Petrology, Geochemistry and Geochronology of Basement Rocks in Bangladesh

A Dissertation Submitted to
the Graduate School of Life and Environmental Sciences,
the University of Tsukuba
in Partial Fulfillment of the Requirements
for the Degree of Doctor of Philosophy in Science
(Doctoral Program in Earth Evolution Sciences)

Ismail HOSSAIN

Contents

Chapter III. Geothermobarometry and fluid inclusions of dioritic rocks in Bangladesh: Implications for emplacement depth and exhumation rate

Chapter IV. Fluid inclusion study of pegmatite and aplite veins of Palaeoproterozoic basement rocks in Bangladesh: Implications for magmatic fluid compositions and crystallization depth.

Abstract

The Palaeoproterozoic (1.7 Ga) basement rocks from Maddhapara, Bangladesh show a large range of chemical variations (e.g., SiO_2 = 50.7–74.7%) and include diorite, quartz diorite, monzodiorite, quartz monzonite and granite. They have a common mineral assemblage of plagioclase, hornblende, biotite, quartz, K-feldspar, titanite, and secondary epidote and chlorite. The pluton overall displays metaluminous, calc-alkaline orogenic suite; mostly I-type suites formed by subduction-related magmatism. The major and trace elements illustrate the unique chemical features by a process that included both partial melting of calc-alkaline lithologies and mixing of mantle-derived magmas, followed by fractional crystallization of largely plagioclase, amphibole and possibly biotite, and by assimilation of country rocks. Some of the fractionated magmas may have mixed with more potassic melts from distinct parts (e.g., metagrewackes) of the continental lithosphere to produce granites.

Application of hornblende thermobarometry to the basement rocks yielded pressure and temperature conditions of 4.9–6.4 kbar and 680–725°C, which probably correspond to crystallization conditions. Zircon saturation thermometry and fluid inclusions data of pegmatite gave reliable condition of ~4.8 kbar and 660–670°C. The basement rocks, therefore, likely crystallized at a depth of ~17–22 km, with a minimum average exhumation rate of ~12–15 m/Ma during Palaeoproterozoic to Lopingian time. Such slow exhumation indicates low relief continental shield surface during this period.

Fluid inclusion studies in dioritic rocks identified aqueous two-phase primary fluid inclusions in plagioclase and quartz. They demonstrate final ice-melting temperatures (T_m) of 0 to –4.0°C, which narrate to $NaCl_{eq}$ salinities of 0 to 6.4 wt.%. Homogenization temperature (T_h) of these inclusions ranges from +259.5 to +358.2°C, which relates to bulk densities of 0.54–0.82 g/cm^3. On the other hand, the fluid inclusions in pegmatite and aplite veins show the T_m and T_h of the dominant carbonic inclusions range from –56.6°C to –58.1°C and from –6.8°C to +30°C, respectively; the T_h values translate into the densities of 0.59–0.97 g/cm^3. Rare aqueous fluid

inclusions in the same rocks have both final T_m values in the range of 0°C to –10.8°C and T_h values in the range of +209.8°C to +405.5°C, which corresponds to bulk densities of 0.52–0.97 g/cm^3. Fluid inclusions in dioritic rocks recommend that low- to medium-salinity (0–6.4 wt.% $NaCl_{eq}$) H_2O-rich fluids are trapped during the crystallization of quartz and plagioclase. Both primary CO_2-rich and H_2O-rich inclusions in pegmatite and aplite veins are present, even in the same inclusion cluster, probably reflecting a single stage of fluid activity during the crystallization of the veins. Therefore, H_2O-rich fluids in dioritic rocks, and CO_2-rich and rare H_2O-rich inclusions in veins as well as lack of H_2O–CO_2 mixed fluids in diorite samples imply two-stage fluid activities (earlier H_2O-rich and by later CO_2-rich fluid).

New U–Pb SHRIMP zircon geochronological data for euhedral zircons from a diorite sample yield a concordia age of 1730±11 Ma, which is interpreted as the crystallization age. The consistent magmatic ages are also common in the Central Indian Tectonic Zone (CITZ), India, the Transamazonian of South America, Bohemian Massif and the Svecofennian, Poland. These areas have identified the sequential growth of the continent through the amalgamation of juvenile terrains, succeeded by a major collisional orogeny. The subduction-related batholiths in different areas in the world signify that the crust contributed effectively to formations of the Palaeoproterozoic supercontinent. The Palaeoproterozoic magmatic age of the examined basement rock and the common occurrences of similar ~1.7 Ga geologic units in the CITZ and Meghalaya-Shillong Plateau in Indian Shield represent their apparent continuation. The consistent Palaeoproterozoic magmatism in the CITZ and Meghalaya-Shillong Plateau as well as the occurrence of ~1.7 Ga geologic units in the Albany-Fraser belt in Australia and East Antarctica indicate that the basement rocks in Bangladesh formed towards the final stages of the assembly of Columbia supercontinent.

Key words: Geochemistry, Calc-alkaline, Amphibole thermobarometry, Fluid inclusion, U–Pb SHRIMP age, Palaeoproterozoic, Basement rocks, Bangladesh, Columbia supercontinent.

List of Figures

Ca: Capricorn, CITZ: Central Indian Tectonic Zone, Eg: Eastern Ghats, Gf: Great Falls, Ke: Ketilidian, Kk: Kola-Karelia, Ma: Mazatzal, Mk: Makkovikian, Ng: Nagssugtoqidian, Pa: Pachemel, Pe: Penokian, Ra: Rayner, Ri: Rinkian, Rj: Rio Negro-Juruena, Ro: Rondonian, Sv: Sveckofennian, Tb: Transamazonian-Birimian, Th: Trans-Hudson, Tt: Thalston-Thelon, Vo: Volhyn, Wb: Windmill Islands-Bunger Hills, Wo: Wopmay, Yv: Yavapai.

List of Tables

CHAPTER I

General Introduction

Bangladesh, as a whole covered by Tertiary and Quaternary sediments without having exposed igneous or metamorphic rocks, is well known for the development of a thick (~22 km) and largest sedimentary succession in the world (Curray, 1991). Dominant Quaternary sediments deposited mainly by Ganges (Padma), Brahmaputra (Jamuna) and Meghna rivers and their numerous distributaries, cover about three quarters of Bangladesh. On the other hand, the Chittagong and Chittagong Hill Tracts, the only extensive hill areas, is lithologically consist of Tertiary sediments. In addition to the hills along the southern spur of the Shillong Massif, a number of hillocks are also covered by Tertiary sediments. Interestingly, the Palaeoproterozoic basement rocks underlie vast areas of the northwestern part of Bangladesh, though sedimentary cover hides such plutonic suites. However, at Maddhapara, study area, the basement rocks occur at a shallow depth from the surface with a successive thin cover of Permian Gondwana Group, Pliocene Dupi Tila Formation, Pleistocene Barind Clay Formation and recent alluvium. Several wells drilled during coal, mineral and hydrocarbon exploratory activities have encountered basement rocks in the area of the Western Foreland Shelf and of the Rangpur Saddle beneath sedimentary cover alluvial deposits. Geophysical studies and drilling showed that the thickness of the sedimentary succession decreases updip from about 5,000 m at the shelf edge to about 150 m in the area of the Rangpur Saddle (Reimann, 1993). Although Archaean to Phanerozoic rocks varieties are widely dominant in Indian subcontinent, the Palaeoproterozoic entity is a conspicuous sparsely in the Central Indian Tectonic Zone (CITZ) with other different areas in India.

In 1959-60, the Standard Vacuum Oil Company first discovered the basement rocks near Kutchma, Bogra at depth 2150 m, and in 1974, Geological Survey of Bangladesh (GSB) discovered the basement rocks at Maddhapara, Dinajpur at shallow depth (128 m), which provide great opportunity to study the basement rocks for petrologists. However, the availability of the basement rocks, detailed petrological and geochemical studies are very limited (Ameen et al., 1998; Kabir, et al., 2001; Zaman et al., 2001, 2002; Hossain et al., 2008a). Recently published some works provide immense opportunity to achieve the decisive remarks (Ameen et al., 2007; Hossain et al., 2007; Hossain and Tsunogae, 2008; Hossain et al., 2008a, 2008b).

The Palaeoproterozoic basement rocks from Maddhapara, Bangladesh characterize a calc-alkaline pluton. In general, calc-alkaline plutons are characteristic of magmatic arcs, and knowledge of their genesis, emplacement, and crystallization is critical in understanding the subduction zone processes that ultimately produce continental crust. However, recent tectonic models for Palaeoproterozoic orogenic belts in North America, Europe, Africa and Asia (CITZ, India) have highlighted mostly similarities with modern subduction and collision zones (e.g., Windley, 1993). Although calc-alkaline plutons have been the subject of many geochemical investigations, detailed studies of evaluation of their crystallization conditions (temperature, pressure, and water and oxygen fugacities) have not commonly been undertaken because of the difficulty of obtaining well-constrained values for intensive parameters. The difficulties arise as these plutons are predominantly composed of quartz, plagioclase, K-feldspar, biotite, hornblende and opaque minerals that are stable over a wide range of crustal conditions.

Careful application of geochemistry, mineral chemistry, appropriate geothermobarometry, and fluid inclusion studies could, nevertheless, yield petrogenetic characterization and reasonable estimates of crystallization conditions, which provide significance improvement for tracking the evolutionary history of a pluton. Information on overall geochemistry, geochronology and crystallization conditions can be used to compare related plutonic units from a particular intrusive complex and from plutons of different terrains, and to evaluate petrogenetic models, which bear on source-region compositions for calc-alkaline magmas and the modification of these magmas by higher-level crustal contaminations. Evaluation of temperature and pressure conditions for plutonic rocks is also important in constraining geophysical and tectonic models of the crust (Zen, 1989).

From overall field observations, data analyses, review of literatures and for obtaining the exact picture of the Palaeoproterozoic basement rocks, I divided the whole topic into four fundamental chapters. Chapter II includes petrography, mineral chemistry, and geochemistry of major, trace and rare earth elements. Petrography is a very important task for getting real idea on minerals, structures and textures of rocks, which is prerequisite for rock characterization. Mineral chemistry gives the clue for minerals formation, what processes were involved. Some major minerals (e.g., feldspars, amphibole, biotite, epidote and titanite) were considered for getting the authentic picture of magmatism. On the other hand, detailed geochemistry of basement rocks in this chapter makes it most valuable part of the dissertation. In this part, I highlighted geochemical classification of rocks, calc-alkalinity, major and trace element

variations with silica, trace and REE spidergrams and different tectonic setting and model, which explained the nature of magmatism significantly. Chapter III includes geothermobarometers and fluid inclusions in dioritic rocks, which offer definite scheme on amphibole thermobarometry for *P–T* conditions, characterized fluid inclusions and comparing its pressure conditions with amphibole barometry. I also extended their application for calculating the emplacement depth and exhumation rate in this chapter, which is very important information for post orogenic conditions of the region. Chapter IV also followed the extension of the fluid inclusion study in the pegmatite and aplite veins, which characterize magmatic fluid compositions and determination of the crystallization pressure and temperature of the host rocks.

In chapter V, I presented U–Pb SHRIMP zircon geochronological data for basement rocks in Bangladesh, and discuss the relationship with the Central Indian Tectonic Zone (CITZ), Meghalaya-Shillong Plateau in Indian Shield and finally palaeogeography of the basement rocks during the formation of the Columbia supercontinent.

CHAPTER II

Petrology and Geochemistry of the Basement Rocks in Bangladesh: A remnant of Palaeoproterozoic magmatism

This chapter is in preparation for the submission to Journal of Petrology

Abstract

The Palaeoproterozoic (1.7 Ga) basement rocks from Maddhapara, Bangladesh show a large range of chemical variations (e.g., SiO_2 = 50.7–74.7%) and include diorite, quartz diorite, monzodiorite, quartz monzonite and granite. The pluton overall displays metaluminous, calc-alkaline orogenic suite, mostly I-type suites formed within subduction-related magmatism. The observed major elements illustrate general trends for fractional crystallization. Trace element contents also indicate the possibility of a fractionation or assimilation; explain the entire variation from diorite to monzonite, even granite. The pluton may have evolved the unique chemical features by a process that included partial melting of calc-alkaline lithologies and mixing of mantle-derived magmas, followed by fractional crystallization, and by assimilation of country rocks. The pluton shows evidence of crystal fractionation involving largely plagioclase, amphibole and possibly biotite. Some of the fractionated magmas may have mixed with more potassic melts from distinct parts (metagrewackes) of the continental lithosphere to produce granites.

The consistent magmatism is also common in the Central Indian Tectonic Zone (CITZ), India, the Transamazonian of South America, Bohemian Massif and the Svecofennian, Poland, that have identified the sequential growth of the continent through the amalgamation of juvenile terrains, succeeded by a major collisional orogeny. Subduction-related batholiths in the Albany-Fraser belt in Australia have similar counterparts in the Windmill islands and Bunger Hills in Antarctica, suggesting that such crust were actively contributing to magmatism in the

Palaeoproterozoic supercontinent.

II. 1. Introduction

U–Pb SHRIMP zircon geochronological results of subsurface basement rocks in Bangladesh reveal the occurrence of Palaeoproterozoic age (~1.72–1.73 Ga; Ameen et al., 2007; Hossain et al., 2007). The common occurrences of similar ~1.7 Ga geologic units in the Central Indian Tectonic Zone (CITZ) and Meghalaya-Shillong Plateau in Indian Shield suggest their apparent continuation with a configuration of the Columbia supercontinent (Hossain et al., 2007). In recent reconstructions of East Gondwana, the composite of the CITZ is recognized as an important Proterozoic collisional zone, along which the North Indian Block (NIB) and the South Indian Block (SIB) were amalgamated during the Palaeoproterozoic to form the Indian subcontinent (Yedekar et al., 1990; Jain et al., 1991; Mishra et al., 2000). The Dinajpur shield, NW Bangladesh, therefore, constitute an integral part of the collisional zone but as it forms a graben due to faulting along the Jamuna (Brahmaputra) and the Ganges, it gets separated on or near the surface between the Chhotonagpur and Shillong Plateaus. These tectonic signatures persuade us to instrument the magmatism of subsurface basement rocks as well as the review of magmatism of different areas of the world during this period.

Although several petrological and geochemical studies on the basement rocks in Bangladesh are available (Ameen et al., 1998; Kabir, et al., 2001; Zaman et al., 2001, 2002; Hossain et al., 2008a, 2008b; Hossain and Tsunogae, 2008), no systematic, in depth, petrogenetic

studies have so far been done from these rocks. Ameen et al. (1998) and Kabir et al. (2001) analyzed major elements (SiO_2, Al_2O_3, K_2O, Na_2O, CaO, MgO and FeO* (*, total) of some boreholes and tunnel samples and concluded that the main rock types (tonalites and granodiorites) belong to I-type granitoid pluton formed under orogenic tectonic environment, which might have subduction-related origin. Zaman et al. (2002) analyzed major, trace and rare earth elements of core samples and suggested that the tonalite-granodiorite suite possibly was derived by partial melting of the granitoid basement and fractionation of Fe–Mg phase. They also pointed out that granites are the partial melting products of the metasediments injected the fractures of the tonalite-granodiorite suite. These works were mostly conventional, which could not focus comprehensive petrological and geochemical aspects. In this point of view, for understanding of petrogenetic characterization, its origin, and specify orogenic signature in Bangladesh, detailed field investigations, petrography, mineral and whole rock geochemistry are very important phenomena. In the present paper, we present subsurface field occurrences of the rocks at stope 1, stope 4 and stope 5 areas in production level with sub-level and ventilation level of mining site in Maddhapara area (Fig. II. 1). A detailed petrography, petrological and geochemical study of the fresh tunnel samples, mostly from production level (-270 m) and sub-level (-246 m) as well as ventilation level (-230 m) of the Maddhapara Granite Mining Company Ltd., and some core samples (GDH-34, GDH-32, BH-11, BH-13, GDH-35, GDH-36) are aimed in order to understand the Palaeoproterozoic magmatism in Bangladesh and compare to similar orogens in other parts of the world.

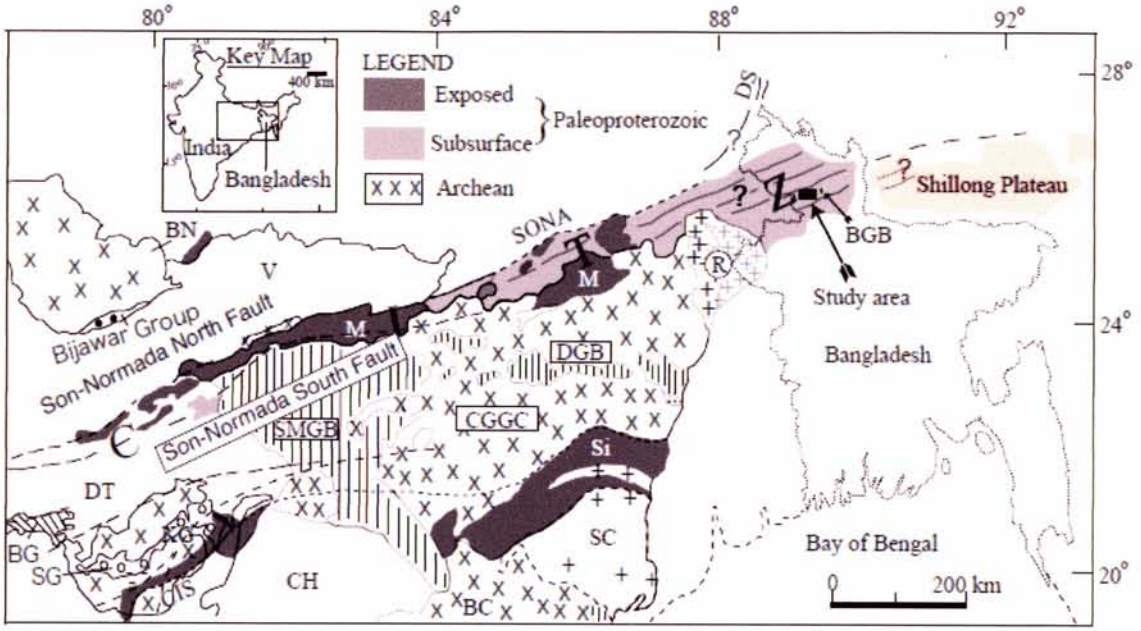

Fig. II. 1. Location map of the Maddhapara basement rocks in Bangladesh, showing different lithological units and tectonic elements of Central Indian Tectonic Zone (CITZ) (modified after Hossain et al., 2007; Acharyya, 2003; Roy et al., 2002). Abbreviations; BC : Bastar Craton, BG : Betul Group, BGB : Barapukuria Gondwana Basin, BN : Bundhelkhand Craton, CGGC : Chotanagpur Granite Gneiss Complex, CH : Chattisgarh, CIS : Central Indian Shear Zone, DGB : Damodar Gondwana Basins, DS : Darjeeling-Sikkim Himalaya, DT : Deccan Trap, KG : Karimnagar Granulite Belt, M : Mohakoshal and equivalents, R : Rajmahal Trap, SG : Sausar Group, SC : Singhbhum Craton, Si : Singhbhum (Palaeoproterozoic), SMGB : Son Mahanadi Gondwana Basins, SONA : Son Narmada Lineament, V : Vindhyan.

II. 2. Geological setting

Bangladesh, a major part of the Bengal Basin, is mainly junction of the Indian and Eurasian plates as well as Burmese sub-plate. It is a composite basin with a varied tectonic history. In between the exposed Peninsular shield and Shillong massif in India lay the Garo-Rajmahal gap corresponding to a shallow basement ridge (Desikachar, 1974) known as Platform flank zone. The Palaeoproterozoic magmatism shaped the platform flank, which was underlain by Permian Gondwana sediments. The Late Cretaceous Rajmahal (117 Ma; Baksi,

1995) basaltic trap flows and Cretaceous-Tertiary sediments in turn have been deposited over the Gondwana sediments. The north-south trending Maldah-Purnea basin and Ghatal-Burdwan basin form a segment of the continental rifted basin zone (Khan and Chouhan, 1996). The zone of Moho unwarping (basement fault) and continental rift mark a mantle activated continental rift zone along which India has been rifted from Australia. Maddhapara, the study area is the shallowest part within an area of the Platform known as Rangpur saddle (Fig. II. 2). It is in the form of a dome bounded by N-S trending faults in the east and the west and slope in the north known as northern slope (Dinajpur slope) and another in the south known as southern slope (Bogra slope). The basement outside the basinal area is directly overlain by Tertiary sediments (Miah et al., 2002). Several drillings in Bangladesh showed that the thickness of the sedimentary succession decreases updip from about 5,000 m at the shelf edge to about 150 m in the area of the Rangpur Saddle (Fig. II. 2).

Regionally two Central Indian Archean cratonic domains (e.g., northern Bundelkhand and southern Bastar cratons) were accreted along ENE–WSW trending CITZ (Fig. II. 1). The CITZ contains Proterozoic supracrustal belts of varied metamorphic grades set in largely undifferentiated migmatitic gneisses and syn- to post-kinematic granitoids. Recent studies have brought out the presence of three granulite belts in this region. The contacts between granulite belts and the adjoining low- to medium-grade supracrustal belts are modified due to deformation and magmatism (Roy et al., 2002). The basement gneisses occur as a lenticular strip from Sindhi to Bansagar between Mahakoshal Group in the south and the Vindhyan sediments in the north. A

large body of granodiorite along with gneisses is exposed near Dudhi to the south of Mahakoshal Group. The overall composition of Dudhi gneiss is hornblende granodiorite. The Son–Normada South Fault shows several phases of sheet-like granite (Palaeoproterozoic) belonging to granodiorite-granite-adamellite (GGA) suite of the shear zone. Important granite bodies are Madanmahal, Barambaba, Jhirgadandi, Tamakhan and Rihad-Renusagar, along with some albite granites. Some of these granites are dated by Rb–Sr isochrones, e.g. Jhirgadandi monzodiorite (1750±100 Ma; 1708±40 Ma and 1813±65 Ma), Tamakhan granite (1856±68 Ma) and Rihand-Renusagar granites (~1730 Ma). Some alkali gabbros indicate a range of Rb-Sr ages from 1610 to 1760 Ma. The available dates suggest an age range of 1700–1800 Ma for Mahakoshal Group, similar to the age of the undeformed sediments of Bijawar Group in the north (Ramakrishnan and Vaidyanadhan, 2008).

The subsurface basement rocks in Bangladesh are dominantly dioritic rocks with minor granitoids. The first discovery of basement rocks at Kuchma, Bogra identified granitic gneiss at a depth of 2150 m (Khan, 1991). Microcline-rich granite, quartz diorite, syenite and quartz monzonite as well as minor metamorphosed rocks such as mica schist/gneiss and hornblende bearing quartz-feldspathic gneiss were also reported from several localities such as the Barapukuria basin (Dinajpur), Badargong, Pirganj, and Mithapukur areas (Rangpur district) (Khan, 1991; Hussain and Curtin, 1995; Uddin et al., 2005).

The basement rocks occur at a shallow depth of 128 m at Maddhapara area and top of this basement has a thin cover of kaolinite with a range of 2–3 m. The rocks of the production

level are mostly fresh and show no significant effect of later hydrothermal alteration, although some altered granitic rocks occur locally. They are sometimes cut by later granitic pegmatite (up to ~50 cm), aplite, and quartz veins. The upper part of basement is highly weathered and the rock exhibits grey to greyish black color, depending on its weathering level. Due to weathering, feldspar was decomposed and ferromagnesian minerals (biotite and amphibole) lost their crystalline forms (Ju and Chun, 2001). Most of the boreholes consist of the whitish granite, which lies at different depth levels and its thickness ranges from 20 cm to 5.4 m but BH-3 shows exceptionally high thickness (27.8 m). The rock contains whitish feldspar, coarse-grained quartz and small amount of dark minerals. In some cases the rock shows pink color. Feldspar, subjected to alteration, imparts light pink color (Ju and Chun, 2001).

In ventilation level, the rocks are altered and fractured in places by the structural influence. Joints and fracture planes are generally filled with thin veins of calcite, while pyrite being locally concentrated. Weathered dioritic rocks are commonly present with whitish granites and/or aplites form as small dykes/veins. Minerals are highly weathered and calcite is dominantly present there. Highly weathered pinkish granite are also common at this level and also in shaft areas. As the depth increases, the rock grades into less weathered and its color becomes more greyish. Sub-level and stope areas in production level are dominantly dioritic with pinkish granitic-pegmatite (Fig. II. 3a) and aplite veins.

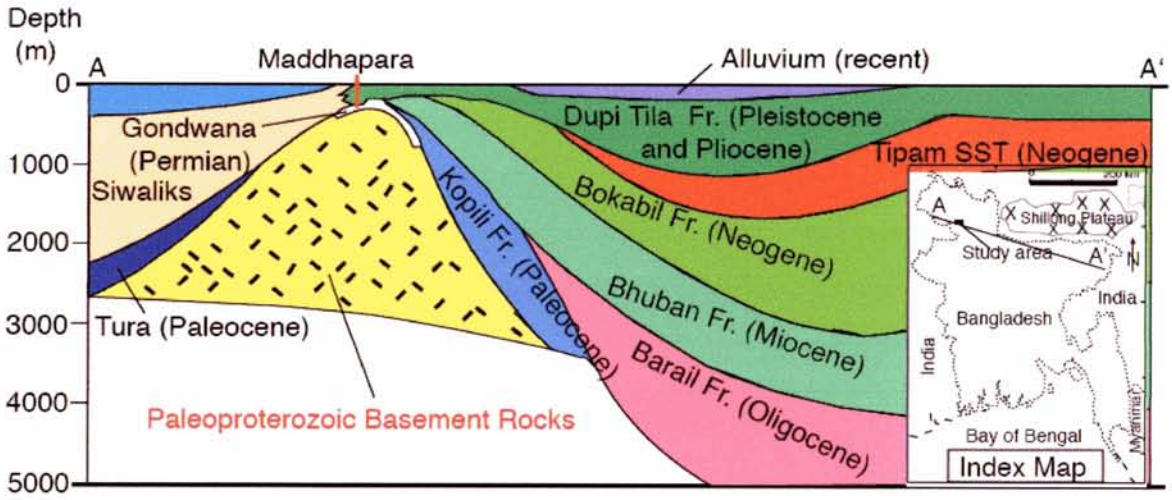

Fig. II. 2. Schematic lithological cross section (WNW-ESE) of Bangladesh (modified after GSB, 1990).

II. 3. Petrography

The main plutonic body at Maddhapara consists of diorite, quartz diorite, granite, monzodiorite, quartz monzonite and syenite (Fig. II. 4). Dioritic rocks are occasionally cut by granitic-pegmatite, aplite and quartz veins. Most of the plutonic rocks are pheneritic with few mylonitic lithologies. Dominant diorite and quartz diorite with monzodiorite and quartz monzonite show similar petrographic features. They are mesocratic to melanocratic, very coarse to medium grained. Modal abundance of minerals in representative samples is listed in Table II. 1. Minor alteration products of these rocks are sericite, chlorite and calcite. Euhedral to subhedral plagioclase show oscillatory zoning, mostly polysynthetically twinned with albite twinning and prismatic-cellular growths. Concentric plagioclase zoning is also present in some rocks (Fig. II. 3g). Medium to coarse grained, subhedral orthoclase are common. Large plagioclase grains sporadically surrounded by hornblende, quartz and biotite indicate porphyritic

texture (Fig. II. 3c). On the other hand fine-grained biotite enclosed in plagioclase indicates poikilitic texture (Fig. II. 3d). Some large plagioclase crystals may contain small quartz, apatite, and/or hornblende inclusions (e.g., samples PLS12, P2). Myrmekitic intergrowths and/or myrmekitic textures are occasionally present (Fig. II. 3e). Large euhedral hornblende crystals are common. Quartz occurs as subhedral to anhedral crystals with irregular cracks and mostly non-undoluse extinction. There is no correlation between the amounts of hornblende and biotite; although hornblende usually dominates. Fine-grained mylonitic diorites show parallel alignment of light (plagioclase, quartz) and dark minerals (hornblende, biotite) (Fig. II. 3h). The studied biotites occur as subhedral to euhedral crystals in close association with plagioclase, hornblende, K-feldspar, quartz, epidote, titanite and apatite (Fig. II. 3b). Epidote occurs as an accessory mineral in diorite (up to 1.7%) and monzodiorite (up to 8.3%) in the studied rocks. Its crystal faces are mildly sub-rounded, singly but general outlines are euhedral. Titanite is a common accessory mineral in diorite (up to 0.8%) and monzodiorite (up to 2%) in studied rocks. Common euhedral, wedge-shaped crystals are relatively fine-grained (0.2–0.7 mm) and are often included in hornblende crystals but themselves generally free of inclusions.

Most of the boreholes from different depth levels are whitish in color (Ju and Chun, 2001). In fact, these rocks are dominantly aplites, composed mainly of fine-grained quartz, plagioclase and K-feldspar. Granitic-pegmatites composed mainly of feldspars (up to 3 cm) and quartz with minor biotite, epidote, chlorite, zircon and apatite. Granite vein contains few garnets showing nearly euhedral crystal form. Quartz occurs as isolated grains and/or aggregates. Rare

quartz intergrowths with K-feldspar and plagioclase formed micrographic and/or granophyric textures. K-feldspars are both microcline (Fig. II. 3f) and orthoclase, forming the majority of phenocrysts. Coarse-grained subhedral orthoclase grains are relatively fresh (e.g. sample P3).

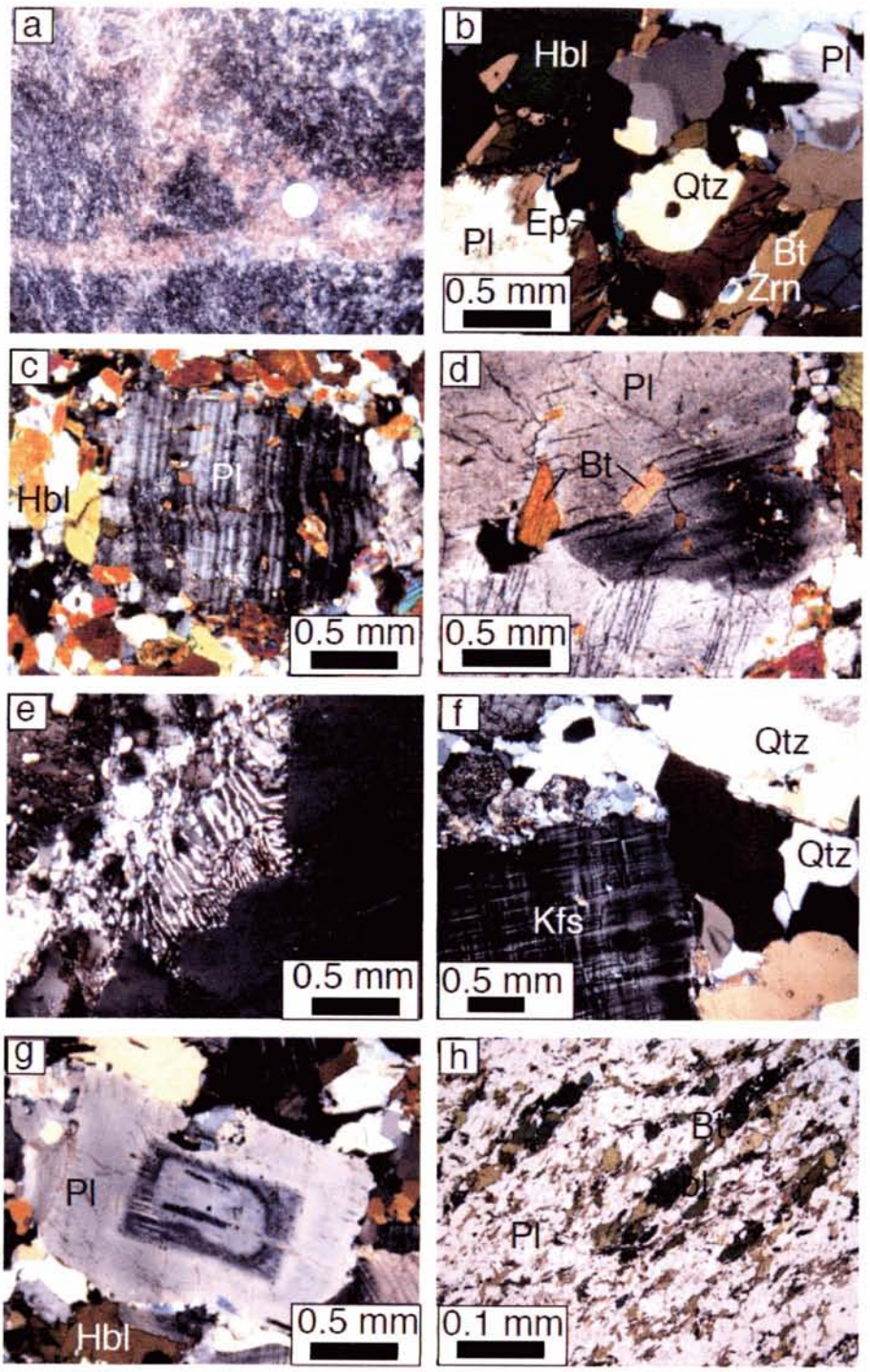

Fig. II. 3. (a) Diorite with cross-cutting pinkish granitic-pegmatite, (b) Mineral assemblages of dioritic rocks (Hbl: hornblende, Pl: plagioclase, Qtz: quartz, Bt: biotite, Zrn: zircon, Ep: epidote, sample P10), (c) Large plagioclase

grain and sporadically surrounded by Hbl, Qtz and Bt indicate porphyritic texture (sample C10), (d) Fine-grained Bt enclosed inside the Pl indicate poikilitic texture (sample PLS2), (e) Myrmekitic intergrowths or textures are rarely present in granitic rocks, (f) Microcline displays cross-hatch twinning and non-perthitic nature, (g) Rare plagioclase zoning present in some dioritic rocks (sample PLS1), (h) Fine-grained mylonitic diorite showing parallel alignment of light (Pl, Qtz) and dark minerals (Hbl, Bt).

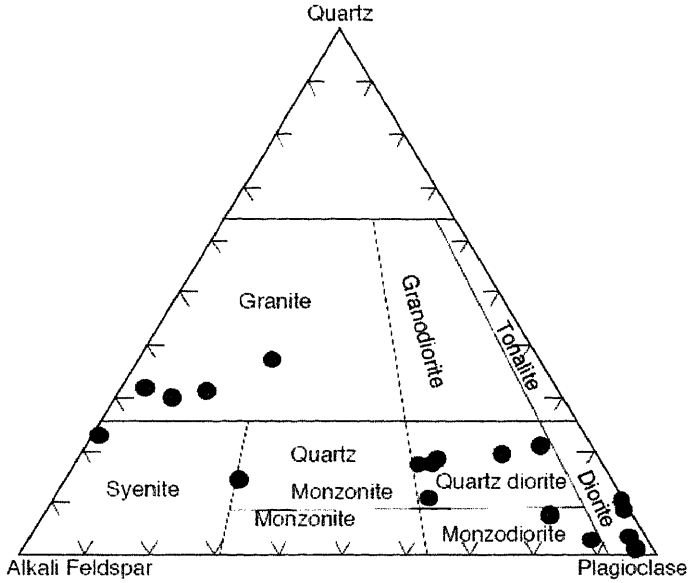

Fig. II. 4. The simplified QAP ternary diagram shows the modal composition of the basement rocks in Bangladesh.

Table II. 1. Modal compositions of basement rocks in Bangladesh.

Sample No.	Rock name	Qtz	Pl	Kfls	Hbl	Bt	Ttn	Ep	Others
PLS2	Diorite	0.7	44.3	1.4	52.5	0.5	0	0.2	0.3
C10	Diorite	1.7	41.7	1.3	52.8	0.8	0.8	0.6	0.2
PLS1	Diorite	4.8	48.2	0.6	40.9	4.7	0.5	0.1	0.2
SL3	Qtz diorite	6.8	56.5	0.5	26.4	7.7	0	1.7	0.3
PL3	Monzodiorite	2.2	60.9	6.5	26.4	2.9	0	0.7	0.3
V1	Monzodiorite	5.8	57.6	10.1	18.8	4	0.1	3.2	0.4
SL2	Qtz diorite	17.7	59.2	7	10.4	5.4	0	0	0.2
PLS12	Qtz diorite	13.4	44.6	10.4	18	9.8	0.3	3.1	0.3
PLS10	Qtz diorite	7.1	37.1	19.9	27.9	5.2	0.4	1.9	0.5
PL8	Qtz diorite	12.7	40.1	19.8	18.4	8.5	0	0.2	0.3
SL4	Qtz diorite	10.4	31.7	14.8	15.5	16.8	2	8.3	1
PLS8	Qtz Monzonite	10	18.1	40.1	24.7	6.3	0.2	0.2	0.1
PL5	Syenite	22.9	0.5	75.8	0.1	0.4	0	0	0.3
C5	Granite	23.4	12.5	26.6	19.4	10.4	0.8	6.6	0.3
PL1	Granite	30	12.4	53	0.7	3.1	0	0.6	0.2
C11(2)	Granite	30	8.2	60.9	0	0.7	0	0	0.2
C9	Granite	30.2	3	61.2	0.1	3.6	0	1.6	0.3

II. 4. Mineral chemistry

II. 4.1. Analytical method

Chemical analyses of minerals in basement rocks were carried out by electron microprobe analyzer (JEOL JXA-8621) at the Chemical Analysis Division of the Research Facility Center for Science and Technology, University of Tsukuba. The analyses were performed under conditions of 20 kV accelerating voltage and 10 nA sample current, and the data were regressed using an oxide-ZAF correction program supplied by JEOL.

II. 4.2. Results

II. 4.2.1. Feldspars

Composition of plagioclase in diorite, quartz diorite, monzodiorite, and quartz monzonite varies from An_{21} (oligoclase) to An_{53} (labradorite). That in diorite shows higher anorthite content of An_{26-53} than that in quartz diorite, monzodiorite, and quartz monzonite (An_{21-36}). Compositional zoning is obvious for plagioclase in some diorites (Fig. II. 3g, sample PLS1), showing anorthite-rich core (An_{53-40}) and albite-rich rim (An_{32-35}). K-feldspar in diorite and monzodiorite has relatively consistent composition of $Or_{91-95} - Ab_{4-9}$.

II. 4.2.2. Calcic-amphibole

Ca-amphibole in the examined samples has a wide compositional variation in X_{Mg}=

Mg/(Fe + Mg) = (0.50–0.66), $(Na+K)^A$ (0.22–0.62 pfu), Si (6.35–6.71 pfu), and Fe^{3+} / (Fe^{2+} + Fe^{3+}) = 0.10–0.45. Most of them are compositionally magnesiohornblende based on the classification of Leake et al. (1997), while some pargasite, magnesiohastingsite, edenite and tschermakite are also present. Although compositions of amphiboles in diorite, quartz diorite, and monzodiorite are generally indistinguishable, rare coarse-grained amphibole in diorite shows slightly higher X_{Mg} (0.52–0.66) than those in quartz diorite and monzodiorite X_{Mg} (0.50–0.63). Slight compositional zoning can be seen for coarse-grained amphibole in diorite in terms of $(Na+K)^A$; the value increases slightly from core (0.45–0.48 pfu) to rim (0.52–0.54 pfu). However, in terms of X_{Mg}, the core and rim value do not show any remarkable variation. Amphibole composition also varies depending on co-existing minerals, with biotite shows lower $(Na+K)^A$ value (0.52–0.55 pfu) than that associated with plagioclase (0.55–0.58 pfu) in diorite sample (P28).

II. 4.2.3. Biotite

Biotite in diorite and monzodiorite has almost consistent composition. Its FeO*/(FeO*+MgO) ratio varies only slightly from 0.49 to 0.62 (Table II. 2). TiO_2 content is also nearly consistent, having the range in quartz diorite (2.1–2.6%), is slightly higher than that in diorite (1.6–2.5%) and monzodiorite (1.8%). The Ti content generally increases with decreasing X_{Mg}.

Table II. 2. Chemical composition of selected biotites from basement rocks in Bangladesh.

Sample Name	SL3.1	SL3.2	SL3.3	PLS1.1	PLS1.2	SL1.1	SL1.2	PLS3.1	PLS3.2	PLS12.1	PLS12.2	PLS12.3	P28.1	P28.2	P28.3
SiO_2	36.40	36.71	36.85	36.84	36.92	36.51	37.31	36.44	35.72	36.74	36.59	32.39	35.61	35.72	36.01
Al_2O_3	15.32	15.20	15.15	14.75	14.77	14.84	15.32	14.75	15.65	15.09	15.32	13.32	15.02	15.42	15.12
TiO_2	2.10	2.05	2.57	2.51	2.50	1.59	1.64	2.18	1.74	1.79	1.77	1.29	1.93	1.76	2.41
Cr_2O_3	0.05	0.00	0.11	0.03	0.00	0.05	0.05	0.06	0.03	0.00	0.04	0.01	0.04	0.03	0.04
FeO*	17.20	16.98	17.03	17.33	17.84	16.66	16.80	17.97	18.28	16.41	16.10	10.92	18.40	17.20	17.88
MnO	0.25	0.26	0.27	0.23	0.23	0.33	0.32	0.28	0.25	0.25	0.29	0.15	0.27	0.19	0.35
MgO	12.84	12.95	12.92	12.83	12.96	13.08	13.48	12.56	13.97	12.94	12.68	11.54	11.28	12.16	11.45
CaO	0.00	0.00	0.02	0.00	0.00	0.01	0.01	0.03	0.06	0.06	0.01	0.14	0.04	0.11	0.01
Na_2O	0.07	0.06	0.02	0.04	0.09	0.03	0.08	0.12	0.05	0.09	0.10	0.11	0.14	0.07	0.12
K_2O	9.69	9.55	9.45	9.72	9.85	9.50	9.46	9.28	7.75	9.46	9.23	6.46	9.69	8.91	9.62
ZnO	0.08	0.02	0.11	0.06	0.02	0.06	0.08	0.04	0.06	0.05	0.00	0.03	0.03	0.08	0.07
Total	93.98	93.78	94.50	94.32	95.19	92.65	94.54	93.71	93.57	92.87	92.11	76.36	92.43	91.65	93.07
FeO*+MgO	30.04	29.93	29.95	30.15	30.80	29.73	30.28	30.53	32.25	29.34	28.78	22.45	29.68	29.36	29.33
FeO*/(FeO*+MgO)	0.57	0.57	0.57	0.57	0.58	0.56	0.55	0.59	0.57	0.56	0.56	0.49	0.62	0.59	0.61

III. 4.2.4. Other minerals

Composition of epidote in diorite and quartz diorite is almost consistent and close to the chemical formula $Ca_2Fe^{3+}Al_2Si_3O_{12}(OH)$. It is remarkably low Cr_2O_3 (<0.1%). No compositional zoning has been identified within singe grain. These minerals occasionally show optical zoning pattern.

Chemical composition of titanite is close to the ideal formula of $CaTiSiO_5$, yet it contains rare Fe_2O_3 of 0.9–1.2%.

II. 5. Whole-rock geochemistry

II. 5.1. Methodology

Nine (9) representative samples of basement rocks collected from different levels and cores, have been analyzed for whole-rock geochemical analyses of major, trace, and rare earth elements. Sampling has been done carefully from different levels and core samples so as to mitigate the possible effects of weathering. Thin sections were made for all the analyzed samples and we confirmed secondary minerals are rare in the rocks. The analyses were obtained from the methods of fusion ICP/MS at the Activation Laboratories Ltd. (Actlabs), Canada as presented in Table II. 3.

II. 5.2. Results

II. 5.2.1. Major elements

The basement rocks in Bangladesh have a large variation of SiO_2 (50.7–74.7 wt%) contents (Table II. 3). The total iron contents are 6.3–10.1 wt% in dioritic rocks and around 1 wt% in granite whereas the content ranges from 4.0 to 11.0 wt% in previous study of the basement rocks (Zaman et al., 2002). The total iron contents in dioritic rocks are very high compare to Bastar granitoids (1.6–4.2 wt%), but Bundelkhand granitoids (2.6–11.0 wt%) and Malanjkhand granitoids (7.0–15.2 wt%), India, show consistent results (Hussain et al., 2004; Kumar and Rino, 2006). Na_2O and K_2O contents of diorite range of 3.0–4.0 wt% and 1.6–2.1

wt%, whereas those of granites are 2.6–3.0 wt% and 5.5–6.2 wt%, respectively. The results are nearly consistent with those of diorite (Na_2O=2.7–4.3 wt%, K_2O=1.5–5.7 wt%) and granite (Na_2O=3.3–4.4 wt%, K_2O=2.0–4.8 wt%) of previous studies (Zaman et al., 2002; Kabir et al., 2001). Most of the rocks analyzed in this study are metaluminous, only a granite (e.g., sample PL5) showing peraluminous in nature (Fig. II. 6) with molar A/CNK values ranging from 0.76 to 1.02.

Table II. 3. Major and trace element abundances of selected samples from basement rocks in Bangladesh.

Elements	SL1	SL2	PLS3	PLS2	PL5	C4	C2	C8	PL9
%									
SiO_2	52.51	58.85	73.56	56.54	74.68	60.01	57.65	55.58	50.68
Al_2O_3	15.64	17.50	13.73	17.01	13.10	16.34	16.99	16.39	16.41
$Fe_2O_3^{(T)}$	10.08	6.25	1.23	7.19	0.83	7.19	6.90	8.40	8.93
MnO	0.18	0.10	0.01	0.14	0.01	0.11	0.11	0.15	0.20
MgO	5.72	3.29	0.40	3.75	0.20	3.29	3.52	4.23	6.57
CaO	7.20	6.17	1.61	6.40	1.42	5.51	6.39	6.56	8.87
Na_2O	2.93	4.00	3.00	3.93	2.59	3.45	3.88	3.87	3.48
K_2O	2.38	1.61	6.22	1.91	5.52	2.02	1.92	1.56	2.08
TiO_2	0.99	0.67	0.11	0.72	0.08	0.72	0.71	0.78	0.91
P_2O_5	0.43	0.29	0.03	0.33	0.02	0.32	0.32	0.28	0.37
LOI	1.18	0.54	1.04	1.34	0.59	1.89	1.45	1.20	1.34
Total	99.24	99.27	99.95	99.25	99.04	100.80	99.84	98.97	99.85
ppm									
Sc	27	16	4	19	2	17	18	24	26
Be	2	2	1	3	< 1	2	2	2	2
V	174	109	21	127	9	118	126	149	177
Cr	120	50	< 20	70	< 20	60	70	130	180
Ni	70	40	< 20	50	< 20	30	40	50	90
Cu	60	30	100	10	< 10	< 10	40	< 10	10
Zn	110	80	< 30	100	< 30	90	90	90	120
Ga	19	19	12	20	11	19	20	20	20
Ge	1.6	1.4	1.2	1.7	0.9	1.5	1.7	1.8	1.7
Rb	82	58	98	85	106	73	64	50	50
Sr	715	860	699	695	675	682	874	632	812
Y	18.9	16.3	2.2	22.6	3	18.7	17.8	18.4	18.1
Zr	122	123	47	131	46	123	147	116	79
Nb	6.6	6.2	3	9.7	3.1	7	6.1	8.9	5.1
Sn	1	1	< 1	2	< 1	1	1	2	1
Sb	1	1	1.1	1.2	0.9	1.1	1.2	1	1.1
Cs	3.2	1.5	1.5	5.4	0.8	2.8	1.7	1.1	0.9
Ba	770	431	2190	374	1806	742	779	253	1047
La	37.2	33.8	12.2	34.2	11.2	41.7	36.1	27	36.9
Ce	75.2	66.2	21	69.2	20.2	79.1	73.1	54	76.4
Pr	8.96	7.63	2.03	8.43	2.06	9.08	8.44	6.44	9.09
Nd	34.7	28.6	6.34	32.8	6.58	33.7	31.7	24.6	34.5
Sm	6.66	5.36	0.87	6.8	1.16	6.18	5.77	4.98	6.53
Eu	1.64	1.44	0.53	1.72	0.61	1.7	1.66	1.43	1.97
Gd	5.31	4.31	0.53	5.46	0.78	4.7	4.57	4.21	4.9
Tb	0.71	0.61	0.06	0.77	0.1	0.68	0.61	0.61	0.68
Dy	3.55	3.02	0.34	3.94	0.55	3.39	3.18	3.26	3.34
Ho	0.65	0.57	0.07	0.74	0.1	0.62	0.59	0.62	0.61
Er	1.79	1.61	0.2	2.21	0.3	1.77	1.65	1.76	1.72
Tm	0.263	0.234	0.032	0.327	0.044	0.259	0.237	0.251	0.242
Yb	1.75	1.49	0.23	2.18	0.31	1.71	1.53	1.59	1.56
Lu	0.257	0.198	0.038	0.324	0.05	0.237	0.226	0.235	0.231
Hf	3.1	3	1.1	3.4	1.8	3.2	3.6	3.1	2.1
Ta	0.46	0.64	0.48	0.8	0.96	0.47	0.59	0.89	0.37
Tl	0.41	0.39	0.41	0.57	0.36	0.51	0.41	0.29	0.27
Pb	19	51	43	33	41	27	31	42	26
Bi	1	0.3	< 0.1	1.4	< 0.1	0.3	0.4	0.3	0.3
Th	4.1	6.49	11.2	8.13	10.5	5.53	5.59	6.28	1.45
U	1.5	1.42	2.17	2.51	2.25	1.83	1.43	1.57	0.45
EuN	18.85	16.55	6.09	19.77	7.01	19.54	19.08	16.44	22.64
Eu*	23.09	18.64	2.75	23.64	3.79	21.06	19.96	17.66	22.14
Eu/Eu*	0.82	0.89	2.22	0.84	1.85	0.93	0.96	0.93	1.02
LaN	101.36	92.10	33.24	93.19	30.52	113.62	98.37	73.57	100.54
YbN	7.06	6.01	0.93	8.79	1.25	6.90	6.17	6.41	6.29
LaN/YbN	14.36	15.33	35.84	10.60	24.41	16.48	15.94	11.47	15.98

The chemical nomenclature of samples based on total alkali versus SiO_2 (TAS) shows that the samples are diorite, granite/alkali granite and gabbro (Cox et al., 1979, Wilson, 1989) (Fig. II. 5a), whereas they are classified as diorite, granite, gabbroic diorite, monzodiorite and monzogabbro based on the classification of Middlemost (1997) (Fig. II. 5b). These classifications are consistent with the results of mode classification except one sample classified as gabbro, although texturally it is similar to other diorites, consists dominantly of plagioclase, hornblende and biotite. Of the different rock types, diorites are the least siliceous (~50 wt.%), with monzodiorite showing intermediate silica contents (~55–60 wt%), and granite showing the highest silica content (~75 wt%).

All the major elements of the basement rocks on silica variation diagram (Fig. II. 9) exhibit decreasing Al_2O_3, FeO*, MgO, CaO, MnO and P_2O_5 contents with increasing SiO_2, whereas K_2O broadly increases. There is no clear trend in Na_2O. Silica variations show clear compositional gap between 61 to 70 wt% SiO_2 contents. Diorite, quartz diorite, monzodiorite and monzonite are relatively mafic and have low molar Al_2O_3/ ($CaO+Na_2O+K_2O$) (A/CNK <1, (0.68–0.91) metaluminous) and molar FeO* / (FeO* +MgO) (0.41–0.52) relatively consistent to the mafic pluton. On the other hand, granites show A/CNK (0.94–1.02) >1, indicating peraluminous nature. Dioritic rocks are characterized by low values of the molar ratio of K_2O/Na_2O (<1) and in general the constituent pluton has higher alkali content (Na_2O+K_2O) and becomes more potassic as a function of increasing SiO_2. On the plot (Na_2O+K_2O) versus SiO_2, the pluton plots within subalkaline field, while they are plotted in calc-alkaline field within

FeO*/MgO versus SiO_2 diagram (Fig. II. 7b). This is consistent with a Peacock (Alkali-Lime) index of about 58, which indicates generally calc-alkaline trend, if plotted (K_2O+Na_2O) –FeO*–MgO (AFM) diagram (Fig. II. 7a).

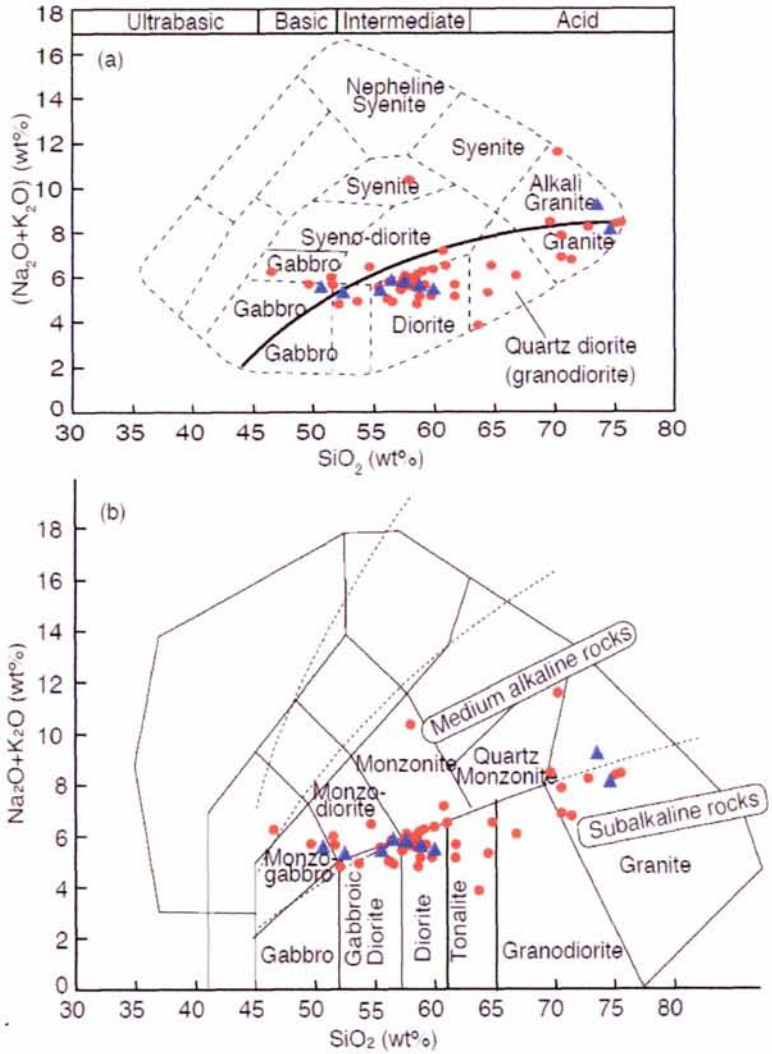

Fig. II. 5. (a) The chemical classification and nomenclature of basement rocks in Bangladesh using the total alkalis versus silica (TAS) diagram of Cox et al. (1979) adapted by Wilson (1989) for plutonic rocks (the curved solid line subdivides the alkalic from subalkalic rocks), (b) TAS diagram after Middlemost (1997). (Symbols: blue triangle, present study, red circle, previous studies (Ameen et al., 1998; Zaman et al., 2001, 2002; Kabir et al., 2001).

Frost et al. (2001) proposed a three-tiered scheme that uses familiar chemical parameters, many of which appear in other geochemical classification schemes for granitoids (Petro et al.,

1979; Maniar and Piccoli, 1989; Barbarin, 1990, 1999). These are (1) Fe# = FeO/(FeO+MgO) or Fe*=FeO*/(FeO*+MgO), (2) the modified alkali lime index (MALI)=Na_2O+K_2O-CaO and (3) the aluminum saturation index (ASI) = Al / (Ca-1.67P+Na+K) (Shand, 1943). The variable Fe* or Fe-number shows the magnesian nature of the analyzed basement rocks (Fig. II. 8a). SiO_2 versus MALI of basement rocks shows that the MALI increases with increasing SiO_2. Most of the analyzed samples show calc-alkalic (78%) and/or alkali-calcic (22%) characters (Fig. II. 8b). ASI values of basement rocks ranges from 0.9 to 0.7, indicating metaluminous nature, only a granite sample (PL5) showing the peraluminous nature (ASI=1.02).

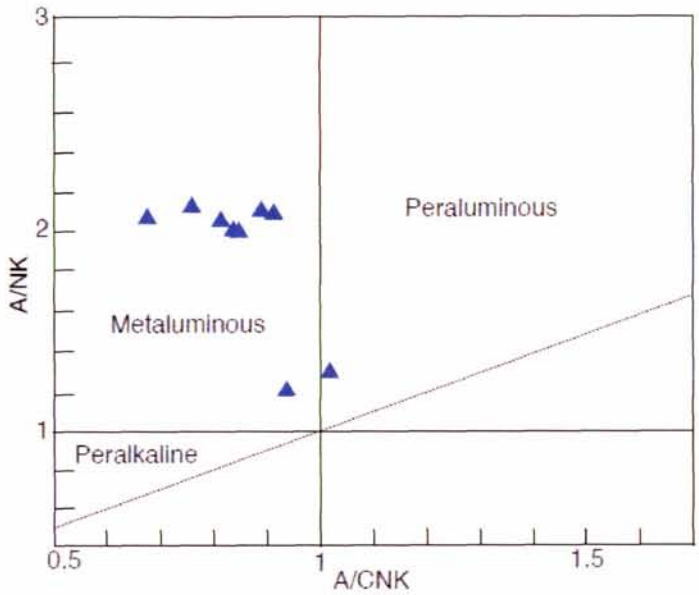

Fig. II. 6. A/CNK versus A/NK Shand index diagram (Maniar and Piccolli, 1989) of basement rocks in Bangladesh.

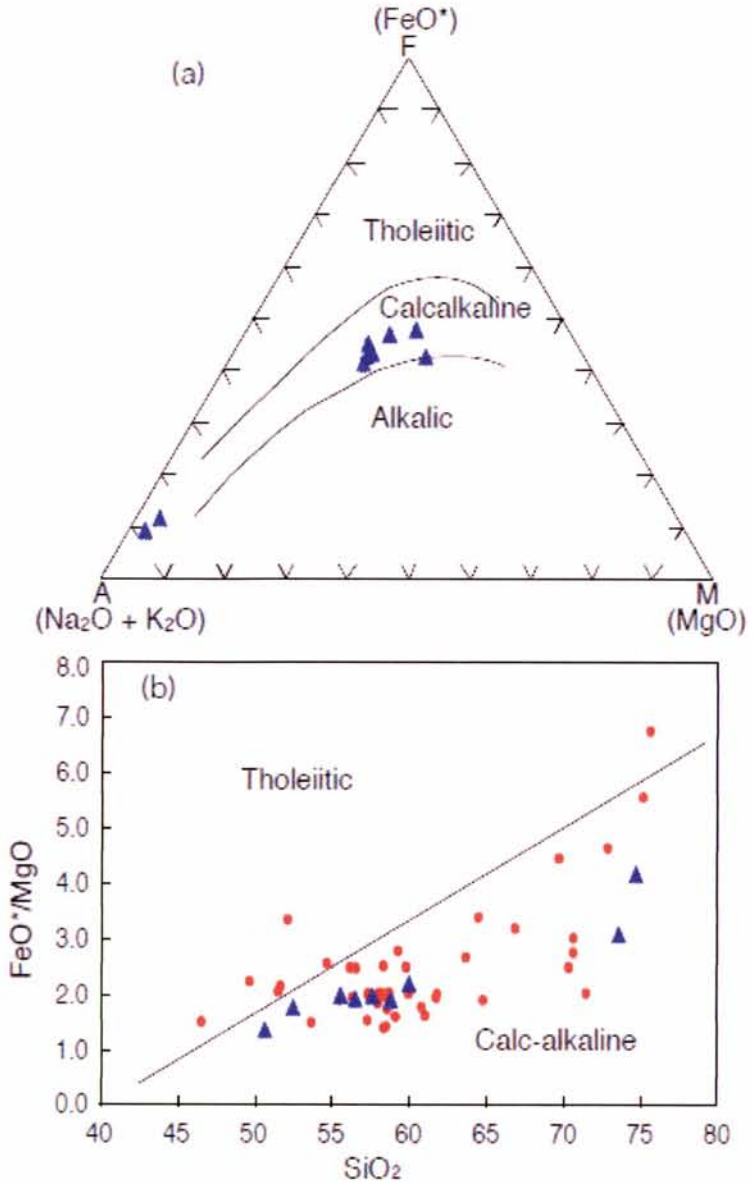

Fig. II. 7. (a) Diagram for (Na_2O + K_2O)-FeO*-MgO (AFM), (b) FeO/MgO* vs SiO_2 diagram with the tholeiitic-calc-alkaline dividing line. Diagrams illustrate the general calc-alkaline trend of the basement rocks (Symbols: blue triangle, present study, red circle, previous studies (Ameen et al., 1998; Zaman et al., 2001, 2002; Kabir et al., 2001).

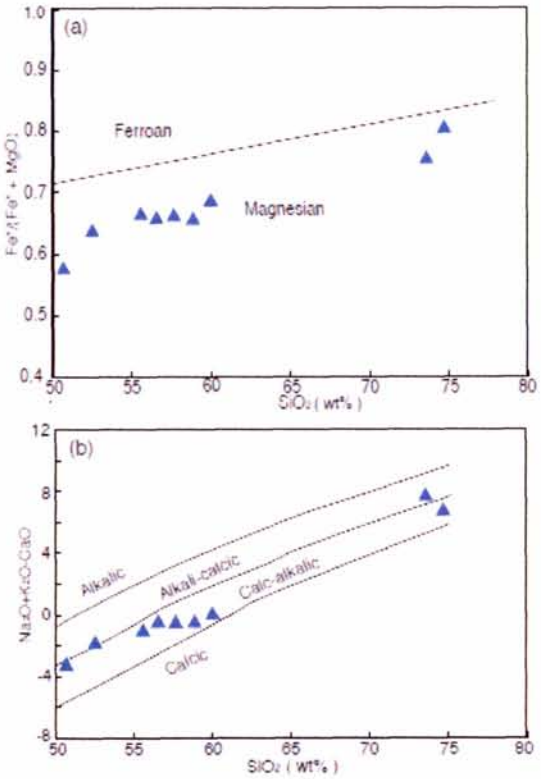

Fig. II. 8. (a) Fe*/(Fe* + MgO) vs SiO_2 and (b) $Na_2O + K_2O$ - CaO vs SiO_2 plots for the basement rocks in Bangladesh (Frost et al., 2001).

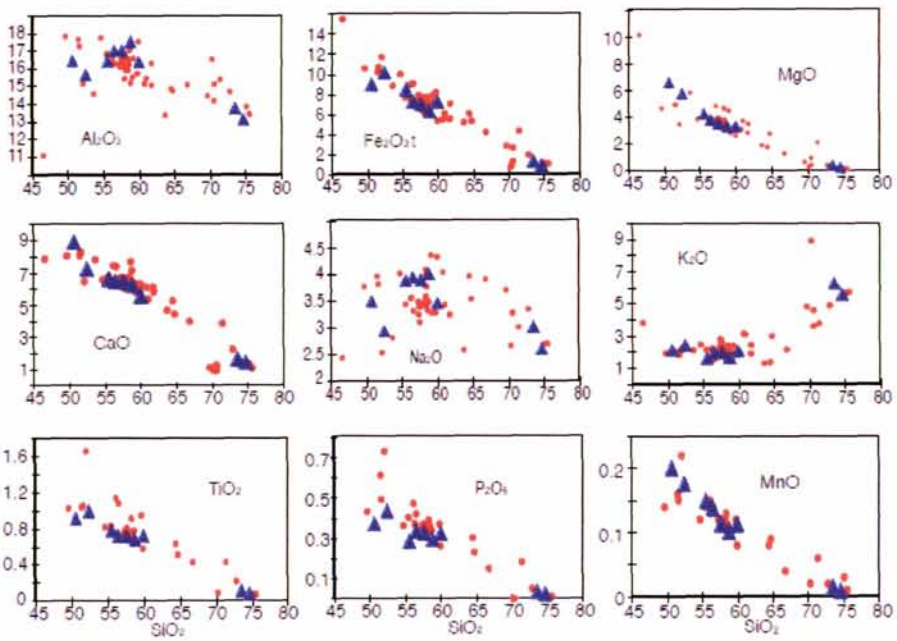

Fig. II. 9. Silica variation diagrams for representative major elements (wt.%) of basement rocks in Bangladesh (Symbols: blue triangle, present study; red circle, previous studies (Ameen et al., 1998; Zaman et al., 2001, 2002; Kabir et al., 2001).

II. 5.2.2. Trace elements

Trace elements abundances generally do not vary systematically with increasing SiO_2 in the analyzed basement rocks. As a whole, those are scattered or non-systematic abundances with increasing SiO_2. Although most trace elements on silica variation diagrams (Fig. II. 10) show negative correlation with SiO_2 (e.g., Nb, Y, and Zr), Rb and Ba show positive trend. The K/Rb values of the rocks range from 294 to 674, there is no systematic variation in K/Rb with SiO_2, broadly comparable to calc-alkaline suites elsewhere (e.g., Bertrand et al., 1984). The values for Zr/Hf (25.5–80.8), Rb/Sr (< 1), Rb/Zr (0.4–2.3) and Nb/Ta (3.2–14.9) of the basement rocks are within the range of plutonic rocks found in continental magmatic arc (after Ayuso and Arth, 1992). These values are inconsistent with a simple origin for the pluton from melting a homogeneous source region. Sr/Y ratio is very high. Some diorites (samples SL1, C8 and PL9) record a high Cr content (up to 180 ppm). Cr, Ni, Zn, Sc abundances generally decrease with SiO_2 (Table II. 3). Yb_N value ranges are 6.0–8.8 in diorite, and 0.9–1.3 in granite. Diorite (sample PL9) has the lowest Rb content (50 ppm), while granite (sample PL5) shows the highest (106 ppm) content.

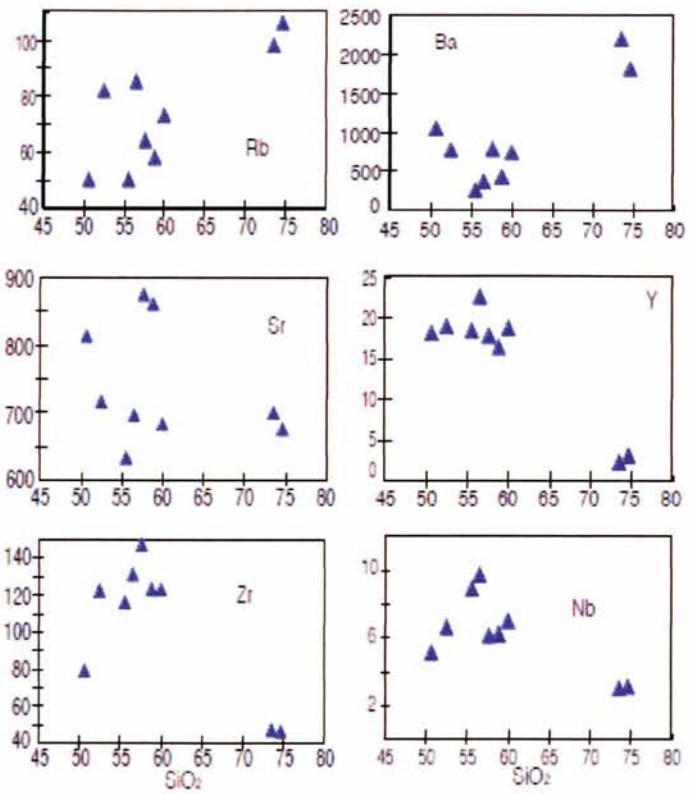

Fig. II. 10. Silica variation diagrams for representative trace elements (ppm) of the basement rocks in Bangladesh.

II. 5.2.3. REE and multi-elemental patterns

Chondrite-normalized rare earth element (REE) patterns (after Taylor and McLennan, 1985) for the basement rocks in Bangladesh show significant light REE (LREE) enrichment and flat heavy REE (HREE) trend (Fig. II. 11). Most of the REE concentrations decrease with increasing SiO_2 contents. In general, dioritic rocks show higher REE content than granites and show nearly neutral Eu anomaly. It also shows a gradual decrease from La to Lu with $(La/Yb)_N$ of 10.6-16.5, Eu/Eu* of 0.8–1.0 and negative Eu anomaly is absent or very small. The rocks with the lowest concentration pattern REE in granites (samples PLS3 and PL5) show a positive Eu anomaly, which may be indicative of feldspar accumulation and also show strongly fractionation

of LREE over HREE with $(La/Yb)_N$ of 24.4–35.8, and Eu/Eu* of 1.9–2.2. MREE patterns are diminutively kinked. The estimated residual assemblage in the examined rocks is dominated by plagioclase and hornblende and includes trace amounts of zircon, titanite and apatite. The strongly fractionated REE patterns and a general trend of decreasing heavy REE, CaO, Y and Co with increasing SiO_2 is consistent with removal of hornblende by crystallization (Arth and Barker, 1976). A volumetrically minor granite representing the most silicic rock in the pluton differs from the bulk of the intrusive because its REE abundances are all lower, though heavy REE show almost flat (Fig. II. 11).

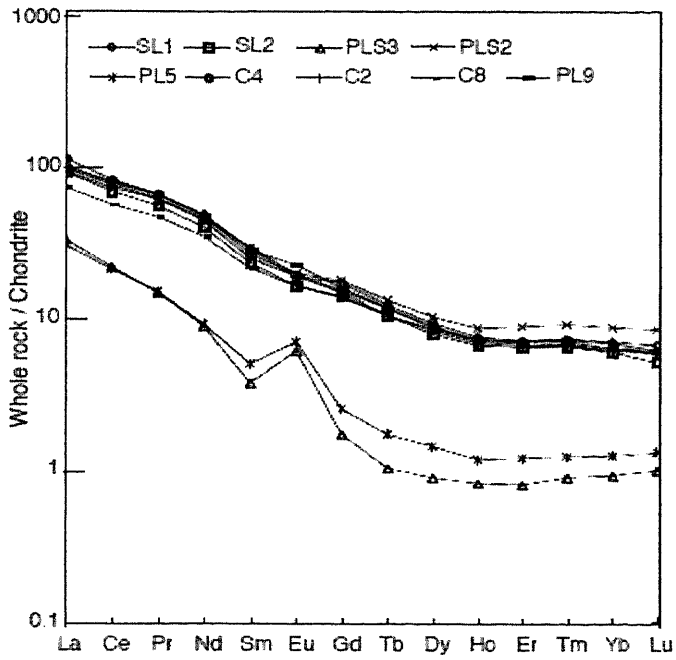

Fig. II. 11. Rare earth element abundances of the basement rocks in Bangladesh, normalized to chondrite values (Taylor and McLennan, 1985).

The primordial mantle normalized multi-elemental patterns (after Taylor and McLennan, 1985) of the analyzed basement rocks show marked enrichment in both the LILE and HFSE in diorite, but granites (samples PLS3 and PL5) show high enrichment of LILE and a lesser

abundance of HFSE. On the other hand, Ba, K, Sr, Sm and Ti show strong positive anomalies and Th, Nb and Tb show strong negative anomalies (Fig. II. 12). The analyzed rocks also show increasing of Th and Ta with increasing SiO_2, which is consistent with the generally incompatible nature of the HFSE and Th in these rocks. However, Zr, Hf and Nb consistent with SiO_2 up to 61%, they are decreased significantly in granitic composition.

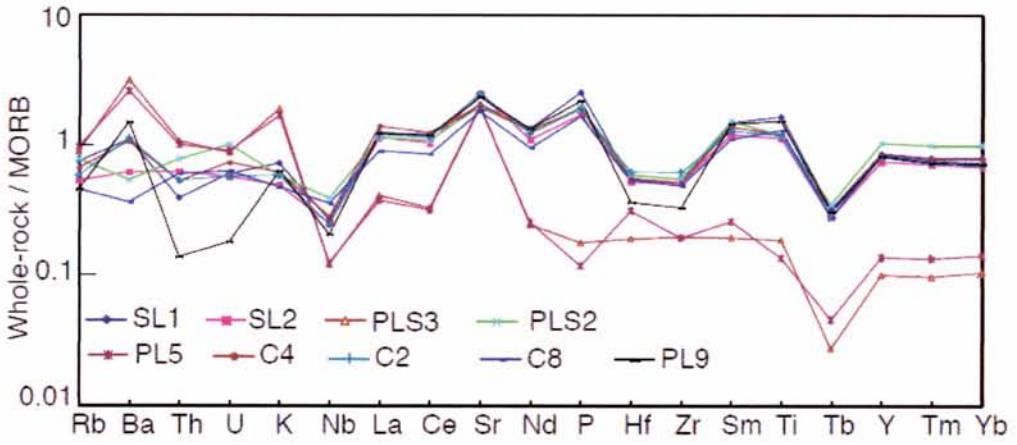

Fig. II. 12. MORB (Sun and McDonough, 1989) normalized trace element plot for the basement rocks in Bangladesh.

II. 6. Discussions

II. 6.1. Implication of geochemical data

Geochemical classification schemes of the analyzed basement rocks indicate that they are mostly calc-alkalic, subalkaline, metaluminous and consistent with a Peacock index (58). Although it is known that calc-alkaline suites consist of rocks that have a wide range of chemical features produced by mixing of magmas from different reservoirs, fractional crystallization, and

crustal assimilation, among others, the relative effect of each process on individual suites of rocks is often difficult to assess (e.g., Taylor 1980; Barker 1981; DePaolo 1981; Gill 1981). Generally calc-alkaline rocks bear the characteristic of magmatic arcs. Metaluminous rock is related to both the magma sources and the conditions of melting (Frost et al., 2001). In contrast, the ASI of a granitic rock is mostly a function of the source of magma, with peraluminous magmas formed from hydrous melting of mafic rocks (Ellis and Thompson, 1986) or melting of pelitic or semipelitic rocks (Holtz and Johannes, 1991). The ASI takes into account the presence of apatite, so that rocks that have ASI > 1·0 are corundum-normative and are termed peraluminous (Zen, 1988). For slightly peraluminous rocks of this phase may be effect of biotite, or forming from a sedimentary source (Chappell and White, 1974), or even by water-excess melting of mafic rocks (Ellis and Thompson, 1986). Metaluminous rocks contain calc-alkalic phases such as hornblende but lack either muscovite or sodic ferromagnesian phases. The distribution of the studied samples allows distinguishing meta-igneous and meta-sedimentary rocks of intermediate to felsic composition; it indicates that all samples of this study derived from igneous protoliths (Werner, 1987). The predominantly metaluminous chemistry, with Na_2O prevailing over K_2O (Janousek et al., 2004; Sokol et al., 2000), corresponds with that of typical I-type granitoids.

Composition of plagioclase in diorite, quartz diorite, monzodiorite, and quartz monzonite varies from oligoclase (An_{21}) to labradorite (An_{53}). Accordingly, the high Mg, Cr, Ni dioritic rocks have a whole-rock chemical composition typical of a cumulate of mafic minerals

(amphibole and biotite) and records of episode of early resorption of anorthite rich core of plagioclase (Pietranik and Weight, 2008). It is also possible that biotite and amphibole formed by reaction between anhydrous mafic minerals and water-rich melt. Such resorption could be an effect of magma mixing or, alternatively, partial melting of mafic lower crust induced by intrusion of hydrous basaltic magma (Annen et al., 2006). The production of a small amount of dioritic magmas by partial melting of lower crust with a basaltic composition is also possible (Annen et al., 2006). The porphyritic texture, occasional existing, represents an early growth of large feldspar crystals during slight cooling of magma followed by fine grains resulting from more rapid cooling due to emplacement at shallow levels (Best, 1982). The latest stage event during exhumation, occasionally observed deformation is supported by the wavy extinction and recrystallization of quartz, kinked biotite, and joints, which are likely responses to post-emplacement regional stresses on basement rocks (Hossain et al., 2008b).

Biotite has a potential to reflect both the nature and the physical conditions of magmas from which it formed (Abdel-Rahman, 1994). The chemical composition of biotite minerals represents three different magmatic rocks (anorogenic extensional-related alkaline rocks, calc-alkaline I-type orogenic suites, and peraluminous including S-type rocks). The analyzed biotite in diorite and quartz monzodiorite in basement rocks shows the FeO*/MgO ratio between 1.25–1.63 (average 1.36). Naturally in the fact that the average FeO*/MgO ratio of biotites doubles from calc-alkaline (1.76), to peraluminous (3.48) to alkaline suites (7.04) (Abdel-Rahman, 1994). According to comparison of biotite discrimination and the examined

basement rocks in Bangladesh also show the field of mostly subduction-related suites including I-type orogenic suite (Abdel-Rahman, 1994). The FeO*/MgO ratio of biotites in Malanjkhand microgranular enclaves and Malanjkhand granitoids is nearly consistent as 1.49 to 2.20 and 1.43 to 1.90, respectively (Kumar and Rino, 2006). In calc-alkaline magmatic rocks, the lack of biotite alteration (to chlorite) and a fresh appearance of plagioclase mostly excludes a later retrograde greenschist-facies overprint and therefore makes it unlikely that epidote formed through a subsolidus reaction (Schmidt and Thompson, 1996).

Major, trace and REE abundances and patterns affected the evolution of the basement rocks of Bangladesh. All the major elements may indicate the presence of some sort of chemical heterogeneity (sub-groups) within larger chemical groupings. Comparable results are observed at Malanjkhand, Bastar and Bundelkhand granitoids (Kumar and Rino, 2006; Hussain et al., 2004). The chemical compositional variations of basement rocks are used to determine the mineral phases that control the two steps. As for example, the decrease in FeO*, MgO, MnO with differentiation indicates crystallization of biotite and/or hornblende, while the decrease in CaO and Al_2O_3 shows crystallization of plagioclase and/or hornblende. The decrease of TiO_2 indicates the involvement of titanite as well as biotite and/or hornblende. The K_2O behavior indicates the involvement of K-feldspars in the evolution (Vaskovic et al., 2004) (Fig. II. 9). The observed major and trace element plots (Fig. II. 9 and Fig. II. 10) are also in agreement with general trends for fractional crystallization. The rocks are related to each other by a process of crystal fractionation, general major element trends as liquid lines of descent. The general decrease of the

Zr, P_2O_5, TiO_2 and V contents and the complex behavior of the immobile trace elements with differentiation were likely due to crystallization/removal of accessory minerals, such as apatite and zircon from the melt. Negative correlation between Y and SiO_2 observed for analyzed rocks (Fig. II. 10) may be due to the early crystallization of Ca-rich accessory phases such as apatite and titanite, which is consistent with the observed depletion in P_2O_5 with increasing SiO_2 (Kumar and Rino, 2006). Fractionation of plagioclase, in addition to hornblende, may have contributed to a trend of increasing Ba and Rb abundances from diorite to granite. Rb/Sr ratios are low (<1) and there is no systematic variation in K/Rb (187–527) with SiO_2 contents, broadly comparable to calc-alkaline suites elsewhere (e.g., Bertrend et al., 1984). Plagioclase contains Sr (and Eu) and any melt produced in the absence of residual plagioclase will be enriched in Sr contents.

The REE pattern remains fractionated in diorite but show a gradual decrease. The REE in granites may be indicative of feldspar accumulation and also show strongly fractionated of light REE over heavy REE. The REE patterns of dioritic rocks are smooth, inclined and parallel, indicating similar source of basement rocks. The REE patterns of the Bundelkhand and Bastar granitoids show flat trends with strong to insignificant Eu anomalies.

The multi-elemental spidergram of the basement rocks show marked enrichment in both LILE and HFSE in diorite but granites show high enrichment of LILE and a lesser abundance of HFSE. Similar patterns were observed in the granitoids of Bundelkhand and Bastar (Hussain et al., 2004). Such multi-elemental patterns are typical of subduction zone magmatism (Peacock,

1990; Saunders et al., 1991; Hawkesworth, 1994). The low contents of Hf (1.1–3.6 ppm) and Zr (47–147 ppm) relate with the patterns of syn- and post-collision granites (Kumar and Rino, 2006). Negative Nb anomalies are characteristic of the continental crust and may be an indicator of crustal involvement in magma processes (Rollinson, 1993).

The signatures of subduction zone magmatism were further disclosed in the tectonic discrimination diagrams especially in the Rb vs. (Y+Nb) of Pearce et al. (1984). All of the samples of the analyzed basement rocks plot within the volcanic arc granite field (Fig. II. 13). In addition, their high Zr/Y ratios (5.8–21.4) (Pearce, 1983) as well as their Th/Yb (0.9–48.7) versus Ta/Yb (0.3–3.1) ratios, and diagrams Th/Yb vs. Ta/Yb (Fig. II. 14a) and Th/Ta vs. Yb (Fig. II. 14b) are compatible with the geochemistry of rocks formed in a continental-margin setting or in a mature island arc (Gorton and Schandl, 2000). The Archaean gneisses and Proterozoic granitoids from Bundelkhand and Bastar show similar results (e.g. Hussain et al., 2004).

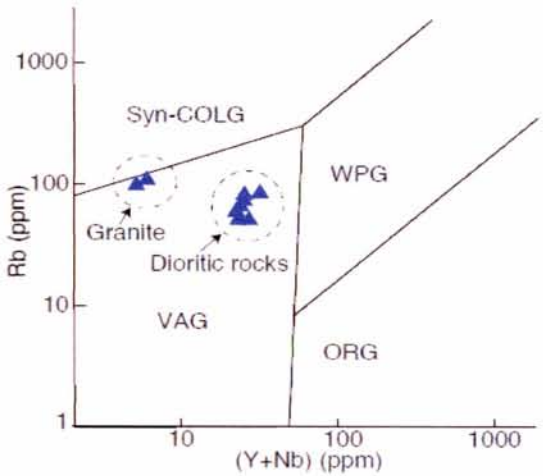

Fig. II. 13. Rb–(Y+Nb) discriminant diagram for the basement rocks in Bangladesh (Abbr., syn-COLG: syn-collision granite, VAG: volcanic arc granite, WPG: within plate granite, ORG: ocean ridge granite).

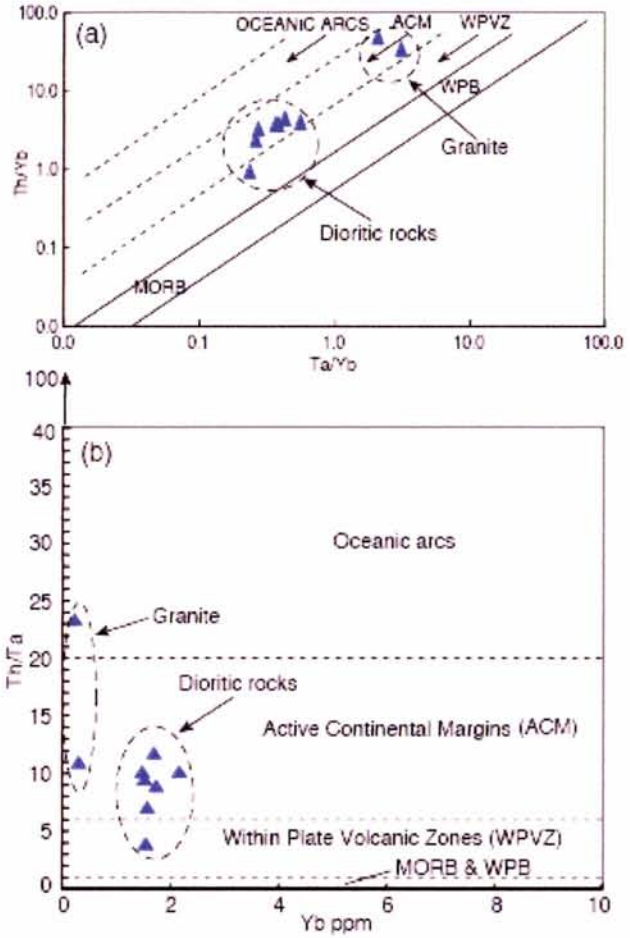

Fig. II. 14. Geodynamic setting of the ca. 1.73 Ga magmatic suite in Bangladesh, (a) Th/Yb vs. Ta/Yb and (b) Th/Ta vs. Yb diagrams of Gorton and Schandl (2000). (Abr., ACM: active continental margins and mature island arcs, WPVZ: within-plate volcanic zones, WPB: within-plate basalts, MORB: mid-oceanic ridge basalts).

II. 6.2. Magma source

Basement rocks in Bangladesh are most likely rocks to represent mantle-derived. The mafic magma is ultimately of mantle origin, which may interact with crustally derived granite melts to form hybrid calc-alkaline rocks (Atherton, 1993), producing very large bodies of granite (Castro et al., 1990). The appreciation of the interaction between contemporaneous mafic and felsic magma can also be viewed as the prime role of mafic magma generating heat energy, i.e.,

mafic magma underplating (Huppert and Sparks, 1988) and volatile supply (Whitney, 1988) to crustal-derived melts. The general view of magmatism in orogenic settings involves intrusion of mantle-derived magmas into the lower crust, remelting of the lower crust (underplated material and pre-existing older crust) to produce dioritic to granitic magmas, and evolution of both mantle- and crustal-derived magmas by fractional crystallization and/or magma-crust interaction (e.g., Annen et al., 2006; Kemp et al., 2007).

Neither pluton, however, has mafic rocks with primitive compositions (Ayuso and Arth, 1992). Values of elemental ratios characteristic of the basement rocks, for example, Ce/Pb=0.5–4.0, Nb/U=1.4–11.3, Rb/Cs=16–65 (abnormal value 133 in sample PL5), Ba/Ta=284–4563, La/Th=1.1–9.1 (abnormal value 25.4 in sample PL9), do not match those of N-type MORB (Ce/Pb=25, Nb/U=50, Rb/Cs=80, Ba/Ta=47, La/Th=21), or ocean island basalts (Ce/Pb=15–31, Nb/U=40–43, Rb/Cs= 70–90, Ba/Ta=130, La/Th=9) (Hofmann, 1988; Sun and McDough, 1989). However, the basement rocks approximate or overlap the range of some relevant ratios characteristic of orogenic andesites (Ce/Pb=2.2–4.8, Nb/U=1.1–6.7, Rb/Cs= ~ 25, Ba/Ta > 450, La/Th=2–7; Gill, 1981). The wide range and especially the high values for La/Yb ratio (16–53) in the pluton resemble the fractionated REE patterns found in andesites from thick continental margins (Thorpe et al., 1979; Bailey, 1981). The Rb/Sr ratio varies 0.06 to 0.14. The corresponding K/Rb ratios of analyzed basement rocks usually vary from 187 to 527; this range is typical of granitoid (Bertrand et al., 1984). Basement rocks can be eliminated as lower crustal components because they are all relatively depleted in Ta (0.4–1.0 ppm) compared to the

batholith (high values of (Hf+Th)/Ta=9.6–25.6) so that mixing of a mantle-derived magma (Ayuso and Arth, 1992). The relatively coherent correlation between Sr and Rb abundances is readily interpretable in term of fractional crystallization model and calculated mineral assemblage (Pl, 46% and Hbl, 54%) and compositions are summarized in Table II. 4.

The assemblage was estimated assuming a starting magma composition represented by the freshest, least evolved rock in the pluton, and using the Rayleigh fractionation or crystal surface-equilibrium model $C_L/C_o=F^{(D-1)}$ (Hanson, 1978), where C_L= concentration of a given elements in residual melt, C_o= concentration of element in the original melt, F= fraction of melt remaining, and D= bulk distribution coefficients are from the compilations of Arth (1976) and Fujimaki et al. (1984).

Fractionation models indicate that the variation in Rb and Sr abundances could well be explained by the predominance of plagioclase in the residue during the evolution of diorite (46% of the assemblage) but this estimate are only approximate. Fractionation of plagioclase, in addition to hornblende, may also have contributed to a trend of increasing Ba and Rb abundances from diorite to quartz monzonite. The processes of the evolution of the basement rocks are difficult to establish, though remarkably trace element variations plotted on compatible-incompatible elements diagrams are used to assess the relative importance of fractional crystallization and partial melting (e.g., McCarthy and Hasty, 1976; Hanson, 1978; Cocherie, 1986). Applications of mathematical approaches for geological variables still have uncertainty. As for example, the exact parental magma composition is generally difficult to

establish, and identification of the residual mineral assemblage is often imperfectly known. Moreover, appropriate partition coefficients as a function of magma evolution often are not available and the full range of compositions of possible contaminants as depth is rarely determined. We simply illustrate possible Rayleigh fractionation assemblage of hypothetical mafic parental magma and selected assimilation path as a means to explain at least some of the trace element variations. Accordingly, it is first necessary to establish the composition and affinities of the mafic rocks of the pluton. The bulk of the evidence presented here also indicates that although fractional crystallization was an important mechanism controlling the evolution of the pluton, a simple fractionation model cannot explain many of the incompatible trace element variations. For example, Cs, Pb, light REE etc., and high and variable ratios of Rb/Cs (2–53), Th/Ta (1–4.4), Th/Yb (34–49), all suggest extensive contributions of crustal components, either as crustal melts or assimilates. Model parameters assumed a parent magma (sample PL9) containing Rb= 50 ppm, Th= 1.45 ppm, Ta= 0.37 ppm and Co= 114 ppm and sample C2 considered a representative contaminant, shows SiO_2= 58 %, Rb= 64 ppm, Th= 5.59 ppm, Ta= 0.59 ppm and Co= 100 ppm. Estimates of the ratios of mass assimilated to mass fractionated are generally <0.5 and the bulk of the variations is explained by reasonable extents of crystallization (<80%); results for a lower ratio of mass assimilated to mass fractionated, R= 0.3, are also shown in Table II. 5.

Table II. 4. Fractional crystallization models for basement rocks.

		Parent	Fractional crystallization			
Elements	D	PL9	FC 20	FC 40	FC 60	FC 80
Rb	0.2	50	60	75	104	182
Sr	1.03	812	807	800	790	774
Ba	0.34	1047	1213	1466	1915	3024
K_2O	0.63	2.08	2.26	2.51	2.92	3.76
Ce	0.53	76.4	85	97	118	164
Nd	0.81	34.5	36	38.1	41.2	47.2
Eu	1.38	1.97	1.81	1.62	1.39	1.07
Yb	0.97	1.56	1.57	1.59	1.61	1.64
Lu	0.92	0.231	0.235	0.24	0.248	0.263
Y	0.6	18.1	19.8	22.2	26.2	34.6
TiO_2	0.89	0.913	0.935	0.964	1.004	1.008
Zr	0.31	79	92	112	148	239
Hf	0.31	2.1	2.4	3	3.9	6.3
Nb	0.47	5.1	5.7	6.7	8.3	11.9
Th	0.3	1.45	1.7	2.1	2.8	4.5
U	0.06	0.45	0.55	0.73	1.06	2
Co	1.17	114	110	105	98	87

Table II. 5. Assimilation-fractional crystallization models for basement rocks.

			Assimilation-fractional crystallization R= 0.3					Assimilation-fractional crystallization R= 0.5			
		Parent	Contaminant								
Elements	D	PL9	C2	20	40	60	80	20	40	60	80
Rb	0.2	50	64	65	89	131	238	72	106	164	301
Sr	1.03	812	874	824	837	854	877	832	853	874	895
Ba	0.34	1047	779	1253	1556	2066	3225	1304	1664	2230	3384
K_2O	0.63	2.08	1.92	2.31	2.61	3.1	3.87	2.38	2.74	3.2	3.88
Ce	0.53	76.4	73.1	88	104	128	176	92	111	138	183
Nd	0.85	34.5	31.7	36.4	38.8	41.9	46.7	37.3	40.4	43.8	47.8
Eu	1.38	1.97	1.66	1.73	1.49	1.24	1	1.64	1.36	1.15	1.01
Yb	0.97	1.56	1.53	1.57	1.59	1.6	1.63	1.57	1.59	1.6	1.62
Lu	0.92	0.231	0.226	0.236	0.242	0.25	0.261	0.237	0.244	0.251	0.259
Y	0.6	18.1	17.8	20.4	23.6	28.2	36.8	21.2	25.1	30.1	37.9
TiO_2	0.89	0.913	0.709	0.924	0.938	0.955	0.981	0.911	0.909	0.907	0.906
Zr	0.31	79	147	104	142	206	356	120	179	272	470
Hf	0.31	2.1	3.6	2.7	3.7	5.3	9.1	3.1	4.6	6.9	11.8
Nb	0.47	5.1	6.1	6.1	7.5	9.7	14.2	6.5	8.4	11.1	15.9
Th	0.3	1.45	5.59	2.22	3.37	5.35	10.03	2.89	4.96	8.32	15.5
U	0.06	0.45	1.43	0.7	1.12	1.91	4.19	0.9	1.62	3.01	6.89
Co	1.17	114	100	107	100	91	81	104	95	86	79

The Hf–Th–Ta diagram further illustrates variations in incompatible element contents in the pluton (Fig. II. 15). The relatively decreasing content of Hf compared to Th and Ta is best attributed to the combined effects of fractionation of a mantle-derived magma coupled with progressive magma mixing and contamination with heterogenous lower crust to produce the least

evolved pluton.

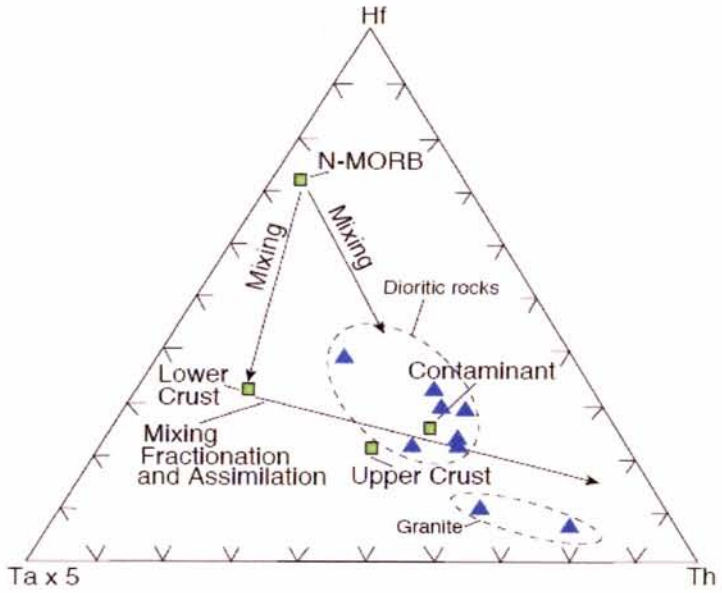

Fig. II. 15. Plot of Hf–Ta x 5–Th. Diagram illustrates the main trend from dioritic to granitic rocks in the Maddhapara, Bangladesh. The compositions of N-type MORB (Sun and McDonough, 1989), average lower and upper crust (Taylor and McLennan, 1985) and potential lower crustal components are shown for comparison (Ayuso and Arth, 1992). Mixing trends between mantle-derived magma and average lower crust are thought to have initiated the evolution. The main trend reflects the effects of fractional crystallization, mixing with Th-enriched crustal melts, and assimilation.

Fractional crystallization estimates have not indicated an important role for garnet in the residue of the pluton, a result in agreement with its evolution in the mid-continental crust, similar results reported our hornblende thermobarometric data (Hossain et al., 2008b). During magmatic differentiation by crystal fractionation, from originally low-volatile silicate melts (yielding normal plutonic rocks), through hydrous silicate melts (yielding pegmatites), to late-stage water-rich fluids (yielding quartz veins), the composition of the residual liquid changes drastically (Roedder, 1992).

The overall enrichment in Th in the main trend of the pluton, from diorites to granites, is

thought to represent a wide variety of interactions with crustal components, and especially the combined effects of assimilation-fractional crystallization (AFC) (Fig. II. 16).

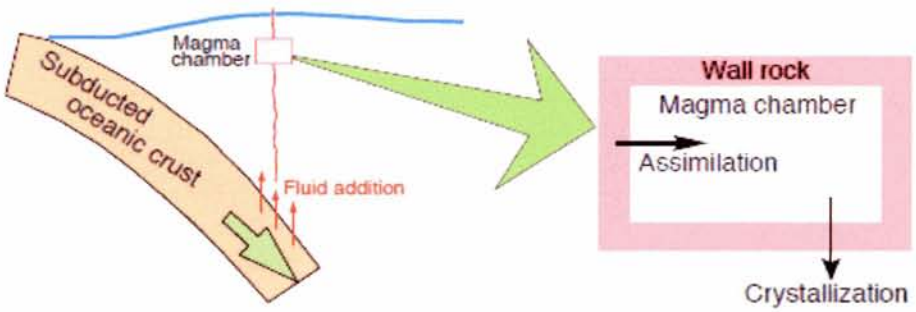

Fig. II. 16. Cartoon for subduction zone and magma chamber at crustal depths. Mass and chemical composition of magma chamber vary due to assimilation and crystallization.

We conclude that it is possible that magmas generated deeper in the crust had a larger component of mantle-derived melt (e.g. diorite), and magma generated higher in the mid-crust contained a larger contribution of sialic material (e.g., Quartz monzonite, granite). High Sr/Y ratio implies partial melting of a basaltic source in a high P_{H2O} environment. This also corresponds to a subduction zone environment (Hussain et al., 2004).

II. 6.3. Magmatism and tectonic evolution during the Columbia supercontinent amalgamation

The bulk of the chemical features of basement rocks thus resemble those of igneous rocks generated in continental arcs where the crust has reached substantial maturity (Brown, 1982; Stephens and Halliday, 1984). Recently Hossain et al. (2007) recognized that 1.7 Ga

Palaeoproterozoic age of the Maddhapara basement rocks and found relationship with the CITZ and Meghalaya-Shillong Plateau in Indian Shield. The CITZ is a complex orogenic belt that has amalgamated the southern Deccan Protocontinent with the northern Buldelkhand Proto-continent in the Proterozoic. The CITZ is bounded to the north by the Son–Normada North Fault (SNNF) and to the south by the Central Indian Shear Zone (CISZ). The CITZ links up with the Chhotonagpur Gneiss in the east, then subsurface Palaeoproterozoic Maddhapara basement rocks continues into Meghalaya plateau (Hossain et al., 2007).

Geographically the CITZ represents a mobile belt of collaged terranes, with a collage of stable crustal blocks and intervening weaker zones of suturing, or remnants of Archaean greenstone belts of rift setting, tectonic zones and magmatic arcs or an aborted rift with mantle activated volcanics (Jain et al., 1995; Acharyya, 1997). The narrow northern belt represents the collapsed early Proterozoic Mahakoshal rift zone, Northern Structural Belt of CITZ which develops into a fold belt and is presently confined to the Son–Narmada (SONA) lineament, which is extended over the alluvial covered Ganga plains and the Bengal Basin to the northeast India as the Brahmaputra lineament (Sen, 1991). The Son–Narmada (SONA) bounded by two major Moho reaching faults (basement fault), the Son-Narmada North Fault (SNNF) and the Son–Narmada South Fault/Shear Zone (SNSF) (Acharyya, 2003). The Deccan Trap covers the western extension of the CITZ, although its northern limiting Narmada lineament can be recognized by the Bouguer gravity anomaly pattern (NGRI, 1978). The Mahakoshal Belt extends without any break from the central to the eastern sectors of the CITZ (Fig. II. 1). The Belt shows

consistent calc-alkaline rocks with present study area, as for examples, calc-alkaline granitoids at Rihand-Renusagar (1.73 Ga), monzodiorite, quartz-syenite at Jhirgadandi (1.75 Ga), syenites at Bori (1.8 Ga) and granite at Barambaba (2.05 Ga), which occur to the north and south of the belt (Sarkar et al., 1998; Roy and Devrajan, 2000). Furthermore, similar precedent Betul Granitoid compositions include tonalite, trondhjemite, granodiorite, quartz-monzonite and granite (Roy et al., 2000). Incredibly recent recognition of mafic/ultramafic magmatism associated with concomitant intra-continental rifting of a Palaeoproterozoic (1891-1883 Ma) large igneous province in the southern Bastar craton and nearby Cuddapah basin from the adjacent Dharwar craton, India followed instinctive trend, and conferred ample justification for sequential growth or accretion of the continent in this region (French et al., 2007; Anand et al., 2003). Yedekar et al. (1990) suggested the time frame for the tectonic activities in the Central Indian Suture (CIS). The oceanic crust between two blocks namely the Bundelkhand craton towards the north and the Bastar craton towards the south started subducting ca. 2.3 Ga. The plutonic activities of calc-alkaline magmatism started almost at the same time giving rise to Malanjkhand and Dongargarh plutons, subsequently ca 2.1 Ga, the Sakoli and the Nandgaon volcanics formed the island arc over the southern block. The collision of the two blocks took place ca. 2.1 to 1.7 Ga and CIS formed. A Palaeoproterozoic deposition age (ca. 1750 Ma) is inferred from the age of a metarhyolite associated with the sediments in the eastern Himalaya, Bhutan (Richards et al., 2006). Towards the northeast, Ghosh et al. (1991, 1994) reported ages as old as 1.7 Ga for basement granitic gneisses from the Meghalaya plateau.

The extensive study of the Palaeoproterozoic crust of the Transamazonian of South America between 2.5–2.0 Ga has identified the sequential growth of the continent through the amalgamation of juvenile terrains, succeeded by a major collisional orogeny (Hartmann, 2004). Similar studies in the ice-covered interior of the East Antarctic shield in exposed basement of the Transantarctic Mountains and Wilkes Land margin suggest correlation with Palaeoproterozoic granitoid rocks and Mesoproterozoic mafic igneous rocks from the Gawler and Curnamona cratons of Australia (Oliver and Fanning, 1997; Peucat et al., 1999; Goodge et al., 2001; Peucat et al., 2002). Subduction-related batholiths between approximately 1.7 and 1.6 Ga in the Albany-Fraser belt in Australia (Nelson et al., 1995) have similar counterparts in the Windmill islands and Bunger Hills in Antarctica, suggesting attachments in pre-drift configuration (Harris, 1995). This type of magmatism is also common in Bohemian Massif, Poland, where the dioritic-tonalitic magmas were in fact derived from ~1.9±0.1 Ga mafic crust, suggesting that such crust was actively contributing to magmatism in the Palaeoproterozoic supercontinent and should be taken into account in geochemical models of basement rocks evolution (Pietranik and Weight, 2008).

The above summary of geochronological information with detailed field investigation, petrography, mineral chemistry and geochemistry of Maddhapara basement rocks suggesting arc-related subduction magmatic activity at ~1.7 Ga, which is consistent with tectonic events of CITZ, Bohemian Massif as well as the Svecofennian (Wiszniewska et al., 2007; Andersson et al., 2006) and others global-scale Palaeoproterozoic magmatic activities.

CHAPTER III

Geothermobarometry and fluid inclusions of dioritic rocks in Bangladesh: Implications for emplacement depth and exhumation rate

This chapter has been published in Journal of Asian Earth Sciences (2008)

(DOI: 10.1016/j.jseaes.2008.10.010)

Abstract

Application of hornblende thermobarometry and fluid inclusion studies to the Palaeoproterozoic (1.7 Ga) basement rocks from Maddhapara, NW Bangladesh, provide information on the pressure and temperature (*P–T*) conditions of crystallization, the emplacement depth and composition of magmatic fluid. The basement rocks are predominantly diorite or quartz diorite with a mineral assemblage of plagioclase, hornblende, biotite, quartz, K-feldspar, titanite, and secondary epidote and chlorite. The calculated *P–T* conditions of the dioritic rocks are 680–725°C and 4.9–6.4 kbar, which probably correspond to crystallization conditions. Fluid inclusion studies suggest that low- to medium-salinity (0–6.4 wt.% $NaCl_{eq}$) H_2O-rich fluids are trapped during the crystallization of quartz and plagioclase. The isochore range calculated for primary aqueous inclusions is consistent with the *P–T* condition obtained by geothermobarometry. The basement rocks likely crystallized at a depth of ~17–22 km, with a minimum average exhumation rate of ~12–15 m/Ma during Palaeoproterozoic to Lopingian time. Such slow exhumation indicates low relief continental shield surface during this period.

III. 1. Introduction

Recent geochronological investigations on basement rocks in the northwestern part of Bangladesh indicate that Palaeoproterozoic (1.72–1.73 Ga; Ameen et al., 2007; Hossain et al., 2007) tonalitic to dioritic rocks, regarded as a continuation of the Central Indian Tectonic Zone in the Columbia supercontinent configuration (Hossain et al., 2007), occur in the Maddhapara

area at a shallow depth (128 m) from the surface. The overlying cover consists of successive units of the Permian Gondwana Group, Pliocene Dupi Tila Formation, Pleistocene Barind Clay Formation and recent alluvium (Fig. III. 1). Although several petrological and geochemical studies on the basement rocks are available (e.g., Ameen et al., 1998; Kabir et al., 2001; Zaman et al., 2001, 2002; Hossain et al., 2008a), no systematic mineralogic, geothermobarometric, and fluid inclusion data have so far been reported from these rocks except for our recent preliminary fluid inclusion study of pegmatite and aplite veins (Hossain and Tsunogae, 2008).

Geothermobarometric studies coupled with fluid inclusion studies are important tools for the estimation of pressure and temperature (*P–T*) conditions of crystallization of igneous rocks (e.g., Anderson and Smith, 1995; Tulloch and Challis, 2000; Zhang et al., 2006; Mishra et al., 2007; Hossain and Tsunogae, 2008). In this study, we apply hornblende thermobarometry to the dioritic rocks from Maddhapara area in northwestern Bangladesh to estimate their *P–T* conditions of crystallization. Microthermometric investigations of trapped fluid inclusions were also carried out to confirm the pressure estimates and to determine the composition of magmatic fluids. We further estimate the emplacement depth of dioritic rocks using the *P–T* and fluid inclusion data, which offer direct evidence for the exhumation history of basement rocks through time.

III. 2. Geologic setting

Bengal Basin, which occupies a major part of Bangladesh, is a composite sedimentary

basin between the Peninsular Indian shield and Shillong massif (Fig. III. 1). It is located near the junction of Indian and Eurasian plates, and Burmese sub-plate. Khan (1991) first reported the discovery of subsurface basement rocks (granitic gneiss) at Kuchma, Bogra at a depth of 2150 m. Microcline-rich granite, quartz diorite, syenite and quartz monzonite as well as minor metamorphosed rocks such as mica schist/gneiss and hornblende bearing quartz-feldspathic gneiss were also reported from several localities such as the Barapukuria basin (Dinajpur), Badargong, Pirganj, and Mithapukur areas (Rangpur district) (Khan, 1991; Hussain and Curtin, 1995; Uddin et al., 2005). In Maddhapara area, the basement rocks occur at a shallow depth of 128 m. The rocks are mostly fresh and show no significant effect of later hydrothermal alteration, although some altered granitic rocks occur locally. They are sometimes cut by later granitic pegmatite (up to ~50 cm), aplite, and quartz veins. The basement rocks in Maddhapara are unconformably overlain by thin sedimentary cover of Permian Gondwana fluvial sediments (Khan and Chouhan, 1996), which is assumed to be of Lopingian (Late Permian) age (~0.26 Ga; ICS, 2004). Although there is no available isotopic age data from the Gondwana fluvial sediments in Bangladesh, Islam et al. (2003) reported Late Permian age from Barapukuria Gondwana coal, in the vicinity of the present study area, based on the presence of miospore genera (e.g., *Protohaploxypinus, Striatopodocarpites, Striatites, Vittatina*, etc.).

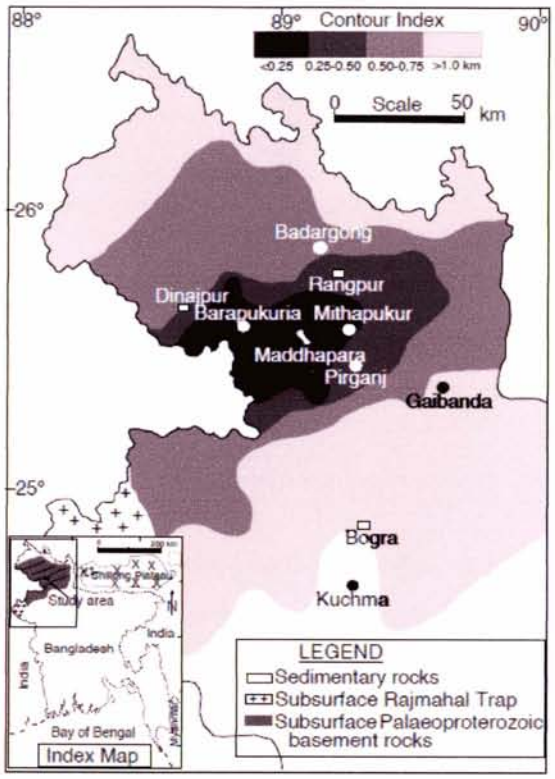

Fig. III. 1. Location map of the Maddhapara basement rocks in Bangladesh showing probable depth of the rocks (modified from Khan, 1991; Hossain et al., 2007). Contour index indicates depth variations of basement rocks from the surface.

III. 3. Petrography

The main plutonic body at Maddhapara consists predominantly of diorite and quartz diorite. Most of the dioritic rock samples were collected from underground tunnel (300 m depth) and sub-level (270 m depth) mining site during detailed underground observations. The dioritic rocks consist of medium- to coarse-grained plagioclase (42–61%), hornblende (19–53%), biotite (1–8%), quartz (1–7%), K-feldspar (1–10%), and titanite (<1%) with accessory epidote, pyrite, chalcopyrite, zircon, and apatite (Fig. III. 2a). Epidote often replaces hornblende and biotite. Plagioclase and biotite are partly altered to sericite and chlorite, respectively.

The dioritic rocks are subdivided into two types; undeformed diorite with large (up to a few mm) subhedral plagioclase (Type 1) and slightly recrystallized and/or mylonitized diorite (Type 2). Samples P14, P15 and P10 are typical examples of Type 1 dioritic rock (Fig. III. 2b). They do not show any evidence of later deformation or recrystallization. Sample P8 (Type 2) also contains subhedral grains of plagioclase and hornblende, but it shows weak foliation and the mineral grains are surrounded by aggregates of fine-grained (<0.3 mm) quartz and biotite (Fig. III. 2d). The fine-grained minerals show wavy extinction (Fig. 2c), probably due to later deformation during uplift. They exhibit deformation textures such as lineation and/or foliation, bending of twin planes, etc. (Fig. III. 2d). Some mylonitic samples (e.g., sample P39) were also collected from fractured zones within dioritic rocks, but their occurrence is restricted along local faults.

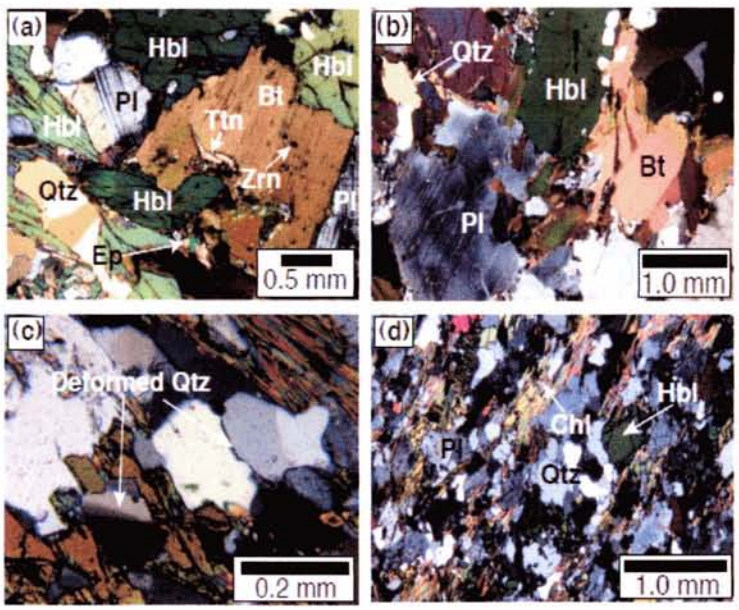

Fig. III. 2. Microphotographs showing representative texture of dioritic rocks. (a) Mineral assemblage and petrographic relationship among hornblende (Hbl), plagioclase (Pl), quartz (Qtz), biotite (Bt), titanite (Ttn), epidote (Ep) and zircon (Zrn) (Type 1), (b) Undeformed diorite (Type 1, sample P10), (c) Wavy extinction in quartz in the Type 2 diorite (sample P8). (d) Internal deformation structures and textures and the occurrence of secondary chlorite

(Chl) in Type 2 diorite.

III. 4. Mineral chemistry

III. 4.1. Analytical methods

Chemical analyses of minerals in dioritic rocks were carried out by electron microprobe analyzer (JEOL JXA-8621) at the Chemical Analysis Division of the Research Facility Center for Science and Technology, the University of Tsukuba, Japan. The analyses were performed under conditions of 20 kV accelerating voltage and 10 nA sample current, and the data regressed using an oxide-ZAF correction program supplied by JEOL. The results of representative analysis of minerals are given in Tables III. 1 and III. 2. Structural formula of amphiboles was calculated based on 23 oxygen and 13 or 15 cations, and partitioning of Fe^{3+} and Fe^{2+} from total iron were calculated following the method outlined by Schumacher (1997).

III. 4.2. Results

III. 4.2.1. Calcic amphiboles

Calcic amphibole in the examined dioritic rocks has a wide compositional variation in X_{Mg} (Mg/(Fe+Mg) = 0.53–0.63), $(Na+K)^A$ (0.40–0.57 pfu), Si (6.41–6.71 pfu), and $Fe^{3+}/(Fe^{2+}+Fe^{3+})$ (0.20–0.34). Most of the amphiboles of the present study are compositionally magnesiohornblende based of the classification of Leake et al. (1997), while some pargasite, magnesiohastingsite, edenite, and tschermakite are also present (Fig. III. 3). The compositional variations mentioned above reflect the slight proportion of tschermakitic, pargasitic, and edenitic

substitutions as a consequence of net-transfer reactions and exchange equilibria, and is often reported for calcic amphiboles from mafic and intermediate rocks (e.g., Hammarstrom and Zen 1986; Hollister et al., 1987; Johnson and Rutherford, 1989). Slight compositional zoning can be seen for coarse-grained amphibole in terms of $(Na+K)^A$; the value decreases slightly from rim (0.52–0.57 pfu) to core (0.40–0.49 pfu), although their X_{Mg} is consistent (0.51–0.52, sample P10). Amphibole composition also varies depending on coexisting minerals; amphiboles with biotite generally show lower $(Na+K)^A$ values (0.52–0.55 pfu) than those associated with plagioclase (0.55–0.57 pfu).

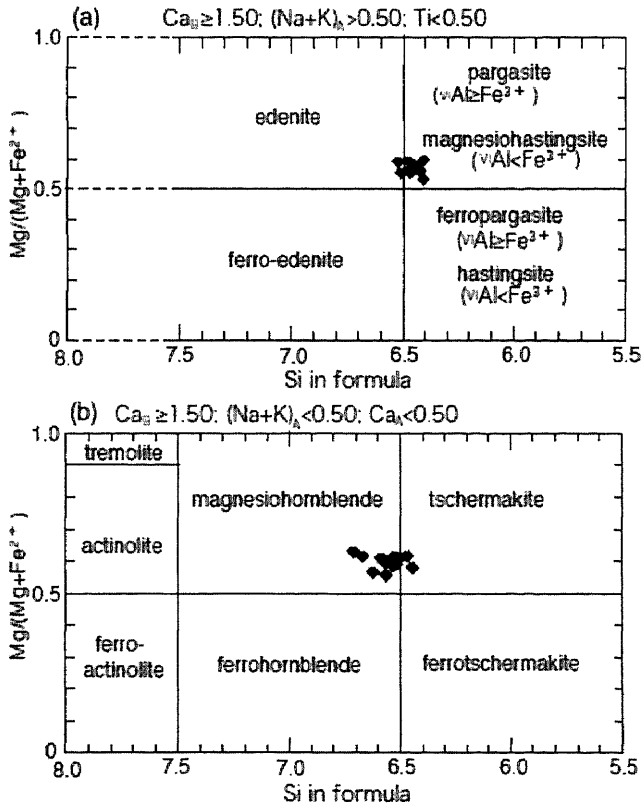

Fig. III. 3. Classification of amphiboles from dioritic rocks according to the nomenclature of Leake et al. (1997).

III. 4.2.2. Feldspars

Table III. 2 provides representative microprobe analyses of plagioclase coexisting with calcic amphiboles. Plagioclase shows a wide compositional range of An_{21-42} (oligoclase to andesine) with ~1% orthoclase component. Rim of plagioclase (An_{21-36}) generally shows lower anorthite content than core (An_{32-42}) for all samples. K-feldspar in dioritic rocks shows a uniform orthoclase-rich composition in all samples (Or_{91-95} Ab_{4-9}).

Table III. 2 Representative plagioclase compositions of the dioritic rocks.

Sample Name	SL3	PLS1	PLS3	PLS3	PLS12	P10	P10	P28
	Rim	Rim	Rim	Core	Rim	Rim	Core	Rim
SiO_2	58.42	58.11	58.32	59.22	60.58	60.23	59.41	58.71
Al_2O_3	25.40	25.41	25.29	25.75	24.93	24.22	25.25	25.30
CaO	7.30	7.31	7.04	7.24	6.16	5.75	6.67	6.91
Na_2O	7.02	7.60	7.41	7.64	8.06	8.31	8.13	8.16
K_2O	0.18	0.09	0.16	0.14	0.13	0.10	0.11	0.06
Total	98.31	98.52	98.22	99.99	99.85	98.62	99.57	99.14
Number of ions on the basis of 8 oxygens								
Si	2.649	2.636	2.648	2.644	2.697	2.714	2.662	2.646
Al	1.357	1.358	1.353	1.355	1.308	1.286	1.333	1.344
Ca	0.354	0.355	0.342	0.346	0.294	0.278	0.320	0.334
Na	0.616	0.668	0.652	0.661	0.695	0.725	0.706	0.712
K	0.010	0.005	0.009	0.008	0.007	0.006	0.006	0.004
Total	4.986	5.022	5.004	5.014	5.001	5.009	5.027	5.040
An%	36.1	34.5	34.6	34.1	29.5	27.5	31.0	31.8
Ab%	62.8	65.0	64.4	65.1	69.8	71.9	68.4	67.9
Or%	1.1	0.5	1.0	0.8	0.7	0.6	0.6	0.3

III. 4.2.3. Other minerals

Biotite in dioritic rocks is Mg-rich (X_{Mg} = 0.52–0.59). Its Ti content is low (1.3–2.6 wt.% TiO_2) and increases slightly with decreasing X_{Mg}. Composition of epidote is close to the ideal chemical formula of $Ca_2Fe^{3+}Al_2Si_3O_{12}(OH)$. No compositional zoning has been identified within

individual grains, although it commonly shows optical zoning patterns. Chemical composition of titanite is also close to the ideal formula of $CaTiSiO_5$, but it contains minor Fe_2O_3, 0.9–1.2 wt.%.

III. 5. Geothermobarometry

Eight samples of dioritic rock were selected for geothermobarometric study. Numerous computations of *P–T* conditions for amphibole crystallization have been proposed (e.g., Blundy and Holland, 1990; Holland and Blundy, 1994; Anderson and Smith, 1995; Anderson, 1996; Ague, 1997), reflecting an increasingly quantitative thermodynamic data base; nevertheless, solid–solution and activity models remain somewhat problematic. For *P–T* calculations, measurements were carried out on rims of coexisting hornblende and plagioclase, which are in contact with quartz and/or K-feldspar – an important prerequisite for application of aluminum-in-hornblende barometry (Stein and Dietl, 2001).

III. 5.1. Al-in-hornblende barometry

Hammarstrom and Zen (1986) and Hollister et al. (1987) suggested that, in the presence of an appropriate buffer assemblage (amphibole + plagioclase + K-feldspar/quartz, at medium to high oxygen fugacity conditions), the total Al content of calcic amphibole increases linearly with pressure of crystallization. Subsequent field-based and experimental studies (e.g., Johnson and Rutherford, 1989; Schmidt, 1992; Rutter et al., 1989; Anderson and Smith, 1995) provided

general confirmation of increasing Al content of hornblende with increasing pressure. In the last two decades, Al-in-hornblende barometry has been widely used to calculate pressures of magmatic crystallization, and to constrain the emplacement depths of batholiths or vertical displacements of crust (e.g., Ague and Brandon, 1992, 1996; Anderson and Smith, 1995; Stein and Dietl, 2001; Zhang et al., 2006). In this study, we have chosen the calibration of Anderson and Smith (1995) to calculate the crystallization pressures of the investigated dioritic rocks, as this calibration is more reliable for considering the influence of temperature and oxygen fugacity on the pressure calculation than the other methods (e.g., Zhang et al., 2006; Stein and Dietl, 2001). The results yielded a pressure range of 4.9–6.4 kbar at 680–725°C (Table III. 1). This is nearly consistent with the ranges obtained by the methods of Hammarstrom and Zen (1986) (4.5–6.4 kbar) and Johnson and Rutherford (1989) (3.7–5.2 kbar), with slightly higher pressure estimates obtained by the methods of Hollister et al. (1987) (4.7–6.8 kbar) and Schmidt (1992) (5.0–6.7 kbar).

III. 5.2. Hornblende-plagioclase thermometer

As hornblende and plagioclase commonly coexist in calc-alkaline igneous rocks, they have been used for thermometry (Blundy and Holland, 1990; Holland and Blundy, 1994). Based on hornblende solid-solution models and well-constrained natural and experimental studies, two geothermometers were calculated by Holland and Blundy (1994) based on the edenite–tremolite reaction (edenite + 4 quartz = tremolite + albite), which is applicable to quartz-bearing igneous

rocks, and edenite–richterite reaction (edenite + albite = richterite + anorthite), which is applicable to both quartz-bearing and quartz-free igneous rocks (Holland and Blundy, 1994; Stein and Dietl, 2001). On the basis of an assessment of the different Al-in-hornblende thermometric algorithms on data from plutonic rocks, Anderson (1996) concluded that edenite–richterite thermometer is the most reliable calibration. Therefore, we used edenite–richterite thermometer to calculate the temperature of crystallization of the basement rocks. The calculated results are 680–725°C (Table III. 1).

Table III. 1 Representative hornblende microprobe analyses from the dioritic rocks and calculated thermobarometric results.

Sample Name	PLS3	PLS12	SL3	PLS1	P10	P28
Wt.%						
SiO_2	42.83	43.72	44.80	42.35	43.25	42.96
TiO_2	1.00	0.85	0.60	0.66	0.82	0.83
Al_2O_3	10.61	10.41	9.51	11.49	10.39	11.01
FeO	17.35	16.84	15.64	16.46	17.52	17.89
MnO	0.38	0.35	0.43	0.39	0.35	0.40
MgO	10.25	10.39	11.29	10.36	10.16	9.73
CaO	11.69	11.38	11.71	11.86	11.70	11.83
Na_2O	1.34	1.31	1.21	1.33	1.06	1.29
K_2O	1.36	1.24	0.86	1.33	1.09	1.25
Total	96.81	96.47	96.05	96.24	96.35	97.19
Formulae per Holland and Blundy (1994)						
T-sites						
Si	6.459	6.583	6.716	6.399	6.521	6.462
Al^{iv}	1.541	1.417	1.284	1.601	1.479	1.538
Sum T	8.000	8.000	8.000	8.000	8.000	8.000
M1,2,3 sites						
Al^{vi}	0.345	0.431	0.397	0.446	0.368	0.414
Ti	0.113	0.096	0.068	0.075	0.093	0.094
Fe^{3+}	0.542	0.455	0.470	0.551	0.630	0.527
Mg	2.304	2.331	2.522	2.333	2.283	2.181
Mn	0.049	0.045	0.055	0.050	0.045	0.051
Fe^{2+}	1.646	1.642	1.489	1.529	1.580	1.723
Ca	0.002	0.000	0.000	0.016	0.002	0.010
Sum M1,2,3	5.000	5.000	5.000	5.000	5.000	5.000
M4 sites						
Fe	0.000	0.023	0.002	0.000	0.000	0.000
Ca	1.887	1.836	1.881	1.904	1.888	1.897
Na	0.113	0.141	0.117	0.096	0.112	0.103
Sum M4	2.000	2.000	2.000	2.000	2.000	2.000
A sites						
Ca	0.000	0.000	0.000	0.000	0.000	0.000
Na	0.279	0.242	0.235	0.294	0.198	0.273
K	0.262	0.238	0.164	0.256	0.210	0.240
Sum A	0.541	0.480	0.399	0.550	0.408	0.513
Sum_cat	15.541	15.480	15.399	15.550	15.408	15.513
Al (Total)	1.886	1.848	1.681	2.047	1.847	1.952
Thermobarometric Results						
T (ed-tr) (°C)	744	682	697	725	697	714
T (ed-ri) (°C)	**723**	**684**	**684**	**700**	**679**	**693**
P-Sch (kbar)	5.97	5.79	4.99	6.73	5.78	6.28
P-J&R (kbar)	4.53	4.37	3.67	5.22	4.37	4.82
P-A&S (kbar)	**5.27**	**5.68**	**4.89**	**6.37**	**5.73**	**6.05**
Depth (km)	**17.9**	**19.3**	**16.6**	**21.6**	**19.5**	**20.6**

III. 6. Fluid inclusions

Five samples of dioritic rocks (P8, P10, P14, P15, and P39) were selected for fluid inclusion study. Samples P14, P15, and P10 correspond to undeformed diorite (Type 1) with

medium- to coarse-grained plagioclase and quartz. Slightly recrystallized diorite (sample P8) and mylonitic diorite (sample P39) (Type 2) were also examined for comparison. Doubly polished thin wafers (~120–150 μm thick) of the rocks were prepared for petrographic and microthermometric studies of fluid inclusions.

III. 6.1. Petrography

Fluid inclusions are generally rare in the dioritic rocks, although they are abundant in the associated pegmatite and aplite veins (Hossain and Tsunogae, 2008). Although they are mostly very small (less than a few microns in size) in both Type 1 and Type 2 rocks, some large fluid inclusions suitable for microthermometric measurements are present in quartz and rarely in plagioclase. It is generally known that feldspars have a better capacity of retaining early fluids as the mineral is more rigid than quartz (cf., Touret, 1987). Rare fluid inclusions are also found in quartz and plagioclase inclusions in hornblendes in Type 2 rocks.

Based on the occurrence, fluid inclusions in the examined samples are classified into three types: primary, pseudosecondary, and secondary (cf., Roedder, 1984). As most inclusions discussed in this study occur as isolated aggregates or local clusters formed away from the grain margins of quartz and plagioclase (Figs. III. 4a, b, and c), they are regarded as primary fluid inclusions that were probably trapped during the crystallization of the host minerals (quartz and plagioclase). Rare fluid inclusions in quartz and plagioclase within hornblende are also regarded to be primary as the inclusions were probably trapped before the crystallization of the host

hornblende. As plagioclase and quartz in Type 1 diorites show no evidence of later deformation and/or recrystallization, primary fluid inclusions in the minerals were probably trapped during the crystallization of host minerals, and they may still preserve initial magmatic fluids.

Primary fluid inclusions are also present within quartz and plagioclase grains in Type 2 diorites as well as Type 1 rocks. Although there is no significant difference in size, shape, and occurrences of primary inclusions between Type 1 and Type 2 rocks, microthermometric data of Type 2 rocks are discussed separately as the latter inclusions might have undergone significant fluid density and composition modification due to later deformation and/or recrystallization.

Secondary inclusions are typically located within healed fractures that intersect the host-crystal boundaries (Fig. III. 4d) probably formed after the crystallization of the mineral. Such inclusions are very small and not suitable for microthermometric measurements. In contrast, pseudosecondary inclusions are formed along micro cracks that develop during the partial growth of the crystal and form arrays that pinch out within the grains.

As discussed below, all the fluid inclusions are H_2O-rich. They are mostly two-phase liquid + vapor inclusions at room temperature, with the occurrence of rare multiphase liquid + vapor + solid (mainly liquid-rich) inclusions. The latter inclusions are present only in quartz and contain one or more solid phases that disappear during heating experiments. All the solids within the fluid inclusion cavities are therefore considered as daughter minerals. The cubic habit and the similar index of refraction as the host quartz suggest that the daughter minerals are probably halite crystals.

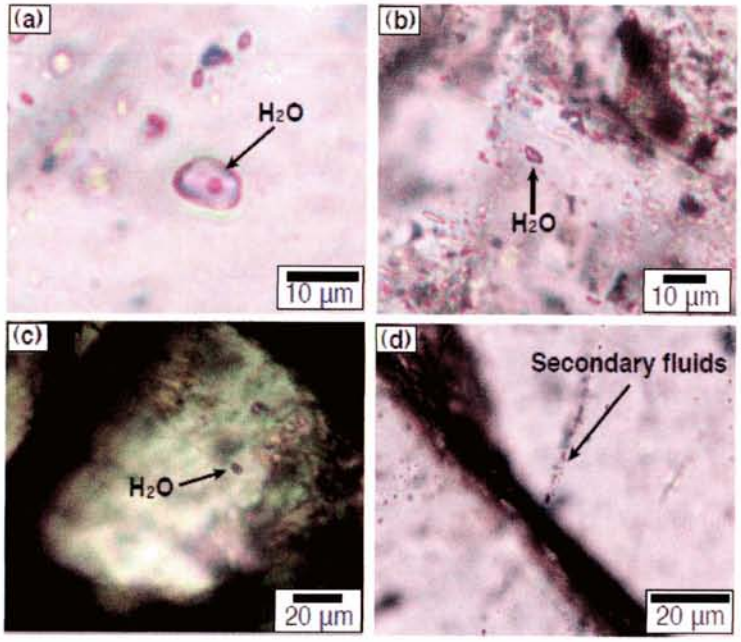

Fig. III. 4. Photomicrographs of representative fluid inclusions in Type 1 dioritic rocks discussed in this study. Isolated primary aqueous fluid inclusions in (a) quartz (sample P14), and (b) plagioclase (sample P10). (c) Primary aqueous fluid inclusions in plagioclase inclusion in hornblende (sample P14). (d) Trails of very small secondary (indicated by arrow) fluid inclusions (sample P10), which are not suitable for microthermometric measurements.

III. 6.2. Microthermometry

III. 6.2.1. Analytical methods

Microthermometric measurements of the fluid inclusions were performed with a Linkam heating/freezing system at the University of Tsukuba, Japan. Calibration was performed using synthetic standard materials supplied by Fluid Inc., Denver, at 0°C (triple point of H_2O) and at 374.1°C (critical point of pure H_2O with a density of 0.317 g/cm^3). During the heating/cooling experiments, the melting temperature (T_m) and homogenization temperature (T_h) of two-phase (gas-vapor) inclusions were measured. Heating rates of the samples were 1°C/min for T_m and 5°C/min for T_h. Repeated microthermometric measurements indicated that the precision of the microthermometric results reported in this study is within ±0.1°C for T_m and ±0.2°C for T_h. The

results of microthermometric measurements are shown in histograms (Fig. III. 5) and summarized in Table III. 3. Relations of salinity and T_h values are shown in Fig. III. 6.

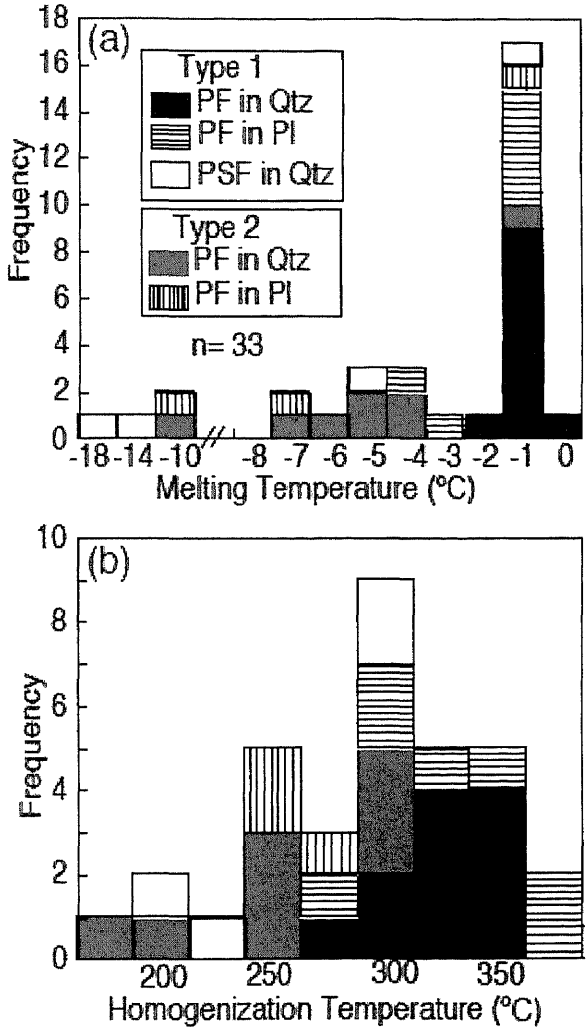

Fig. III. 5. Histograms showing the distribution of (a) melting temperature (T_m), and (b) homogenization temperatures (T_h) of aqueous fluid inclusions in dioritic rocks. PF: primary fluid inclusions, PSF: pseudosecondary fluid inclusions.

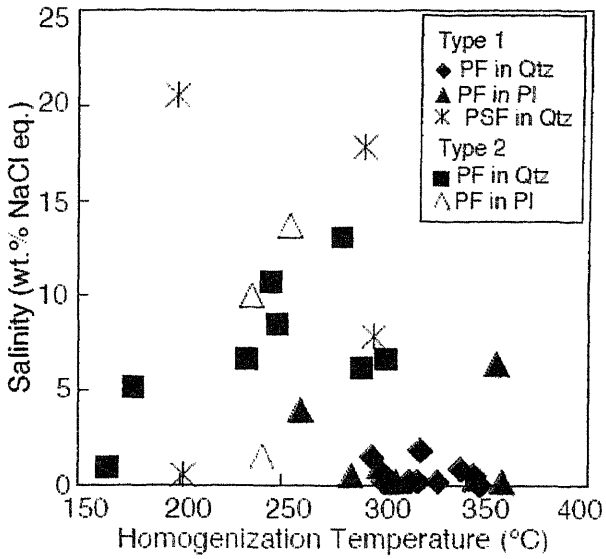

Fig. III. 6. Correlation between homogenization temperatures and salinities of aqueous fluid inclusions in dioritic rocks.

Table III. 3. Microthermometric data for aqueous fluid inclusions of dioritic rocks in Bangladesh

Sample	Melting Temperature (°C)			Homogenization Temperature (°C)			Wt.%	Density	Inclusion type	Size
Number	Min.	Max.	Average	Min.	Max.	Average	NaCl eq.	(g/cm^3)	& Host mineral	(μm)
P14, P15, P10 (Type 1)	-4.0	-1.0	-1.1	259.5	358.2	315	0.17-6.4	0.54-0.73	PF & Pl	2-7
P14, P15 (Type 1)	-1.1	0.0	-0.3	294.1	347.4	318	0.0-1.8	0.57-0.72	PF & Qtz	3-16
P8, P39 (Type 2)	-9.2	-0.6	-4.8	164.9	301	242	1.0-13.1	0.79-0.93	PF & Qtz	2-8
P8, P39 (Type 2)	-9.7	-0.9	-5.7	235.5	254.8	244	1.5-13.6	0.82-0.92	PF & Pl	2-4
P14, P15 (Type 1)	-17.3	-0.3	-9.2	199.1	295.1	247	0.5-20.4	0.81-1.02	PSF & Qtz	4-8

Pl, plagioclase; Qtz, quartz; PF, primary fluid inclusions; PSF, pseudosecondary fluid inclusions

III. 6.2.2. Results

The results of microthermometric measurements show clear difference between the two categories of samples (Type 1 and Type 2). Primary two-phase fluid inclusions in plagioclase and quartz in Type 1 samples show final ice-melting temperatures ($T_{m,\,ice}$) of 0 to –4.0°C (Fig. III. 5a), which correspond to $NaCl_{eq}$ salinities of 0 to 6.4 wt.%. T_h of these inclusions ranges from +259.5 to +358.2°C (Fig. III. 5b), which correspond to bulk densities of 0.54–0.82 g/cm^3 (Table III. 3). There is no obvious difference between the inclusions trapped in plagioclase and quartz. There is

no correlation between T_h and salinity of the Type 1 inclusions (Fig. III. 6).

On the other hand, $T_{m,\,ice}$ of primary fluid inclusions trapped in quartz and plagioclase in Type 2 samples is slightly low at –0.6 to –9.7°C (Fig. III. 5b), which correspond to higher $NaCl_{eq}$ salinities of 1.0–13.6 wt.%. Their T_h is also low (+164.9°C to +301.0°C; Fig. III. 5b), which correspond to bulk densities of 0.72–1.01 g/cm^3 (Table III. 3). The density range is higher than those of primary inclusions in Type 1 samples. As shown in Fig. III. 6, aqueous fluids in Type 2 quartz show a correlation of T_h and salinity. The $T_{m,\,ice}$ and T_h ranges of rare pseudosecondary inclusions (Type 1) in quartz (–0.3°C to –17.3°C and +199.1°C to +295.1°C, respectively) are consistent with the results of Type 2 samples.

The composition and density of aqueous fluids trapped within inclusions can be represented through an isochore (line of constant volume) in P–T space. The fluid densities and isochores were calculated using the computer program "MacFlinCor," developed by Brown and Hagemann (1994), using the equation and thermodynamic data of Bodnar and Vityk (1994). For construction of isochores in Fig. III. 7, the T_h values were adopted for each category of inclusion. The implication of the results will be discussed in the next section.

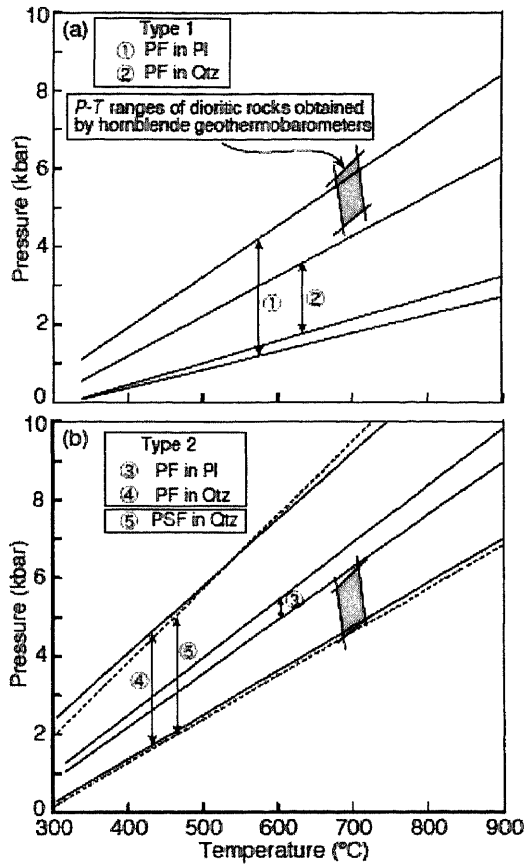

Fig. III. 7. *P-T* diagram showing isochores for aqueous fluid inclusions in various host minerals within Type 1 (a) and Type 2 (b) dioritic rocks. The dark shaded area indicates the temperature and pressure ranges of dioritic rocks obtained by hornblende geothermometry (680–725°C) and Al-in-hornblende geobarometry (4.9–6.4 kbar).

III. 7. Discussion

III. 7.1. Characterization of magmatic fluid

Detailed petrographic and microthermometric investigations of fluid inclusions in dioritic rocks from northwestern Bangladesh indicate that H_2O-rich fluids are trapped in quartz and plagioclase. Primary nature of occurrence of the inclusions in coarse-grained minerals in Type 1 diorites indicates that the fluids were trapped during the crystallization of the host minerals, and that the trapped H_2O-rich fluid can be regarded as a trace of magmatic fluid. As shown in Fig. III. 7a, isochores for primary high-density fluid inclusions in plagioclase in Type 1 diorite intersect

the *P–T* condition of the rocks at ~6.0 kbar and ca. 710°C, which broadly corresponds to the crystallization conditions of the rocks (680–725°C and 4.9–6.4 kbar in Fig. III. 7) obtained from geothermobarometry. However, isochores for some primary fluid inclusions within quartz in Type 1 rocks show slightly depleted pressure (~4.5 kbar at 725°C). The primary fluid inclusions in Type 1 diorite thus have a wide density variation, and some plot below the *P–T* range in Fig. III. 7a due to low-density. However, both the high- and low-density inclusions are often present in the same inclusion clusters, suggesting that they were trapped at the same stage. Such a wide density range is probably due to later slight density modification of some inclusions during exhumation, which is a common feature of fluid inclusions in orogenic belts (e.g., Ohyama et al., 2008; Tsunogae et al., 2002, 2008; Santosh and Tsunogae, 2003; Santosh et al., 2008). In contrast, isochores for Type 2 diorites are plotted around lower-*T* side of the Type 1 isochores (Fig. III. 7b), suggesting that the rocks underwent significant recrystallization and/or deformation during cooling. Fluid inclusions in such deformed samples are therefore not suitable for characterization of the magmatic fluids (e.g., Wilkins and Barkas, 1978).

Our microthermometric results suggest that the magmatic fluids related to the crystallization of dioritic rocks are H_2O-rich ($T_{m,\,ice}$ = 0 to –4.0°C) with low to medium-salinity (0–6.4 wt.% $NaCl_{eq}$), although aqueous fluids with slightly higher density is also present in Type 2 diorite (up to 13.6 wt.% $NaCl_{eq}$). However, this result contrasts to the occurrence of CO_2-rich fluids in late pegmatite and aplite veins cutting across the diorite (Hossain and Tsunogae, 2008). Such occurrences of both H_2O- and CO_2-rich fluids in single plutonic complex have been

reported as results of fluid immiscibility (e.g., Roedder, 1971, 1979; Bodnar, 1995; Heinrich, 1995, Reyf, 1997). However, in this case, different intrusion stages of dioritic rocks and veins as well as lack of H_2O–CO_2 mixed fluids in diorite samples suggest two-stage fluid activities (earlier H_2O-rich and by later CO_2-rich fluid), which have been reported for dioritic rocks elsewhere (Roedder, 1992).

III. 7.2. Emplacement depth and exhumation history

The crystallization temperature and pressure conditions of the dioritic rocks have been estimated to be 680–725°C and 4.9–6.4 kbar by hornblende–plagioclase and Al-in-hornblende geothermobarometers. As the *P–T* condition has been obtained from coarse-grained plagioclase and hornblende pairs in undeformed (Type 1) dioritic rocks, it can be regarded as the condition of magmatic crystallization, although we cannot neglect possible slight modification of mineral compositions during cooling. The *P–T* conditions are nearly consistent with the range of isochores estimated from primary aqueous fluid inclusions trapped in quartz and plagioclase in Type 1 dioritic rocks, which further indicates that the trapped fluid is a trace of magmatic fluid.

The pressure range enables us to estimate minimum emplacement depth of the dioritic rocks at ~17–22 km, if the rock density is assumed to be ~3 g/cm^3. The result is nearly consistent with available palaeodepth estimates for pegmatite and aplite veins intruding the dioritic rocks (~16 km/~4.8 kbar; Hossain and Tsunogae, 2008) and also for plutonic rocks in the Central Indian Tectonic Zone (~17 km/≥5 kbar; Mishra et al., 2007). As the basement rocks in the study

area is located close to the surface, the thickness of eroded rocks after the crystallization of the dioritic rocks can be estimated to be ~17–22 km from the pressure range. As the Maddhapara basement rocks were overlain by thin cover of Lopingian (~0.26 Ga) Gondwana fluvial sediments, we estimate the erosional period of the basement rocks to be 1.47 billion years (=1.73–0.26), and the minimum average rate of exhumation of the rocks as ~12–15 m/Ma, suggesting relatively slow exhumation during Palaeoproterozoic to Lopingian time. The estimation of minimum average exhumation rate was done by considering the entire depth versus time, following the method of Rubatto and Hermann (2001). Here we considered the extent of time between the time of crystallization of basement rocks (U–Pb SHRIMP zircon age) and the Lopingian sedimentation age record. The exhumation rate results are comparable with estimates from other orogenic belts made by different methods, including cosmogenic isotope, apatite fission track, and the volume of sediments in streams or deposits (e.g., Yoshinobu et al., 2002; McInnes et al., 2005). The exhumation rate calculated from the emplacement depth of the pluton is only a minimum estimate. The pluton might be reburied and/or some sedimentation might have occurred during the period of over 1.47 billion years. Although the sedimentation of Lopingian time is the oldest similar event in Bangladesh and most parts of the CITZ and adjoining areas, rare Upper Carboniferous to Permian Gondwana sediments in eastern and south–central India, and also few isolated areas (in India) have also been reported (Tewari, 1999). The slow exhumation rate could indicate low relief continental shield surface for the northwestern Bangladesh during the Neoproterozoic to Palaeozoic. Our *P–T* and fluid inclusion

data therefore provide valuable information on the exhumation rate of the basement rocks in Bangladesh, which is crucial to understand the earth's geologic cycles, including the geographic evolution of continental surfaces (e.g., Wilkinson and Kesler, 2007). The basement rocks were probably uplifted along the Son–Narmada lineament that corresponds to an ENE–WSW trending deep crustal fault (Acharyya, 2003), and subsequently covered by alluvial sediments during the Lopingian. The exhumation rate of these Palaeoproterozoic basement rocks were probably decreased soon after the termination of tectonic activity (Matmon et al., 2003). Then the basement remained relatively stable and the subsequent rock uplift was in equilibrium with denudation since the tectonic activity terminated. As a result, the landscape was facilitated to approach a balance in terms of mass loss over time when considered on such long time scales (Pazzaglia and Brandon, 2001). The longevity and topographic persistence of the basement might also explain the existence of a thickened crust.

Our study provides the first emplacement depth and exhumation rate data as well as the characterization of magmatic fluid in dioritic rocks in Bangladesh. The results will be useful in further understanding the tectonic activities in CITZ and adjoining areas in India.

CHAPTER IV

Fluid inclusion study of pegmatite and aplite veins of Palaeoproterozoic basement rocks in Bangladesh: Implications for magmatic fluid compositions and crystallization depth.

This chapter has been published in Journal of Mineralogical and Petrological Sciences

(2008, Vol. 103, pp. 121-125)

Abstract

We report the first fluid inclusion data on Palaeoproterozoic basement rocks in Bangladesh for the characterization of magmatic fluid compositions and determination of the crystallization pressure and temperature of the host rock. Fluid inclusions are present as primary and pseudosecondary types in quartz grains within pegmatite and aplite, which occur as veins in dioritic rocks. Both primary CO_2-rich and H_2O-rich inclusions are present, even in the same inclusion cluster, probably reflecting a single stage of fluid activity during the crystallization of the veins. The melting temperature (T_m) and homogenization temperature (T_h) of the dominant carbonic inclusions are in the ranges of –56.6°C to –58.1°C and –6.8°C to +30°C, respectively; the T_h values translate into densities of 0.59–0.97 g/cm^3. Rare aqueous fluid inclusions have a final T_m value in the range of 0°C to –10.8°C and a T_h value in the range of +209.8°C to +405.5°C, which corresponds to bulk densities of 0.52–0.97 g/cm^3. Isochores of the inclusions and temperatures obtained from the zircon saturation thermometry of pegmatite indicate that the veins crystallized at ~4.8 kbar and 660–670°C (depth of ~ 16 km). The results of this study will be useful in understanding the magmatism and metallogeny of felsic igneous rocks of Bangladesh, which are related to the formation of the Columbia supercontinent.

IV. 1. Introduction

Recent geochronological studies on basement rocks in Bangladesh indicate that Palaeoproterozoic (1.72-1.73 Ga; Ameen et al., 2007; Hossain et al., 2007) tonalitic and dioritic rocks exist in the Maddhapara area (Fig. IV. 1), which are regarded as a continuation of the Central Indian Tectonic Zone (CITZ) as a possible remnant of the Columbia supercontinent (Hossain et al., 2007). Although petrographical and geochemical data on basement rocks is available, no detailed geothermobarometric and fluid inclusion studies have thus far been conducted on them. Fluid inclusions in such igneous rocks are regarded as a powerful tool for the characterization of magmatic fluids and estimation of the trapping depth of the fluids, which are

useful for the determination of the physicochemical conditions of the source magma.

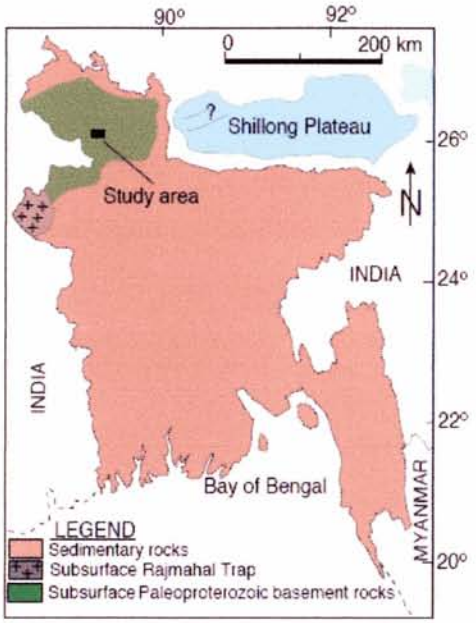

Fig. IV. 1. Geological map of Bangladesh showing sample location of the study area.

In this study, we report the first fluid inclusion data on Palaeoproterozoic basement rocks in Bangladesh. A limited number of fluid inclusion studies have been conducted on CITZ rocks; most of these studies have been conducted on metamorphic rocks (e.g., Santosh et al., 2006). In comparison, few studies on magmatic fluid inclusions have been published in igneous rocks related to the formation of the Columbia supercontinent (e.g., Nabelek and Ternes, 1997; Reyf, 1997). Therefore, we have attempted to identify the magmatic fluid phases, densities, and *P-T* conditions of the crystallization of the magma. The results of this study will be useful in understanding the magmatism and metallogeny of the felsic igneous rocks of Bangladesh, which are related to the formation of the CITZ as well as Columbia supercontinent.

IV. 2. Sample

The basement rocks in Bangladesh are predominantly dioritic rocks. Due to the absence of fluid inclusions in this type of rock, we focused on inclusions trapped in quartz grains within pegmatite (samples PLS3 and PL12) and aplite (sample PL7). Both pegmatite and aplite occur as

veins having a thickness of up to 50 cm; these veins were possibly intruded together in the cooling stage. Pegmatite is mainly composed of K-feldspar (orthoclase and microcline, up to 2 cm in length), quartz, and albite with accessory zircon, while aplite, which is a typical intrusive rock, is mainly composed of fine-grained plagioclase and quartz.

The temperature of crystallization of pegmatite was estimated using zircon saturation geothermometry. Results of previous experimental studies and the amount of zirconium required for saturation were used to estimate the temperature at which zircon was crystallized (e.g., Watson, 1979; Watson and Harrison, 1983; Ayers and Watson, 1991). Watson and Harrison (1983) revisited the thermometry and investigated the relation between zircon crystallization and melt composition, which is given by the solubility model: T_{Zr} = 12900/[2.95 + 0.85 x M + ln (496000/Zr_{melt})], where M = molar [(Na + K + 2 x Ca)/(Al x Si)]. Consequently, T_{Zr} provided a minimum estimate of the magma temperature before extensive crystallization, probably effectively on crystallization depth.

In this study, we adopted the calibration of Miller et al. (2003) to minimize the errors in the calculated value of T_{Zr}. The crystallization temperature of pegmatite was estimated as 660–670 °C using the Zr content (46–47 ppm) and M values (1.4–1.5, where SiO_2 = 73.5–74.7 wt%, Al_2O_3 = 13.1–13.7 wt%, Na_2O = 2.6–3.0 wt%, K_2O = 5.5–6.2 wt%, and CaO = 1.4–1.6 wt%) of bulk rock.

IV. 3. Fluid inclusions

Fluid inclusions are classified into three types on the basis of their occurrence: primary, pseudosecondary, and secondary (cf., Roedder, 1984). As the inclusions examined in this study occur as isolated aggregates or local clusters formed away from the grain margins of quartz, they are regarded as primary fluid inclusions that were probably trapped during the growth of the host mineral. However, we cannot exclude the possibility that they were trapped in healed and annealed early fractures as pseudosecondary inclusions (e.g., Touret, 2001) (Figs. IV. 2a-2c).

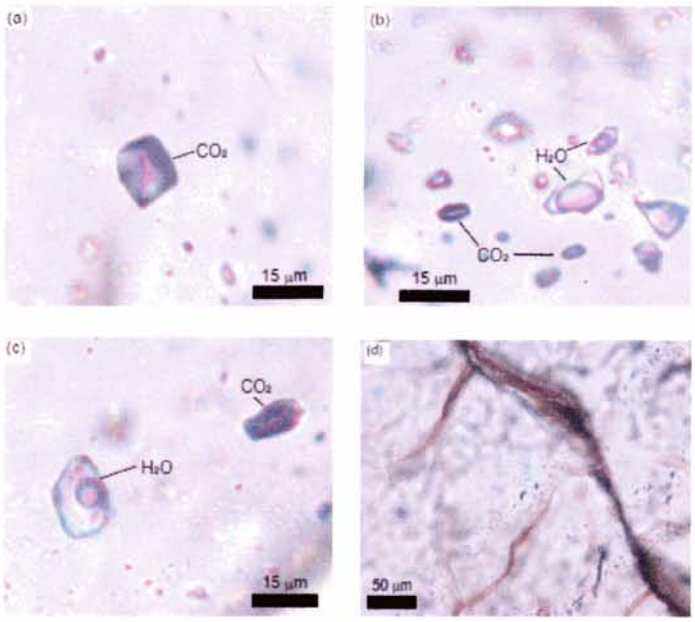

Fig. IV. 2. Photomicrographs of representative fluid inclusions discussed in this study. (a) Isolated primary carbonic fluid inclusions in pegmatite (sample PLS3). (b) A cluster of fluid inclusions, showing co-existence of primary carbonic and aqueous fluid inclusions in pegmatite (sample PLS3). (c) Relatively large primary aqueous and carbonic fluid inclusions having clear evidence for the co-existence in pegmatite (Sample PLS3). (d) Trails of very small secondary fluid inclusions (sample PL7), which are not suitable for microthermometric measurement.

They are totally contained within a grain and rarely develop along identifiable cracks. These inclusions commonly occur along crystal growth surfaces and show a general scattered distribution in sections. Secondary inclusions are those inclusions that are formed after the crystallization of a mineral. They are typically located within healed fractures that intersect the host-crystal boundaries (Fig. 2d). Pseudosecondary inclusions are formed along microcracks that develop during the partial growth of the crystal and form arrays that pinch out within the grains.

As discussed below, both primary CO_2-rich and H_2O-rich inclusions are present, even in a single inclusion cluster (Figs. IV. 2b and 2c). Some lengthened inclusions that form trails are also trapped during the growth of the host mineral as pseudosecondary inclusions. Further, there exist sòme arrays of very small secondary fluid inclusions, which are not suitable for microthermometric measurement. As shown in Figure IV. 2d, the occurrence and size of the secondary inclusions are clearly different from those of the primary inclusions (Figs. IV. 2a-2c). Although feldspar grains have rare primary fluid inclusions, they are very small and unsuitable

for analysis. No boiling evidence is recognized in the studied samples.

Table IV. 1. Summary of microthermometric measurements of carbonic and aqueous fluid inclusions in pegmatites and aplite.

Sample	Rock/ fluid	Melting temperature (°C)			Homogenization temperature (°C)			Density	Wt %	Type of	Size
No.	types	Min.	Max.	Average*	Min.	Max.	Average*	(g/cm³)	salt	inclusion	(μm)
PLS3	Pg/ CO_2	-57.6	-56.6	-56.9±0.4	7.4	30.0	23.1±12.1	0.59–0.88	-	Primary	2–7
PL12	Pg/ CO_2	-57.9	-56.6	-57.2±0.3	-6.4	29.1	16.1±6.3	0.63–0.96	-	Primary	2–12
PL7	Ap/ CO_2	-58.1	-56.7	-57.1±0.3	-6.8	29.8	16.7±9.5	0.60–0.97	-	Primary	2–16
PL12	Pg/ CO_2	-57.2	-56.6	-56.8±0.2	15.7	30.0	25.9±5.3	0.59–0.82	-	PS	4–10
PL7	Ap/ H_2O	-10.8	-6.5	-9.0±2.2	209.8	405.2	275.5±112.3	0.63–0.97	9.8–14.8	Primary	4–10
PL12	Pg/ H_2O	-3.4	0	-1.0±1.5	249.6	405.5	319.0±60.9	0.52–0.83	0–5.5	Primary	4–12

Microthermometric measurements of the fluid inclusions were performed with a Linkam heating/freezing system at the University of Tsukuba. Calibration was performed using synthetic standard materials supplied by Fluid Inc., Denver. The calibrations were performed at 0 °C (triple point of H_2O), –56.6 °C (triple point of CO_2), and the critical point of pure H_2O with a density of 0.317 g/cm ^{3} (374.1 °C). In the heating/cooling experiment, the melting temperature (T_m) and homogenization temperature (T_h) of two-phase (gas-vapor) inclusions were measured. The heating rates of the samples were 1 °C/min for T_m and 5 °C /min for T_h. Repeated microthermometric measurements indicated that the precision of the microthermometric results reported in this study was within ±0.1 °C for T_m and ±0.2 °C for T_h. The results are shown in histograms (Fig. IV. 3) and summarized in Table IV. 1. The T_m values of primary carbonic inclusions are in the ranges of –56.6 °C to –57.9 °C (pegmatite) and –56.7 °C to –58.1 °C (aplite); these values are close to the triple point of pure CO_2 (–56.6 °C). The slight depression in the T_m values of some inclusions suggests the probable presence of traces of additional fluid components such as N_2 and CH_4 in the dominant CO_2-rich fluid (Fig. IV. 3a). Continuous heating leads to the homogenization of the inclusions into the liquid phase at a T_h value in the range of –5.8 °C to +30 °C for pegmatite and –6.8 °C to +29.8 °C for aplite (Fig. IV. 3b). When the T_h data is compiled into histograms, most of them show a T_h range of +14 °C to +30 °C. These T_h values translate into CO_2 densities of 0.59–0.97 g/cm^3 (Table IV. 1). The T_m and T_h values of rare

pseudosecondary inclusions lie in the ranges of –56.6°C to –57.2°C and +15.7°C to +30°C, respectively; these values are similar to those of primary inclusions.

Aqueous fluid inclusions in pegmatite and aplite yield final T_m values ranging from 0°C to –10.8°C and T_h values ranging from +209.8°C to +405.5°C (Fig. IV. 3c), which correspond to bulk densities of 0.52–0.97 g/cm^3 (Table IV. 1). Their equivalent NaCl concentrations are 0.17–14.8 wt%.

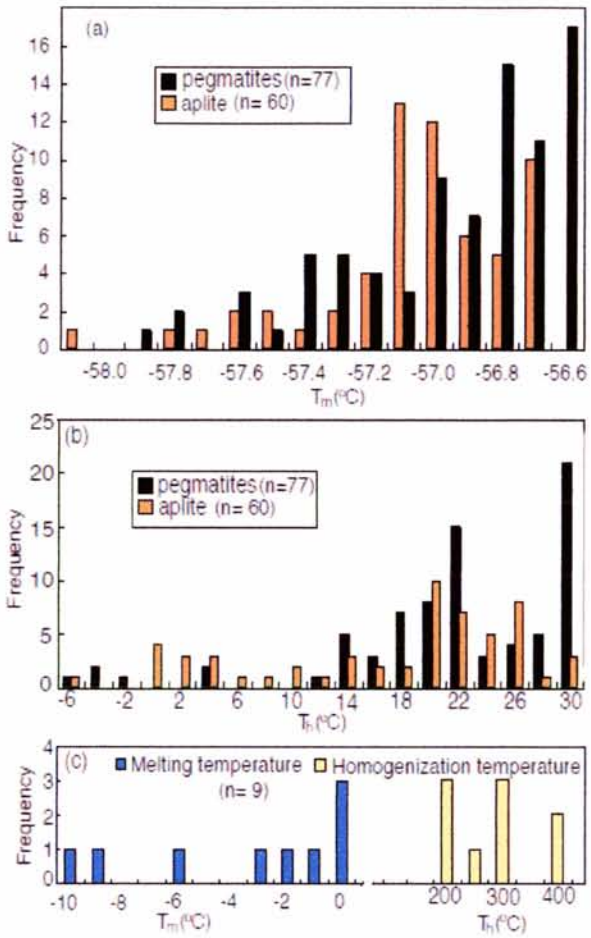

Fig. IV. 3. Histograms showing the distribution of melting (a) and homogenization (b) temperatures of carbonic fluid inclusions, and aqueous fluid inclusions (c) temperatures in pegmatite and aplite.

The composition and density of the fluid phase trapped within the inclusions can be represented through a specific isochore (line of constant volume) in *P-T* space. The carbonic and aqueous inclusions analyzed in this study have been used for constructing the isochores shown in

Figure IV. 4. The fluid densities and isochores were calculated with the computer program "MacFlinCor," which was developed by Brown and Hagemann (1994), using the equation and thermodynamic data of Brown and Lamb (1989). For the construction of the isochores shown in Figure IV. 4, the minimum and maximum values of T_h were adopted for each category of inclusion. Separate isochores were also computed for the highest-density primary CO_2 fluid inclusion in the quartz present in pegmatite and aplite (T_h = –5.8°C to –6.8°C).

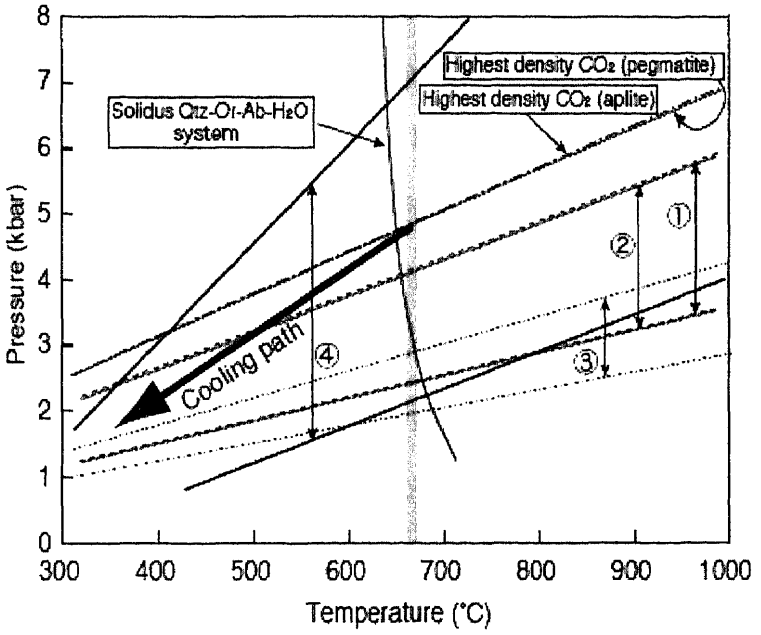

Fig. IV. 4. P-T diagram showing isochores for carbonic (dash lines) and aqueous (heavy solid lines) fluid inclusions in pegmatite and aplite. The isochore ranges correspond to errors in calculated densities in Table 1 for primary CO_2 inclusions of pegmatite (1), primary CO_2 inclusions of aplite (2), pseudosecondary CO_2 inclusions (3) and aqueous fluid inclusions (4). Individual isochores for highest density CO_2 values (not corrected) for pegmatite and aplite (dash lines). Shaded area indicates temperature range of pegmatite obtained from zircon saturation thermometry (660-670°C). Solidus of Qtz-Or-Ab-H_2O system was taken from Johannes (1984).

IV. 4. Discussion

The petrographic and microthermometric measurements of the fluid inclusions in the pegmatite and aplite veins of the basement rocks in Bangladesh indicate that dominant CO_2-rich and rare H_2O-rich fluids are trapped in quartz at the same stage. Primary to pseudosecondary occurrences of the inclusions suggest that they were trapped during the crystallization of host

minerals and that the trapped fluids are magmatic in origin. Some H_2O-rich inclusions are saline with equivalent NaCl concentrations of 0.17–14.8 wt%. Previous studies on fluid inclusions in magmatic rocks suggest that occurrences of such CO_2 + saline H_2O fluids and the dominant CO_2-rich fluid in late-stage pegmatite and aplite are common (Roedder, 1979; Konnerup-Madsen et al., 1985; Reyf, 1997; Nabelek and Ternes, 1997). This is probably due to the separation of the magmatic fluid into two immiscible phases at low temperatures—CO_2-rich gas and salt-rich liquid (brine) (Reyf, 1997)—and/or the change in fluid compositions from H_2O-CO_2 to CO_2 during the crystallization stage (Nabelek and Ternes, 1997). The primary fluid inclusions, which are probably trapped during the growth of quartz, have a wide density range (0.59–0.97 g/cm^3). Although most of them have a low density (0.59–0.81 g/cm^3), rare high-density inclusions (0.96–0.97 g/cm^3) are also present. It is interesting to note that they are trapped together with high-T_h (low-density) inclusions. Such a wide density variation and the preservation of the rare high-density inclusions suggest that all the primary fluid inclusions were probably trapped together, and their density decreased significantly during exhumation (Ohyama et al., 2008). Therefore, we infer that the CO_2-rich inclusions with the highest-density values preserve the fluid at magmatic crystallization.

In this study, the crystallization temperature of pegmatite has been estimated to be 660–670°C by the zircon saturation thermometry of pegmatite. Since both carbonic and aqueous inclusions were apparently trapped in a single stage of fluid activity during the formation of veins, the overlapping ranges of H_2O and the highest-density CO_2 isochores shown in Figure IV. 4 (4.8 kbar at 660–670°C) probably correspond to the pressure of crystallization of the veins. The pressure of crystallization corresponds to the depth of crystallization at ~ 16 km when the rock density is assumed to be ~ 3 g/cm^3. The *P–T* condition is consistent with the solidus of the Qtz-Or-Ab-H_2O system (Johannes, 1984, Fig. IV. 4), suggesting that the mineral assemblages of pegmatite discussed in this study (quartz + K-feldspar + albite) may have been stable at the *P–T* condition. Isochores for some low-density carbonic and aqueous inclusions possibly suggest later

modification of the fluid density because the cooling path in Figure IV. 4 intersects the isochores, which is a common feature of retrogressed high-grade metamorphic rocks (Tsunogae and van Reenen, 2007; Ohyama et al., 2008). The crystallization depth of the host diorite is, therefore, regarded to be more than 16 km.

This study provides the first magmatic fluid inclusion data of the basement rocks in Bangladesh formed during the amalgamation of the Columbia supercontinent. The results will be useful in understanding the magmatic activity and metallogeny of basement rocks.

CHAPTER V

Palaeoproterozoic U-Pb SHRIMP zircon age from basement rocks in Bangladesh: A possible remnant of Columbia Supercontinent

This chapter has been published in Comptes Rendus Geoscience

(2007, Vol. 339, pp. 979-986)

Abstract

We present new U–Pb SHRIMP zircon geochronological data for basement rocks in Bangladesh, and discuss the relationship with the formation of Columbia Supercontinent. Euhedral zircons from a diorite sample yield a concordia age of 1730±11 Ma, which is interpreted as the crystallization age. The Palaeoproterozoic age of the examined basement rock and the common occurrences of similar ~1.7 Ga geologic units in the Central Indian Tectonic Zone and Meghalaya-Shillong Plateau in Indian Shield suggest their apparent continuation. This, together with the occurrence of similar ~1.7 Ga geologic units in the Albany-Fraser belt in Australia and East Antarctica are used to suggest that the basement rocks in Bangladesh formed towards the final stages of the assembly of Columbia Supercontinent.

V. 1. Introduction

Supercontinents containing most of the earth's continental crust are considered to have existed at least twice in Proterozoic time. The younger one, Rodinia, formed ~1.0 Ga (Hoffman, 1991) by accretion and collision of fragments produced by breakup of the older supercontinent, Columbia, which was assembled by global-scale 2.0–1.8 Ga collisional events (Rogers and Santosh, 2002). Based on the distribution of U–Pb zircon ages, coupled with Nd and Hf isotope data, Condie (2004) recognized that there is a major peak in juvenile crustal production rate at *ca.* 1.9 Ga (Fig. 1). The ~2.1–1.7 Ga distribution in Fig. V. 1 probably corresponds to inboard manifestations of subduction/collision/post-collision related magmatism associated with the

formation of Columbia supercontinent. As with the case of any supercontinent, the exact configuration of Columbia supercontinent awaits more and precise geochronologic information from separated continental fragments, providing a means to establish former linkages.

Basement rocks from Bangladesh were never considered in the configuration of Columbia, partly due to the lack of exposed igneous or metamorphic rocks. The geology of Bangladesh is characterized by extensive Tertiary and Quaternary successions, forming part of one of the largest continental sedimentary depositories in the world (Curray, 1991). Drill-hole geological investigations from the Maddhapara area (between 89°03′30″E to 89°04′53″E and 25°33′15″N to 25°34′15″N; Fig. V. 2), northwestern part of Bangladesh reveals that basement rocks occur at a shallow depth (~128 m; e.g., Khan, 1991). Ameen et al. (2007) recently reported a U–Pb SHRIMP age of 1722±6 Ma from a tonalitic core sample from this area (obtained at a depth of 227.48 m in drill hole BH-2). They consider the buried rocks at Maddhapara to represent a separate and discrete microcontinental fragment that was trapped by the northward migration of India during Gondwana dispersal. Here we report new U–Pb SHRIMP zircon age for a dioritic sample (obtained from tunnel, at a depth of 276 m), and based on a literature survey, attempt to evaluate the significance of basement rocks in Bangladesh in a supercontinent framework. We suggest the possibility of basement rocks in Bangladesh forming the continuation of the Central Indian Tectonic Zone and Meghalaya-Shillong Plateau in Indian Shield on the basis of available geochronological and paleogeographical information.

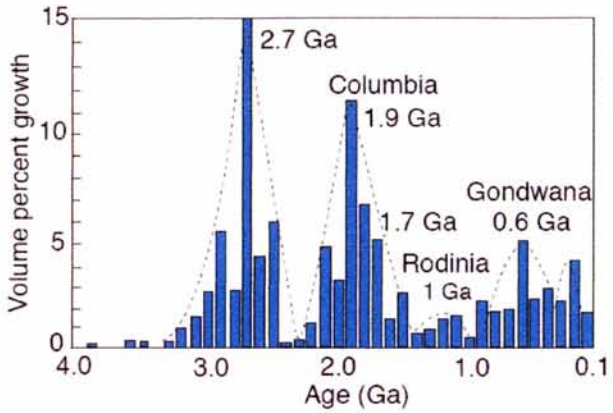

Fig. V. 1. Frequency distribution of juvenile crustal production with time. Juvenile crust ages are U–Pb zircon ages used in conjunction with Nd and Hf isotope data (modified after Groves et al., 2005).

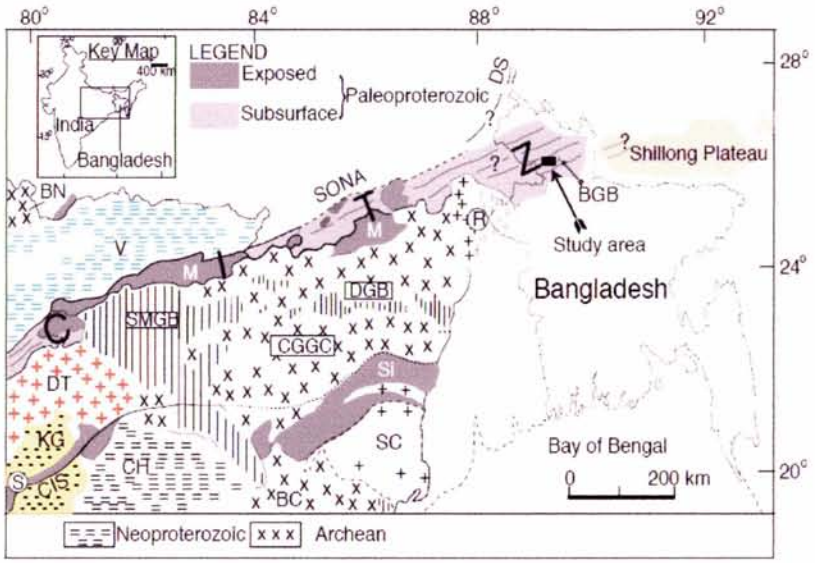

Fig. V. 2. Location map of the Maddhapara basement rocks in Bangladesh, showing tectonic elements and its relationship with CITZ (modified after Khan, 1991; Rao and Reddy, 2002; Acharyya, 2003). Abbreviations; BC : Bastar Craton, BN : Bundhelkhand Craton, BGB : Barapukuria Gondwana Basin, CGGC : Chotanagpur Granite Gneiss Complex, CH : Chattisgarh, CIS : Central Indian Shear Zone, DGB : Damodar Gondwana Basins, DS : Darjeeling-Sikkim Himalaya, DT : Deccan Trap, KG : Karimnagar Granulite Belt, M : Mohakoshal and equivalents, R : Rajmahal Trap, S : Sausar, SC : Singhbhum Craton, Si : Singhbhum (Paleoproterozoic), SMGB : Son Mahanadi Gondwana Basins, SONA : Son Narmada Lineament, V : Vindhyan.

V. 2. Geologic and petrographic information

The basement rocks in Bangladesh are dominantly dioritic rocks with minor granitoids. Amphibole and biotite form the dominant mafic minerals in all the rock types. Although late

hydrothermal alteration is observed in some of the collected samples, the diorite sample (SL1) from which zircons were extracted for geochronology is fresh and show no evidence of alteration. The sample is medium to coarse-grained and composed dominantly of plagioclase, hornblende, biotite and quartz (Fig. V. 3A). Light pink to colorless zircon crystals (size range: 120 to 440 μm; length/width ratios: 3:2 to 4:1) are commonly included in large euhedral hornblende and subhedral to euhedral biotite. They exhibit typical magmatic oscillatory zoning, as seen in cathodoluminescence (CL) images (Fig. V. 3B). Some coarse zircons have isolated cores mantled by concentric zoning (e.g., grain SL1-6 in Fig. V. 3B). However, they do not show obvious age differences as illustrated below. This suggests that all parts of the zircon grains grew close and probably preserves the magmatic crystallization age.

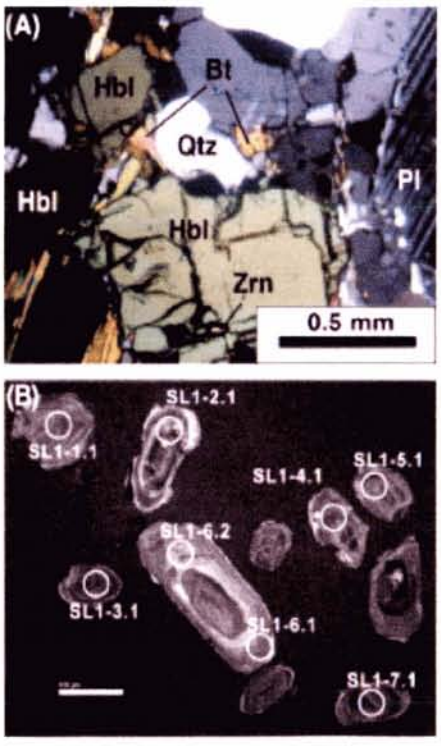

Fig. V. 3. Photomicrograph of zircons examined in this study. (A) Photomicrograph showing typical mineral assemblage of analyzed diorite (sample SL1). Crossed polars. Hbl: hornblende, Bt: biotite, Pl: plagioclase, Qtz: quartz, Zrn: zircon. (B) CL image of zircons in sample SL1 with analyzed spots.

V. 3. Geochronology methods

For U–Pb SHRIMP zircon dating, zircons were separated from the diorite sample (SL1) using conventional techniques. The zircon crystals were mounted in an epoxy disc together with standard zircon, and then polished to expose their cores. The internal structure for analyzed zircons was observed using CL images (e.g., Fig. V. 3B). Using guidance from the CL images, zoned mantle parts of zircons were analyzed for U–Pb isotopes and U, Th and Pb concentrations using a SHRIMP II ion microprobe at the Institute of Geology, Chinese Academy of Geological Sciences, Beijing. The analysis follows the methods of Compston et al. (1992) and Williams and Claesson (1987). Measurements were corrected using reference zircon standard Temora (417 Ma; Black et al., 2003). The common Pb was estimated from ^{204}Pb counts, and the data processing was carried out using Isoplot (Ludwig, 1997).

V. 4. Results

The analytical results of zircons in sample SL1 are listed in Table V. 1, and all analyzed zircons are shown in Fig. V. 3B. Ages are weighted means with 1σ errors. Eight individual analyses were carried out for seven zircon grains. The measurements have been done on large core or mantle parts of the grains. Although the analyzed spots have a wide range in concentrations of U (137–1159 ppm), Th (79–479 ppm) and ^{206}Pb (29.9–307 ppm), there is no systematic correlation between the estimated $^{207}Pb/^{206}Pb$ and U, Th and Pb contents, and Th/U ratio (Table V. 1). Seven spots of zircons have a consistent $^{206}Pb/^{238}U$ age between 1720±45 to

1791±44 Ma, yet spot SL1.6.1 yielded younger $^{206}Pb/^{238}U$ age of 1440±37 Ma (Table V. 1). This is due to recent Pb-loss of the analyzed spot as shown in the concordia diagram (Fig. V. 4A). None of the zircon analyses showed any inheritance. All the analyzed zircons gave $^{207}Pb/^{206}Pb$ ages of 1678±34 to 1737±7 Ma. Seven concordant data yielded a concordia age of 1730±11 Ma (95% confidence limit, MSWD = 0.6, probability of concordance = 0.24) (Fig. V. 4A). As the MSWD is indistinguishable from unity for this number of data points, it is not statistically significant to attempt any editing of the analyses. The concordia age is almost consistent with the weighted mean $^{207}Pb/^{206}Pb$ age of 1728±11 Ma for all eight spots (95% confidence limit, MSWD = 0.78, probability of equivalence = 0.60) (Fig. V. 4B). Our U–Pb SHRIMP age is consistent with available SHRIMP zircon age of 1722±6 Ma for tonalite from the same area (Ameen et al., 2007). Therefore, it can be concluded that the magmatic crystallization of the basement rocks in Bangladesh took place at *ca.* 1.7 Ga.

Table V. 1. Summary of zircon U-Th-Pb analyses in sample SL1 from Maddhapara.

Spots	U	Th	$^{206}Pb^*$	$^{206}Pb_c$	$^{232}Th/^{238}U$	Age (Ma)**			Isotope ratios (±%)**			
	(ppm)	(ppm)	(ppm)	(%)		$^{206}Pb/^{238}U$	$^{207}Pb/^{206}Pb$	$^{208}Pb/^{232}Th$	$^{238}U/^{206}Pb^*$	$^{207}Pb^*/^{206}Pb^*$	$^{207}Pb^*/^{235}U$	$^{206}Pb^*/^{238}U$
SL1.6.1	137	79	29.9	1.22	0.59	1,440 ±37	1,723 ±48	1,455 ±74	4.000±2.9	0.1055±2.6	3.64±3.9	0.2502±2.9
SL1.6.2	208	130	57.9	0.88	0.65	1,791 ±44	1,678 ±34	1,799 ±65	3.122±2.8	0.1030±1.9	4.55±3.4	0.3203±2.8
SL1.5.1	318	238	86.0	0.35	0.77	1,759 ±42	1,708 ±21	1,753 ±53	3.188±2.7	0.1046±1.1	4.52±3.0	0.3137±2.7
SL1.4.1	1159	479	307.0	0.10	0.43	1,729 ±41	1,737 ± 7	1,677 ±51	3.250±2.7	0.1063±0.4	4.51±2.7	0.3077±2.7
SL1-3.1	258	192	69.8	0.70	0.77	1,754 ±44	1,722 ±25	1,786 ±66	3.198±2.9	0.1054±1.4	4.55±3.2	0.3127±2.9
SL1-2.1	295	202	77.9	0.59	0.71	1,720 ±45	1,719 ±22	1,668 ±56	3.271±3.0	0.1053±1.2	4.44±3.2	0.3057±3.0
SL1-1.1	414	325	111.0	0.39	0.81	1,751 ±42	1,714 ±18	1,736 ±50	3.204±2.7	0.1050±1.0	4.52±2.9	0.3121±2.7
SL1-7.1	271	153	73.2	0.32	0.58	1,757 ±44	1,724 ±20	1,804 ±58	3.192±2.9	0.1056±1.1	4.56±3.1	0.3133±2.9

Errors are 1-sigma; Pb_c and Pb^* indicate the common and radiogenic portions, respectively.

Error in Standard calibration was 0.74%(not included in above errors but required when comparing data from different mounts).

** Common Pb corrected using measured ^{204}Pb.

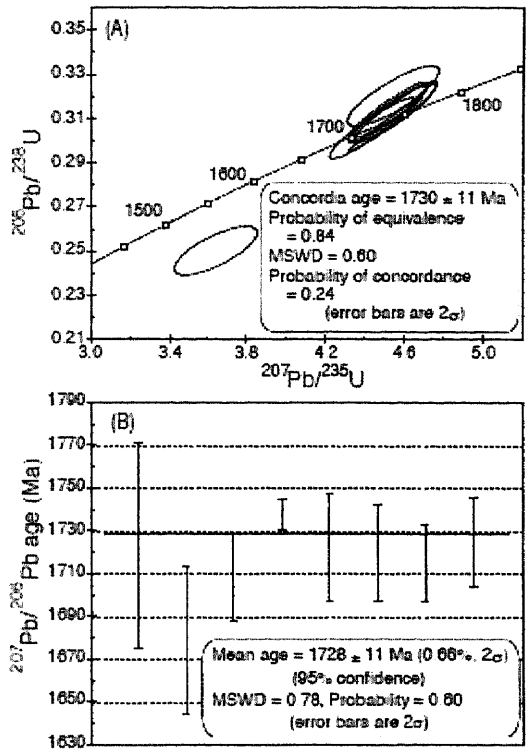

Fig. V. 4. (A) Concordia diagram showing SHRIMP analyses of zircons in sample SL1. (B) Diagram showing the weighted mean age for zircons in sample SL1 from Maddhapara.

V. 5. Discussion

Interpretations of configuration of Proterozoic supercontinents are controversial because of the inherent difficulties and uncertainties in matching continental fragments that were dispersed prior to the assembly and subsequent breakup and dispersal. The case of Columbia supercontinent is no different. The recognition of the 2.1 to 1.8 Ga collision/accretionary events on nearly every continent, including the Transamazonian of South America, the Birimian of West Africa, the Trans-Hudson and its age-equivalent of North America, the Svecofennian and Kola-Karelia of northern Europe, the Akitan and Central Aldan of Siberia, the Capricorn of Western Australia, the Transantarctic Mountains of Antarctica, the Trans-North China in North China, the Central Indian Tectonic Zone in India, etc., led geologists to consider that they represent the

fragments of a pre-Rodinia supercontinent that formed in response to global-scale collision at this time (e.g., Rogers and Santosh, 2002; Condie, 2004; Zhao et al., 2002; Zhao et al., 2006).

The two possible configurations of Columbia, proposed by Rogers and Santosh (2002) and Zhao et al. (2002), differ mainly in the position of North China Craton (NCC), with the former considering that NCC was adjacent to the Baltic and Amazonian cratons, while the latter placing the eastern margin of NCC against the western margin of Indian Shield. Recent studies reported the occurrence of ~1.8 Ga to ~1.65 Ga mafic-felsic intrusions, including anorthosite-mangereite-charnockite-granite (AMCG) suites and rapakivi granites, in NCC (e.g., Zhang et al., 2007; Zhao et al., 2003). Similar Palaeoproterozoic AMCG and rapakivi magmatism is wide spread along the margin of Amazonia and Baltica (Geraldes et al., 2001). No such magmatism is reported from the western margin of Indian shield during the concerned time frame. Hence we follow the configuration of Columbia supercontinent given in Rogers and Santosh (2004) (Fig. V. 5), where NCC is placed adjacent to Baltica. If Bangladesh was part of this configuration, it is most likely to be placed between eastern India, East Antarctica and south-western Australia. To evaluate this, we review the Palaeoproterozoic rock record from these continental fragments.

Although the geology of the ice-covered interior of the East Antarctic shield is poorly known, recent geological studies in exposed basement of the Transantarctic Mountains and Wilkes Land margin suggest correlation with Palaeoproterozoic granitoid rocks and Mesoproterozoic mafic igneous rocks from the Gawler and Curnamona cratons of Australia

(Oliver and Fanning, 1997; Peucat et al., 1999; Goodge et al., 2001; Peucat et al., 2002). Subduction-related batholiths between approximately 1.7 and 1.6 Ga in the Albany-Fraser belt in Australia (Nelson et al., 1995) have similar counterparts in the Windmill islands and Bunger Hills in Antarctica, suggesting attachments in pre-drift configuration (Harris, 1995).

In eastern India, zircons with core ages of 1.7–1.6 Ga from granulites (e.g., Santosh et al., 2004) occurring along the flanks of Palaeoproterozoic rift basins suggest new growth at this time. These rift basins, which had matching rifts in the Columbia region of western North America, were instrumental in Roger and Santosh (2002) proposed configuration of Columbia. One of the prominent features from Indian shield which figures in the Columbia supercontinent configuration is the Central Indian Tectonic Zone (CITZ), considered as the collision zone along which the North and South Indian Blocks amalgamated during the Palaeoproterozoic (Fig. V. 2) (Yedekar et al., 1990; Jain et al., 1995; Mishra et al., 2000). Although recent works showed Mesoproterozoic (~1.5 Ga) reworking of some of the Palaeoproterozoic lithologies from CITZ (Bhowmik et al., 2005), the available geochronological data (Sarkar, 1980; Deb et al., 1989) suggest that the collision in central India progressed between 2100 and 1700 Ma. This is supported by the 2040–2090 Ma age of the ultra-high temperature metamorphic event (Bhowmik et al., 2005) and a number of granitoid magmatic events, bracketed between 2.0–1.7 Ga, from the CITZ (Ray Barman et al., 1990; Ray Barman and Bishui, 1994; Sarkar et al., 1998; Roy and Devrajan, 2000; Acharyya, 2003).

Further up north, extensive occurrence of ~1.9 Ga old porphyritic granites is observed in

the lesser Himalayas (Trevedi, 1990; Valdiya, 1995). DeCelles et al. (2000) reported detrital zircon ages of ~2.0 to 1.8 Ga range from the Lesser Himalaya of Nepal. Granitic gneiss dated at ~1.7 Ga occurs in the Darjeeling-Sikkhim Himalaya (Paul et al., 1996). Towards the north-east, Ghosh et al. (1991, 1994) reported ages as old as 1.7 Ga for basement granitic gneisses from the Meghalaya plateau, while Chatterjee et al. (2007) reported ages of 1.5 Ga from gneissic rocks within the Shillong Plateau.

The above summary of geochronological information give ample justification for the consideration of basement rocks in Bangladesh to be apparent continuation of the Central Indian Tectonic Zone with further extension into the Meghalaya-Shillong Plateau. This differs from the suggestion of Ameen et al. (2007) that the basement rocks in Bangladesh constitute a unique and separate entity, with no meaningful comparison with the CITZ and/or Meghalaya-Shillong Plateau. Finally the common occurrence of ~1.7 Ga geologic units on nearly every continent (e.g., Rogers and Santosh, 2002; Condie, 2004; Zhao et al., 2002; Zhao et al., 2006) warrants the consideration of basement rocks of Bangladesh in the Columbia supercontinent framework. Thus, U–Pb SHRIMP zircon ages of diorite (1730±11 Ma; this study) and tonalite (1722±6 Ma; Ameen et al., 2007) indicate that the basement rocks in Bangladesh formed towards the final stages of the assembly of Columbia supercontinent (~1.9–1.7 Ga).

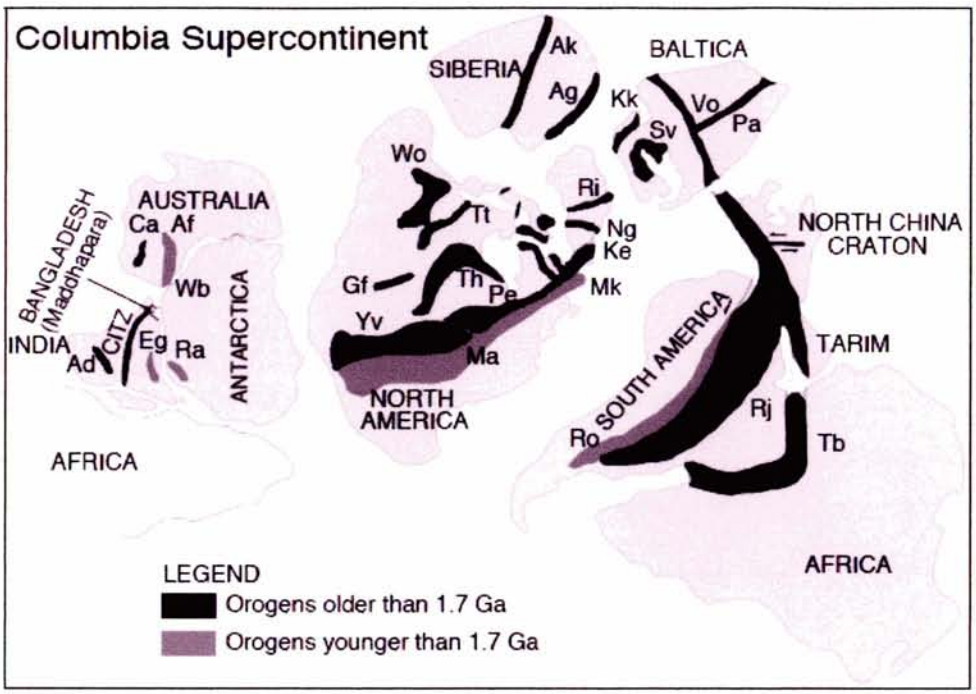

Fig. V. 5. Schematic map showing the Columbia Supercontinent with its remnant in Bangladesh, as a continuation of the CITZ (modified after Rogers and Santosh, 2002). Abbreviations of orogens; Af: Albany-Fraser, Ad: Aravalli-Delhi, Ag: Angara, Ak: Akitkan, Ca: Capricorn, CITZ: Central Indian Tectonic Zone, Eg: Eastern Ghats, Gf: Great Falls, Ke: Ketilidian, Kk: Kola-Karelia, Ma: Mazatzal, Mk: Makkovikian, Ng: Nagssugtoqidian, Pa: Pachemel, Pe: Penokian, Ra: Rayner, Ri: Rinkian, Rj: Rio Negro-Juruena, Ro: Rondonian, Sv: Sveckofennian, Tb: Transamazonian-Birimian, Th: Trans-Hudson, Tt: Thalston-Thelon, Vo: Volhyn, Wb: Windmill Islands-Bunger Hills, Wo: Wopmay, Yv: Yavapai.

CHAPTER VI

General Summary

The Palaeoproterozoic (1.7 Ga) basement rocks from Bangladesh exhibit spatial association of diorite, quartz diorite, monzodiorite, quartz monzonite and granite. About the different rock types and their geochemistry, I discussed the most of their features in chapter II. Generally the petrography, mineral chemistry, major and trace elements, REE data and different models were constructed for explaining magmatism of the pluton. The pluton overall displays metaluminous, calc-alkaline orogenic suite; mostly I-type suites formed within subduction-related magmatism. The major elements show general trends for fractional crystallization. Trace element contents also indicate the possibility of a fractionation or assimilation that can explain the entire variation from diorite to monzonite, even granite. The main trend of the pluton, from diorites to granites, is thought to represent various degrees of interactions with crustal components, and especially the combined effects of assimilation-fractional crystallization (AFC). These results were also verified by the Rayleigh fractionation and assimilation fractional crystallization models. The pluton may have evolved the unique chemical features by a process that included partial melting of calc-alkaline lithologies and mixing of mantle-derived magmas, followed by fractional crystallization, and by assimilation of country rocks. It is possible that the magmas generated deeper in the crust had a larger component of mantle-derived melt (e.g. diorite), and that the magma generated higher in the mid-crust contained a larger contribution of sialic material (e.g., quartz monzonite, granite). Parallel REE patterns discussed in chapter II indicate similar source of the basement rocks. From an extensive search of literatures on the Palaeoproterozoic magmatism of Indian subcontinent,

consistent magmatism is found to be very rare, except on the CITZ (e.g. Barambaba, Jhirgadandi, Bori, Rihand-Renusagar and Betul Granitoid), due to intense metamorphism and evolution of the entire shield area. However, recent recognition of a Palaeoproterozoic large igneous province in the southern Bastar craton and nearby Cuddapah basin in the adjacent Dharwar craton, India followed instinctive trend, and conferred ample justification for sequential growth or accretion of the continent in this region.

In chapters III and IV, hornblende thermobarometry and fluid inclusions of dioritic rocks and cross-cutting pegmatite and aplite veins were discussed to provide information on the *P–T* conditions of crystallization, the emplacement depth and exhumation. The crystallization (*P–T*) conditions of the dioritic rocks have been estimated to be 680–725°C and 4.9–6.4 kbar by hornblende–plagioclase and Al-in-hornblende thermobarometry. Zircon saturation thermometry also offers the crystallization temperature of pegmatite at 660–670°C. The fluid inclusion data on Palaeoproterozoic basement rocks in Bangladesh also make available information on the characterization of magmatic fluid compositions and determination of the crystallization pressure and temperature of the host rock. The microthermometric results suggest that these magmatic fluids (H_2O-rich with low to medium salinity) related to the crystallization of dioritic rocks. However, this result contrasts with the occurrence of CO_2-rich fluids in late pegmatite and aplite veins cutting across the diorite (Hossain and Tsunogae, 2008). The occurrences of both H_2O- and CO_2-rich fluids in single plutonic complex have been reported as being caused by fluid immiscibility (e.g., Roedder, 1971, 1979; Bodnar, 1995; Heinrich, 1995, Reyf, 1997). However,

in this case, both different intrusion stages of dioritic rocks and veins as well as lack of H_2O–CO_2 mixed fluids in diorite samples imply two-stage fluid activities (earlier H_2O-rich and by later CO_2-rich fluid), which have been reported for dioritic rocks elsewhere (Roedder, 1992).

The pressure of crystallization of the pegmatite and aplite veins corresponds to the depth of crystallization at ~16 km. The *P–T* condition is consistent with the solidus of the Qtz-Or-Ab-H_2O system (Johannes, 1984), instructing that the mineral assemblages of pegmatite discussed in this study (quartz + K-feldspar + albite) may have been stable in the *P–T* condition. It is interesting to note that the solidification stages of diorite and aplite might be different, but their source magmas were identical in origin.

The crystallization depth of the host diorite is ~17–22 km, which is also consistent with *P-T* conditions of the fluid inclusions in dioritic rocks. Therefore, the *P–T* and fluid inclusion data provide the exhumation rate of ~12–15 m/Ma during Palaeoproterozoic to Lopingian time of the basement rocks in Bangladesh, which is crucial in understanding the earth's geologic cycles, including the geographic evolution of continental surfaces (e.g., Wilkinson and Kesler, 2007). The basement rocks were probably uplifted along the Son–Narmada lineament that corresponds to an ENE–WSW trending deep crustal fault (Acharyya, 2003), and subsequently covered by alluvial sediments during the Lopingian. The exhumation rate of these Palaeoproterozoic basement rocks was probably decreased soon after the termination of tectonic activity (Matmon et al., 2003). Then the basement remained relatively stable and the subsequent rock uplift led to denudation since the tectonic activity (e.g., exhumation, crustal shortening and

thickening) terminated. As a result, the landscape was facilitated to approach a balance in terms of mass loss over time when considered on such long time scales (Pazzaglia and Brandon, 2001). The longevity and topographic persistence of the basement might also explain the existence of a thickened crust. The results will be useful in well understanding the tectonic activities in CITZ and adjoining areas in India.

In chapter V, geochronology provides ample justification for the consideration of basement rocks in Bangladesh as being the apparent continuation of the CITZ with its further extension into the Meghalaya-Shillong Plateau. U–Pb SHRIMP zircon age from a diorite sample yields a concordia age 1730±11 Ma, which is interpreted as the crystallization age of basement rocks in Bangladesh. In eastern India, zircons with core ages of 1.7–1.6 Ga from granulites (e.g., Santosh et al., 2004) occurring along the flanks of Palaeoproterozoic rift basins suggest new growth at this time. These rift basins, which had matching rifts in the Columbia region of western North America, were instrumental in a proposed configuration of Columbia (Roger and Santosh, 2002). One of the prominent features from Indian shield which figures in the Columbia supercontinent configuration is the CITZ, considered as the collision zone along which the North and South Indian Blocks amalgamated during the Palaeoproterozoic (Yedekar et al., 1990; Jain et al., 1995; Mishra et al., 2000). Although recent works showed Mesoproterozoic (~1.5 Ga) reworking of some of the Palaeoproterozoic lithologies from CITZ (Bhowmik et al., 2005), the available geochronological data (Sarkar, 1980; Deb et al., 1989) suggest that the collision in central India progressed between 2100 and 1700 Ma. This is supported by a number of granitoid

magmatic events ages of 2.0–1.7 Ga from the CITZ (Sarkar et al., 1998; Roy and Devrajan, 2000; Acharyya, 2003).

Towards the northeast, Ghosh et al. (1991, 1994) reported ages as old as 1.7 Ga for basement granitic gneisses from the Meghalaya plateau, while Chatterjee et al. (2007) reported ages of 1.5 Ga from gneissic rocks within the Shillong Plateau.

Interpretations of configuration of Proterozoic supercontinents and the recognition of the 2.1 to 1.8 Ga collision/accretionary events on nearly every continent, led geologists to consider that they represent the fragments of a pre-Rodinia supercontinent that formed in response to global-scale collision at this time (e.g., Rogers and Santosh, 2002; Condie, 2004; Zhao et al., 2002; Zhao et al., 2006). The extensive study of the Palaeoproterozoic crust of the Transamazonian of South America has identified the sequential growth of the continent through the amalgamation of juvenile terrains, succeeded by a major collisional orogeny. Subduction-related batholiths in the Albany-Fraser belt in Australia have similar counterparts in the Windmill islands and Bunger Hills in Antarctica. This type of magmatism is also common in Bohemian Massif and the Svecofennian, Poland, where the dioritic-tonalitic magmas were in fact mafic-derived crust, signify that the crust actively contributed to the evolution of magmatism in the Palaeoproterozoic supercontinent.

The above summary of geochemical and geochronological information gives ample justification for the consideration of basement rocks in Bangladesh to be apparent continuation of the CITZ with further extension into the Meghalaya-Shillong Plateau. This differs from the

suggestion of Ameen et al. (2007) that the basement rocks in Bangladesh constitute a unique and separate entity, with no meaningful comparison with the CITZ and/or Meghalaya-Shillong Plateau.

Finally the common occurrence of ~1.7 Ga geologic units on nearly every continent (e.g., Rogers and Santosh, 2002; Condie, 2004; Zhao et al., 2002; Zhao et al., 2006) warrants the consideration of basement rocks of Bangladesh in the Columbia supercontinent framework. Thus, U–Pb SHRIMP zircon ages of diorite indicate that the basement rocks in Bangladesh formed towards the final stages of the assembly of Columbia supercontinent (~1.9–1.7 Ga).

Acknowledgements

I would like to express my profound gratitude to my supervisor Dr. Toshiaki Tsunogae for his constant guidance, all sorts of facilitate, sharing his knowledge of various geological areas and constructive comments for improving this thesis. I am grateful to Professor Yoji Arakawa and Professor Bin Chen for their support to analyze U–Pb SHRIMP zircon age at the Institute of Geology, Chinese Academy of Geological Sciences, Beijing. I am deeply indebted to Professor Yujiro Ogawa and Ken-ichiro Hisada for their support, encouragement and valuable suggestions. I am also grateful to my respectable teachers and colleagues of the department of Geology and Mining, University of Rajshahi, Bangladesh for their encouragements and inspiration during the research. I wish to thank Chairman, Petrobangla and Managing Director, Maddhapara Granite Mining Company Ltd. for their kind permission for sampling and supports. I also acknowledged to Mr. Md. Abdul Hannan, DGM, Mr. Md. Abu Taleb Farazi, Manager, Mr. Hasan Mahmudul Islam (Sumon), Deputy Manager, Mr. Md. Razeeun Nabi, Deputy Manager, Mr. Saiful Islam, Deputy Manager, Mr. Bmesh Chandra Roy, Deputy Manager, Mr. Md. Mojibul Sajjad, Deputy Manager and Mr. Md. Ahasan Habib Shahin, Assistant Manager at Maddhapara Granite Mining Company Ltd. for their assistance of underground mine site observation and assistance in samples collection. Special thanks are due to Dr. N. Nishida for his assistance on microprobe analyses. Mr. Hiroyuki Ohyama is also acknowledged for his constant guidance during the microthermometric measurements. Special thanks to H.M. Rajesh for his constructive

discussions and comments for improving this thesis. I am grateful to my colleagues Y. Miyagi, H. Ohyama, S. Ishii, A. Yamada, H. Tadokoro, T. Kanazawa, N. Kondou, Y. Nishimiya, and H. Shimizu for discussions and supports. I always feel my indebted patience to my parents and every family member who encourage me in different ways. I am very much grateful to my wife and son who support and encourage me in tough moment. Finally, I would like to thank the Ministry of Education, Culture, Sports, Science and Technology (Monbukagakusho) of Japan for allowing me a prestigious scholarship. This study was supported by a Grant-in-Aid from the Japanese Ministry of Education, Sports, Culture, Science and Technology (Nos. 17340158 and 20340148) and JSPS-INSA Joint Research Program (No. BDD20023) to TT.

References

Abdel-Rahman, A.F.M., 1994. Nature of Biotites from Alkaline, Calc-alkaline, and Peraluminous Magmas. Journal of Petrology 35, 525-541.

Acharyya, S.K., 1997. Evolutionary character of the Gondwanic Indian Crust. Indian Minerals 51, 1-24.

Acharyya, S.K., 2003. The nature of Mesoproterozoic Central Indian Tectonic Zone with Exhumed and Reworked Older Granulites. Gondwana Research 6, 197-214.

Ague, J.J., 1997. Thermodynamic calculation of emplacement pressures for batholithic rocks, California; implications for the aluminium-in-hornblende barometer. Geology 25, 563-566.

Ague, J.J., Brandon, M.T., 1992. Tilt and northward offset of Cordilleran batholiths resolved using igneous barometry. Nature 360, 146-149.

Ague, J.J., Brandon, M.T., 1996. Regional tilt of the Mount Stuart batholith, Washington, determined using aluminum-in-hornblende barometry: Implications for northward translation of Baja British Columbia. Geological Society of American Bulletin 108, 471-488.

Ameen, S.M.M., Khan, M.S.H., Akon, E., Kazi, A.I., 1998. Petrography and major oxide chemistry of some Precambrian crystalline rocks from Madhyapara, Dinajpur. Bangladesh Geoscience Journal 4, 1-19.

Ameen, S.M.M., Wilde, S.A., Kabir, M.Z., Akon, E, Chowdhury, K.R., Khan, M.S.H., 2007. Paleoproterozoic granitoids in the basement of Bangladesh: A piece of the Indian shield or an exotic fragment of the Gondwana jigsaw? Gondwana Research, 12, 280-387.

Anand, M., Gibson, S.A., Subbarao, K.V., Kelly, S.P., Dickin, A.P., 2003. Early Proterozoic melt generation processes beneath the intracratonic Cuddapah Basin, southern India. Journal of Petrology 44, 2139-2171.

Anderson, J.L., 1996. Status of thermobarometry in granitic batholiths. Transactions of Royal Society Edinburgh, Earth Sciences 87, 125-138.

Anderson, J.L., Smith, D.R., 1995. The effects of temperature and f_{O2} on the Al-in-hornblende barometer. American Mineralogist 80, 549-559.

Andersson, U.B., Eklund, O., Fröjdö, S., Konopelko, D., 2006. 1.8 Ga magmatism in the Fennoscandian Shield; lateral variations in subcontinental mantle enrichment. Lithos 86, 110-136.

Annen, C., Blundy, J.D., Sparks, R.S.J, 2006. The genesis of intermediate and silicic magmas in deep crustal hot zones. Journal of Petrology 47, 505-539.

Arth, J.G., 1976. Behavior of trace elements during magmatic processes — a summary of theoretical models and their applications. Journal Research U.S. Geological Survey 4, 41-47.

Arth, J.G., Barker, F., 1976. REE partitioning between hornblende and dacite liquid and implications for the genesis of trondhjemitic-tonalitic magmas. Geology 4, 534-536.

Atherton, M.P., 1993. Granite magmatism. Journal of Geological Society London 150, 1009-1023.

Ayers, J.C., Watson, E.B., 1991. Solubility of apatite, monazite, zircon, and rutile in supercritical aqueous fluids with implications for subduction zone geochemistry. Philosophical Transactions of the Royal Society London, A 335, 365-375.

Ayuso, R.A., Arth, J.G., 1992. The Northeast Kingdom batholith, Vermont: magmatic evolution and geochemical constraints on the origin of Acadian granitic rocks. Contributions of Mineralogy and Petrology 111, 1-23.

Bailey, J.C., 1981. Geochemical criteria for a refined tectonic discrimination of orogenic andesites. Chemical Geology 32, 139-154.

Baksi, A.K., 1995. Petrogenesis and timing of volcanism in the Rajmahal flood basalt province,

northeastern India. Chemical Geology 121, 73-90.

Barbarin, B., 1990. Granitoids: main petrogenetic classification in relation to origin and tectonic setting. Geological Journal 25, 227-238.

Barbarin, B., 1999. A review of the relationships between granitoid types, their origins and their geodynamic environments. Lithos 46, 605-626.

Barker, F., 1981. Introduction to special issue on granites and rhyolite: A commentary for the non-specialist. Journal of Geophysical Research 86, 10131-10135.

Bertrend, J.M., Duppy, C., Dostal, J., Davison, I., 1984. Geochemistry and geotectonic interpretation of granitoids from Central Iforas (Mali, W. Africa). Precambrian Research 26, 265-283.

Best, M.G., 1982. Igneous and Metamorphic Petrology. W.H. Freeman, San Francisco, 630pp.

Bhowmik S.K., Basu Sarbadhikari, A., Spiering, B., Raith, M., 2005. Mesoproterozoic reworking of Paleoproterozoic ultrahigh-temperature granulites in the Central Indian Tectonic Zone and its implications. Journal of Petrology 46, 1085-1119.

Black, L.P., Kamo, S.L., Allen, C.M., Aleinikoff, J.N., Davis, D.W., Korsch, R.J., Foudoulis, C., 2003. TEMORA 1: a new zircon standard for Phanerozoic U-Pb geochronology. Chemical Geology 200, 155-170.

Blundy, J.D., Holland, T.J.B., 1990. Calcic amphibole equilibria and a new amphibole-plagioclase geothermometer. Contributions to Mineralogy and Petrology 104, 208-224.

Bodnar, R.J., 1995. Fluid-inclusion evidence for a magmatic source for metal in porphyry copper deposits. In: Thompson, J.F.H. (Ed.), Magmas, Fluids, and Ore Deposits. Mineralogical Association of Canada, Short Course Series 23, 139-152.

Bodnar, R.J., Vityk, M.O., 1994. Interpretation of microthermometric data for H_2O-NaCl fluid

inclusions. In: De Vivo, B., Frezzotti, M.-L. (Eds.), Fluid Inclusions in Minerals, Methods and Applications. Short Course International Mineralogical Association, VPI Press, pp. 117-130.

Brown, G.C., 1982. Calc-alkaline intrusive rocks: their diversity, evolution, and relation to volcanic arcs. In: Thorpe, R.S. (ed.) Andesites. John Wiley and Sons, pp. 437-461.

Brown, P.E., Hagemann, S.G., 1994. MacFlinCor: a computer program for fluid inclusion data reduction and manipulation. In: De Vivo, B., Frezzotti, M.-L. (Eds.), Fluid inclusions in minerals: methods and applications. Short Course International Mineralogical Association, VPI Press, pp. 231-250.

Brown, P.E., Lamb, W.M., 1989. P-V-T properties of fluids in the system H_2O-CO_2-NaCl: New graphical presentations and implications for fluid inclusion studies. Geochimica et Cosmochimica Acta 53, 1209-1221.

Castro, A., Rosa, J.D., Stephens, W.E., 1990. Magma mixing in the subvolcanic environment: petrology of the Gerena interaction zone near Seville, Spain. Contributions to Mineralogy and Petrology 106, 9-26.

Chappell, B.W., White, A.J.R., 1974. Two contrasting granite types. Pacific Geology 8, 173-174.

Chatterjee, N., Mazumdar, A.C., Bhattacharya, A., Saikia, R.R., 2007. Mesoproterozoic granulites of the Shillong-Meghalaya Plateau: Evidence of westward continuation of the Prydz Bay Pan-African suture into Northeastern India. Precambrian Research 152, 1-26.

Cocherie, A., 1986. Systematic use of trace element distribution patterns in log-log diagrams for plutonic suites. Geochimica et Cosmochimica Acta 50, 2517-2522.

Compston, W., Williams, I.S., Kirschvink, J.L., 1992. Zircon U-Pb ages of early Cambrian time-scale. Journal of Geological Society 149, 171-184.

Condie, K.C., 2004. Supercontinents and superplume events: distinguishing signals in the

geologic record. Physics of the Earth and Planetary Interiors 146, 319-332.

Cox, K.G., Bell, J.D., Pankhurst, R.J., 1979. The Interpretation of Igneous Rocks. George Allen and Unwin, London, 450pp.

Curray, J.R., 1991. Geological history of the Bengal geosyncline. Journal of Association of Exploration Geophysicists 12, 209-219.

De Paolo, D.J., 1981. Trace element and isotopic effects of combined wall-rock assimilation and fractional crystallization. Earth and Planetary Science Letters 53, 189-202.

Deb, M., Thorpe, R.I., Cumming, G.L., Wagner, P.A., 1989. Age, source and stratigraphic implications of Pb isotope data for conformable, sediment-hosted, basemetal deposits in the Proterozoic Aravalli Delhi orogenic belt, NW India. Precambrian Research 43, 1-22.

Decelles, P.G., Gehrels, G.E., Quade, J., Lareau, B., Spurlin, M., 2000. Tectonic Implications of U-Pb Zircon Ages Himalayan Orogenic Belt in Nepal. Science 288, 497-499.

Desikachar, S.V., 1974. A review of the tectonic and geological history of eastern India in terms of plate tectonics theory. Journal of Geological Society India 15, 137-149.

Ellis, D.J., Thompson, A.B., 1986. Subsolidus and partial melting reactions in the quartz-excess $CaO+MgO+Al_2O_3+SiO_2+H_2O$ system under water-excess and water-deficient conditions to 10 kb: some implications for the origin of peraluminous melts from mafic rocks. Journal of Petrology 25, 91-121.

French, J.E., Heaman, L.M., Chacko, T., Srivastava, R.K., 2007. 1891-1883 Ma Southern Bastar-Cuddapah mafic igneous events, India: A newly recognized large igneous province. Precambrian Research 160, 308-322.

Frost, B.R., Barnes, C.G., Collins, W.J., Arculus, R.J., Ellis, D.J., Frost, C.D., 2001. A geochemical Classification for Granitic Rocks. Journal of Petrology 42, 2033-2048.

Fujimaki, H., Tatsumoto, M., Aoki, K., 1984. Partition coefficients of Hf, Zr, and REE between

phenocrysts and groundmasses. Proceedings of the fourteenth lunar and planetary science conference, Part 2. Journal of Geophysical Research 89, suppl. B662-B672.

Geraldes, M.C., Van Schmus, W.R., Condie, K.C., Bell, S., Teixeira, W., Babinski, M., 2001. Proterozoic geologic evolution of the SW part of the Amazonian Craton in Mato Grosso state, Brazil. Precambrian Research 111, 91-128.

Ghosh, S., Chakraborty, S., Paul, D.K., Sarkar, A., Bhalla, J.K., Bishui, P.K., Gupta, S.N., 1991. Geochronology and geochemistry of granite plutons from East Khasi Hills, Meghalaya. Journal of Geological Society of India, 137, 331-342.

Ghosh, S., Chakraborty, S., Paul, D.K., Bhalla, J.K., Bishui, P.K., Gupta, S.N., 1994. New Rb-Sr isotopic ages and geochemistry of granitoids from Meghalaya and their significance in middle- to late-Proterozoic crustal evolution. Indian Minerals 48, 33-44.

Gill, J.B., 1981. Orogenic Andesites and Plate Tectonics. Berlin: Springer-Verlag, 390pp.

Goodge, J.W., Fanning, C.M., Bennett, V.C., 2001. U-Pb evidence of approximately 1.7 Ga crustal tectonism during the Nimrod Orogeny in the Transantarctic Mountains, Antarctica; implications for Proterozoic plate reconstructions. Precambrian Research 112, 261-288.

Gorton, M.P., Schandl, E.V., 2000. From continents to island arcs: a geochemical index of tectonic setting for arc-related and within plate felsic to intermediate volcanic rocks. Canadian Mineralogist 38, 1065-1073.

Groves, D.I., Condie, K.C., Goldfarb, R.J., Hronsky, J.M.A., Vielreicher, R.M., 2005. Secular changes in global tectonic processes and their influence on the temporal distribution of gold-bearing mineral deposits. 100th Anniversary Special Paper, Economic Geology 100, 203-224.

GSB, 1990. Geological Map of Bangladesh. Geological Survey of Bangladesh.

Hammarstrom, J.M., Zen, E., 1986. Aluminum in hornblende; an empirical igneous

geobarometer. American Mineralogist, 71, 1297-1313.

Hanson, G.N., 1978. The application of trace elements to the petrogenesis of igneous rocks of granitic composition. Earth and Planetary Science Letters 38, 26-43.

Harris, L.B., 1995. Correlation between the Albany, Fraser and Darling mobile belts of western Australia and Mirnvy to Windmill Islands in the East Antarctic shield: implications for Proterozoic Gondwanaland reconstructions. In: M. Yoshida, M. Santosh (Eds.) India and Antarctica during the Precambrian. Geological Society of India Memoir 34, pp. 47-71.

Hartmann, L.A., 2004. Early Paleoproterozoic (2.5-2.0 Ga) tectonic evolution of South America. Geological Society of America (Abstract) 36, 339.

Hawkesworth, C.J., Gallagher, K., Hergt, J.M., McDermott, F., 1994. Destructive plate margin magmatism: Geochemistry and melt generation. Lithos 33, 169-188.

Heinrich, C.A., 1995. Geochemical evolution and hydrothermal mineral deposition in Sn (-W-base metal) and other granite-related ore systems: some conclusions from Australian examples. In: Thompson, J.F.H. (Ed.), Magmas, Fluids, and Ore Deposits. Mineralogical Association of Canada, Short Course Series, 23, 203-220.

Hoffman, P.F., 1991. Did the breakout of Laurentia turn Gondwana inside out? Science 252, 1409-1412.

Hofmann, A.W., 1988. Chemical differentiation of the Earth: the relationship between mantle, continental crust, and oceanic crust. Earth and Planetary Science Letters 90, 297-314.

Holland, T., Blundy, J., 1994. Non-ideal interactions in calcic amphiboles and their bearing on amphibole-plagioclase thermometry. Contributions to Mineralogy and Petrology 116, 433-447.

Hollister, L.S., Grissom, G.C., Peters, E.K., Stowell, H.H., Sisson, V.B., 1987. Confirmation of the empirical correlation of Al in hornblende with pressure of solidification of calc-alkaline

plutons. American Mineralogist 72, 231-239.

Holtz, F., Johannes, W., 1991. Genesis of peraluminous granites. Experimental investigation of melt compositions at 3 and 5 kb and various H_2O-activities. Journal of Petrology 32, 935-958.

Hossain, I., Tsunogae, T., 2008. Fluid inclusion study of pegmatite and aplite veins of Palaeoproterozoic basement rocks in Bangladesh: Implications for magmatic fluid compositions and crystallization depth. Journal of Mineralogical and Petrological Sciences 103, 121-125.

Hossain, I., Tsunogae, T., Rajesh, H.M., Chen, B., Arakawa, Y., 2007. Palaeoproterozoic U-Pb SHRIMP zircon age from basement rocks in Bangladesh: A possible remnant of Columbia Supercontinent. Comptes Rendus Geoscience 339, 979-986.

Hossain, I., Tsunogae, T., Rajesh, H.M., 2008a. Petrogenetic characterization of Palaeoproterozoic basement rocks from Bangladesh: A remnant of magmatism associated with the Columbia supercontinent amalgamation. Geochimica et Cosmochimica Acta 72, A394.

Hossain, I., Tsunogae, T., Rajesh, H.M., 2008b. Geothermobarometry and fluid inclusions of dioritic rocks in Bangladesh: Implications for emplacement depth and exhumation rate. Journal of Asian Earth Sciences (2008), doi: 10.1016/j.jseaes.2008.10.010.

Huppert, H.E. and Sparks, R.S.J., 1988. The Generation of Granitic Magmas by Intrusion of Basalt into Continental Crust. Journal of Petrology 29, 599-624.

Hussain, M.F., Mondal, M.E.A., Ahmad, T., 2004. Geodynamic evolution and crustal growth of the central Indian Shield: Evidence from geochemistry of gneisses and granitoids. Proc. of Indian Academy of Science (Earth Planetary Science) 113, 699-714.

Hussain, M.M., Curtin, G.C., 1995. Results of petrographic studies and chemical analyses of the crystalline drill cores from the Barapukuria area, Parbatipur Thana, Dinajpur District,

Bangladesh. Records of the Geological Survey of Bangladesh 7(5), pp. 3.

ICS, 2004. The International Commission of Stratigraphy. International Stratigraphic Chert, Cambridge University Press.

Islam, M.S., D'Rozario, A., Chowdhury, K.R., Banerjee, M., 2003. Palynostratigraphy of the Gondwana Sequence in the Barapukuria coal basin, Bangladesh. Bangladesh Geoscience Journal 9, 1-29.

Jain, S.C., Yedekar, D.B., Nair, K.K.K., 1991. Central Indian shear zone: a major Pre-cambrian crustal boundary. Journal of Geological Society of India 37, 521-531.

Jain, S.C., Nair, K.K.K., Yedekar, D.B., 1995. Geology of the Son-Narmada-Tapti lineament zone in Central India. In: Chakraborti, B.K. (Ed.), Geoscientific studies of the Son-Narmada-Tapti Lineament Zone. Project Crumansonata, Geological Survey of India, Special Publication 10, pp. 1-154.

Janousek, V., Braithwaite, C.J.R, Bowes, D.R., Gerdes, A., 2004. Magma-mixing in the genesis of Hercynian calc-alkaline granitoids: an integrated petrographic and geochemical study of the Sazava intrusion, Central Bohemian Pluton, Czech Republic. Lithos 78, 67-99.

Johannes, W., 1984. Beginning of melting in the granite system Qz-Or-Ab-An-H_2O. Contributions to Mineralogy and Petrology 86, 264-273.

Johnson, M.C., Rutherford, M.J., 1989. Experimental calibration of the aluminum-in- hornblende geobarometer with application to Long Valley caldera (California) volcanic rocks. Geology 17, 837-841.

Ju, J.S., Chun, J.S., 2001. Report on geological survey of boreholes (2nd revision), Maddhapara Hardrock Mining Project, 223pp.

Kabir, M.Z.K., Chowdhury, K.R., Akon, E., Kazi, A.I., Ameen, S.M.M., 2001. Petrogenetic Study of Precambrian Basement Rocks from Maddhapara, Dinajpur, Bangladesh. Bangladesh

Geoscience Journal 7, 1-18.

Kemp, A.I.S., Hawkesworth, C.J., Foster, G.L., Paterson, B.A., Woodhead, J.D., Hergt, J.M., Gray, C.M., Whitehouse, M.J., 2007. Magmatic and crustal differentiation history of granitic rocks from Hf–O isotopes in zircon. Science 315, 980-983.

Khan, A.A., Chouhan, R.K.S., 1996. The crustal dynamics and the tectonic trends in the Bengal Basin. Journal of Geodynamics 22, 267-286.

Khan, F.H., 1991. Geology of Bangladesh. Wiley Eastern Limited, 207pp.

Konnerup-Madsen, J., Dubessy, J., Rose-Hansen, J., 1985. Combined Raman microprobe spectrometry and microthermometry of fluid inclusions in minerals from igneous rocks of the Gardar province (South Greenland). Lithos 18, 271-280.

Kumar, S., Rino, V., 2006. Mineralogy and geochemistry of microgranular enclaves in Palaeoproterozoic Malanjkhand granitoids, central India: evidence of magma mixing, mingling, and chemical equilibration Contributions of Mineralogy and Petrology 152, 591-609.

Leake, B.E., Woolley, A.R., Arps, C.E.S., Birch, W.D., Gilbert, M.C., Grice, J.D., Hawthorne, F.C., Kato, A., Kisch, H.J., Krivovichev, V.G., Linthout, K., Laird, J., Mandarino, J.A., Maresch, W.V., Nickel, E.H., Rock, N.M.S., Schumacher, J.C., Smith, D.C., Stephenson, N.C.N., Ungaretti, L., Whittaker, E.J.W., Youzhi, G., 1997. Nomenclature of amphiboles: report of the subcommittee on amphiboles of the international mineralogical association, Commission on new minerals and minerals name. Canadian Mineralogist 35, 219-246.

Ludwig, K.R., 1997. Using Isoplot/EX, version 2, in A Geochronolgical Toolkit for Microsoft Excel. Berkeley Geochronological Center Special Publication 47.

Maniar, P.D., Piccoli, P.M., 1989. Tectonic discrimination of granitoids. Geological Society of America Bulletin 101, 673-689.

Matmon, A., Bierman, P.R., Larsen, J., Southworth, S., Pavich, M., Caffee, M., 2003. Temporally and spatially uniform rates of erosion in the southern Appalachian Great Smoky Mountains. Geology 31, 155-158.

McCarthy, T.S., Hasty, R.A., 1976. Trace element distribution patterns and their relation to the crystallization of granitic melts. Geochimica et Cosmochimica Acta 40, 1351-1358.

McInnes, B.I.A., Evans, N.J., Fu, F.Q., Garwin, S., 2005. Application of thermochronology to hydrothermal ore deposits. Reviews in Mineralogy and Geochemistry 58, 467-498.

Miah, I., Arefin, K.M.S., Arifuzzaman, M., 2002. Prospect of Metallic Minerals in Madhyapara Hard Rocks: A Geoelectrical Analysis. Bangladesh Journal of Geology 21, 1-7.

Middlemost, E., 1997. Magmas, Rocks and Planetary Development. Longman, Harlow, 299pp.

Miller, C.F., McDowell, S.M., Mapes, R.W., 2003. Hot and cold granites? Implications of zircon saturation temperatures and preservation of inheritance. Geology 31, 529-532.

Mishra, B., Saravanan, C.S., Bhattacharya, A., Goon, S., Mahato, S., Bernhardt, H.J., 2007. Implications of super dense carbonic and hypersaline fluid inclusions in granites from the Ranchi area, Chottanagpur Gneissic Complex, Eastern India. Gondwana Research 11, 504-515.

Mishra, D.C., Singh, B., Tiwari, V.M., Gupta, S.B., Rao, M.B.S.V., 2000. Two cases of continental collisions and related tectonics during the Proterozoic period in India: insights from gravity modelling constrained by seismic and magnetotelluric studies. Precambrian Research 99, 149-169.

Nabelek P.I., Ternes, K., 1997. Fluid inclusions in the Harney Peak granite, Black Hills, South Dakota, USA: implications for solubility and evolution of magmatic volatiles and crystallization of leucogranite magmas. Geochimica et Cosmochimica Acta 61, 1447-1465.

Nelson, D.R., Myers, J.S., Nutman, A.P., 1995. Chronology and evolution of the Middle

Proterozoic Albany-Fraser orogen, Western Australia, Australian Journal of Earth Science 42, 481-495.

NGRI, 1978. In: Gravity Maps of India. National Geophysical Research Institute, Hyderabad, pp. 1-5.

Ohyama, H., Tsunogae, T., Santosh, M., 2008. CO_2-rich fluid inclusions in staurolite and associated minerals in a high-pressure ultrahigh-temperature granulite from the Gondwana suture in southern India. Lithos 101, 177-190.

Oliver, R.L., Fanning, C.M., 1997. Australia and Antarctica: precise correlation of Paleoproterozoic terrains. In: Ricci, C.A. (Ed.), The Antarctic Region: Geological Evolution and Processes. Terra Antarctica Publications, Siena, pp. 163-172.

Paul, D.K., McNaughton, N.J., Chattopadhyay, S., Ray, K.K., 1996. Geochronology and Geochemistry of the Lingtse Gneiss, Darjeeling-Sikkim Himalaya: Revisited. Journal of Geological Society of India 48, 497-506.

Pazzaglia, F.J., Brandon, M.T., 2001. A fluvial record of long-term steady-state uplift and erosion across the Cascadia forearc high, western Washington State. American Journal of Science 301, 385-431.

Peacock, S.M., 1990. Numerical simulation of metamorphic pressure-temperature-time paths and fluid production in subducting slabs. Tectonics 9, 1197-1211.

Pearce, J.A., 1983. Role of the sub-continental lithosphere in magma genesis at active continental margins. In: Hawkesworth, C.J., Norry, M.J. (Eds.), Continental Basalts and Mantle Xenoliths. Shiva Publishers, pp. 230-249.

Pearce, J.A., Harris, N.B.W., Tindle, A.G., 1984. Trace element discrimination diagrams for the tectonic interpretation of granitic rocks. Journal of Petrology 25, 956-983.

Petro, W.L., Vogel, T.A., Wilband, J.T., 1979. Major-element chemistry of plutonic rock suites

from compressional and extensional plate boundaries. Chemical Geology 26, 217-235.

Peucat, J.J., Meno, R.P., Monnier, O., Fanning, C.M., 1999. The Terre Adélie basement in the East-Antarctica shield: geological and isotopic evidence for a major 1.7 Ga thermal event: comparison with the Gawler craton in South Australia, Precambrian Research 94, 205-224.

Peucat, J.J., Capdevila, R., Fanning, C.M., Menot, R.P., Pecora, L., Testut, L., 2002. 1.60 Ga felsic volcanic blocks in the moraines of the Terre Adélie Craton, Antarctica: comparisons with the Gawler Range Volcanics, South Australia, Australian Journal of Earth Sciences 49, 831-845.

Pietranik, A., Weight, T.E., 2008. Processes and Sources during Late Variscan Diorite-Tonalitic Magmatism: Insights from Plagioclase chemistry (Gęsiniec Intrusion, NE Bohemian Massif, Poland). Journal of Petrology 49, 1619-1645.

Ramakrishnan, M., Vaidyanadhan, R., 2008. Geology of India. Geological Society of India, Bangalore, volume 1, 556pp.

Rao, V.V., Reddy, P.R., 2002. A Mesoproterozoic Supercontinent: Evidence from the Indian Shield. Gondwana Research 5, 63-74.

Ray Barman, T., Bishui, P.K., 1994. Dating of Chotonagpur gneissic complex of eastern Indian Precambrian shield. Records Geological Survey of India 127, 25-27.

Ray Barman, T., Bishui, P.K., Sarkar, A., 1990. Dating of early Precambrian Granite-Greenstone Complex of the Eastern Indian Precambrian shield with special reference to Chhotanagpur Granite Gneiss Complex. Records Geological Survey of India 123, 25-27.

Reimann, K.U., 1993. Geology of Bangladesh. Gebrüder, Borntraeger, Berlin, 160pp.

Reyf, F.G., 1997. Direct evolution of W-rich brines from crystallizing melt within the Mariktikan granite pluton, west Transbaikalia. Mineralium Deposita 32, 475-490.

Richards, A., Parrish, A., Harris, N., Argles, T., Zhang, L., 2006. Correlation of lithotectonic

units across the eastern Himalaya, Bhutan. Geology 34, 341-344.

Roedder, E., 1971. Fluid inclusion studies on the porphyry-type ore deposits at Bingham, Utah, Butte, Montana, and Climax, Colorado. Economic Geology 66, 98-120.

Roedder, E., 1979. Origin and significance of magmatic inclusions. Bulletin de Mineralogie 102, 487-510.

Roedder, E., 1984. Fluid inclusions. Mineralogical Society of America, Washington, D.C. Reviews in Mineralogy 12, 644pp.

Roedder, E., 1992. Fluid inclusion evidence for immiscibility in magmatic differentiation. Geochimica et Cosmochimica Acta 56, 5-20.

Rogers, J.J.W., Santosh, M., 2002. Configuration of Columbia, a Mesoproterozoic Supercontinent. Gondwana Research 5, 5-22.

Rogers, J.J.W., Santosh, M., 2004. Continents and Supercontinents. Oxford University Press, USA, 289pp.

Rollinson, H.R., 1993. Using Geochemical Data: Evaluation, Presentation, Interpretation. Addison Wesley Longman, Harlow, 352pp.

Roy, A., Devrajan, M.K., 2000. A reappraisal of the stratigraphy and tectonics of the Palaeoproterozoic Mahakoshal supracrustal belt, Central India, Proc. In: Proc. Int. Nat. Sem. Precambrian crust in Eastern and Central India, UNESCO-IUGS-IGCP-368, Geological Survey of India, Special Publications 57, 79-97.

Roy, A., Ramachandra, H.M., Bandyopadhyay, B.K., 2000. Supracrustal belts and their significance in the crustal evolution of Central India. In: Proc. Dr. M. S. Krisnan Birth Cent. Sem., Geological Survey of India, Special Publications 55, 361-380.

Roy, A., Prasad M.H., Devrajan, M.K., 2002. Low pressure Metamorphism, Deformation and Syntectonic Granite Emplacement in the Palaeoproterozoic Mahakoshal Supracrustal Belt,

Central India. Gondwana Research 5, 489-500.

Rubatto, D., Hermann, J., 2001. Exhumation as fast as subduction? Geology 29, 3-6.

Rutter, M.J., Van der Laan, S.R., Wyllie, P.J., 1989. Experimental data for a proposed empirical igneous geobarometer: Aluminium in hornblende at 10 kbar pressure. Geology 17, 897-900.

Santosh, M., Tsunogae, T., 2003. Extremely high density pure CO_2 fluid inclusions in a garnet granulite from southern India. Journal of Geology 111, 1-16.

Santosh, M., Yokoyama, K., Acharyya, S.K., 2004. Geochronology and Tectonic Evolution of Karimnagar and Bhopalpatnam Granulite Belts, Central India. Gondwana Research 7, 501-518.

Santosh, M., Tsunogae, T., Iki, T., Vansutre, S., Hari, K.R., 2006. Petrology, fluid inclusions and metamorphic history of Bhopalpatnam granulites, Central India. Journal of Asian Earth Sciences 28, 81-98.

Santosh, M., Tsunogae, T., Ohyama, H., Sato, K., Li, J.H., Liu, S.J., 2008. Carbonic metamorphism at ultrahigh-temperatures: Evidence from North China Craton. Earth and Planetary Science Letters 266, 149-165.

Sarkar, A., Bodas, M.S., Kundu, H.K., Mamgain, V.D., Shanker, R., 1998. Geochronology and geochemistry of Mesoproterozoic intrusive plutonites from the eastern segment of the Mahakoshal greenstone belt, Central India. In: Int. Nat. Sem. Precambrian crust in Eastern and Central India, UNESCO-IUGS-IGCP-368, Geological Survey of India (Abstract), pp. 82-86.

Sarkar, S.N., 1980. Precambrian stratigraphy and geochronology of Peninsular India: a review. Indian Journal of Earth Science 7, 12-26.

Saunders, A.D., Norry, M.J., Tarney, J., 1991. Fluid influence on the trace element composition of subduction zone magmas; Philosophical Transactions of the Royal Society of London 335,

377-392.

Schmidt, M.W., 1992. Amphibole composition in tonalite as a function of pressure: an experimental calibration of the Al-in-hornblende barometer. Contributions to Mineralogy and Petrology 110, 304-310.

Schmidt, M.W., Thompson, A.B., 1996. Epidote in calc-alkaline magmas: An experimental study of stability, phase relationships, and the role of epidote in magmatic evolution. American Mineralogist, 81, 462-474.

Schumacher, J.C. 1997. Appendix 2: the estimate of ferric iron in electron microprobe analysis of amphiboles. Canadian Mineralogist 35, 238-246.

Sen, N., 1991. The Narmada-Son-Brahmaputra transform: a Mesozoic fracture zone in Gondwanic India. Tectonophysics 67, 647-670.

Shand, S.J., 1943. The Eruptive Rocks, 2nd edn. New York: John Wiley, 444pp.

Sokol, A., Domecka, K., Breiter, K., Janousek, V., 2000. The underground gas storage near Pribram — a source of new information about granitoids of the Central Bohemian Pluton. Bulletin of Czech Geological Survey 75, 89-104.

Stein, E., Dietl, C., 2001. Hornblende thermobarometry of granitoids from the Central Odenwald (Germany) and their implications for the geotectonic development of the Odenwald. Mineralogy and Petrology 72, 185-207.

Stephens, W.E., Halliday, A.N., 1984. Geochemical contrasts between late Caledonian granitoid plutons of northern, central and southern Scotland. Transactions of the Royal Society of Edinburgh, Earth Sciences, 75, 259-273.

Sun, S.S., McDough, W.F., 1989. Chemical and isotopic systematics of oceanic basalts: implications for mantle composition and processes. In: Magmatism in the Ocean Basins (eds.) Saunders, A.D., Norry, M.J., Geological Society of London, Special Publication 42,

313-345.

Taylor, H.P., 1980. The effects of assimilation of country rocks by magmas on $^{18}O/^{16}O$ and $^{87}Sr/^{86}Sr$ systematics in igneous rocks. Earth and Planetary Science Letters 47, 243-254.

Taylor, S.R., McLennan, S.M., 1985. The continental crust: its composition and evolution. Blackwell, Oxford, 312pp.

Tewari, R.C., 1999. Sedimentary-Tectonic Status of Permian-Triassic Boundary (250 Ma) in Gondwana Stratigraphy of Peninsular India. Gondwana Research 2, 185-189.

Thorpe, R.S., Francis, P.W., Moorbath, S., 1979. REE and Sr isotope evidence concerning the petrogenesis of North Chilean ignimbrites. Earth and Planetary Science Letters 42, 259-267.

Touret, J.L.R., 1987. Metamorphic fluids: data from fluid inclusions. In: Helgeson, H.C. (Ed.), Chemical transport in metasomatic processes. NATO-ASI Series C218, Reidel, Dordrecht, pp. 91-121.

Touret, J.L.R., 2001. Fluids in metamorphic rocks. Lithos 55, 1-26.

Trivedi, J.R., 1990. Geochronological studies of Himalayan granitoids, Ph.D. thesis (unpub.), Gujarat University, Ahmedabad, India, 170pp.

Tsunogae, T., Santosh, M., Osanai, Y., Owada, M., Toyoshima, T., Hokada, T., 2002. Very high-density carbonic fluid inclusions in sapphirine-bearing granulites from Tonagh Island in the Archean Napier Complex, East Antarctica: implications for CO_2 infiltration during ultrahigh-temperature (T>1100°C) metamorphism. Contributions to Mineralogy and Petrology 143, 279-299.

Tsunogae, T., van Reenen, D.D., 2007. Carbonic fluid inclusions in sapphirine + quartz bearing garnet granulite from the Limpopo Belt, southern Africa. Journal of Mineralogical and Petrological Sciences 102, 57-60.

Tsunogae, T., Santosh, M., Dubessy, J., 2008. Fluid characteristics of high- to

ultrahigh-temperature metamorphism in southern India: a quantitative Raman spectroscopic study. Precambrian Research 162, 198-211.

Tulloch, A.J., Challis, G.A., 2000. Emplacement depths of Paleozoic-Mesozoic plutons from western New Zealand estimated by hornblende-Al geobarometry. New Zealand Journal of Geology and Geophysics 43, 555-567.

Uddin, M.N., Ahmed, M., Ahsan, K., 2005. Stratigraphy of Badarganj Basin, Rangpur District. Bangladesh Journal of Geology 24, 65-73.

Valdiya, K.S., 1995. Proterozoic sedimentation and Pan-African geodynamic development in the Himalaya. Precambrian Research 74, 35-55.

Vaskovic, N., Koroneos, A., Christofides, G., Sreckovic-Batocanin, D., Milovanovic, D., 2004. Mineralogy and Petrology of the Brnjica Granitoids (Eastern Serbia). Bulletin of the Geological Society of Greece 36, 615-624.

Watson, E.B., 1979. Zircon saturation in felsic liquids: experimental results and applications to trace element geochemistry. Contributions to Mineralogy and Petrology 70, 407-419.

Watson, E.B., Harrison, T.M., 1983. Zircon saturation revisited: Temperature and composition effects in a variety of crustal magma types. Earth and Planetary Science Letters 64, 295-304.

Werner, C.D., 1987. Saxonian granulites- a contribution to the geochemical diagnosis of original rocks in high-metamorphic complexes. Gerlands Beitr. Geophys. 96, 271-290.

Whitney, J.A., 1988. The origin of granite; the role and source of water in the evolution of granitic magmas. GSA Bulletin, 100, 1886-1897.

Wilkins, R.W.T., Barkas, J.P., 1978. Fluid Inclusions, Deformation and Recrystallization in Granite Tectonites. Contributions to Mineralogy and Petrology 65, 293-299.

Wilkinson, B.H., Kesler, S.E., 2007. Tectonism and Exhumation in Convergent Margin Orogens: Insights from Ore Deposits. Journal of Geology 115, 611-627.

Williams, I.S., Claesson, S., 1987. Isotope evidence for the Precambrian province and Caledonian metamorphism of high-grade paragneiss from the Seve Nappes, Scandinavian Caledonides, II. Ion microprobe zircon U-Th-Pb. Contributions to Mineralogy and Petrology 97, 205-217.

Wilson, M., 1989. Igneous petrogenesis. Unwin Hyman, London, 456pp.

Windley, B.F., 1993. Uniformitarianism today: plate tectonics is the key to the past. Journal of the Geological Society, London 150, 7-19.

Wiszniewska, J., Krzeminska, E., Dörr, W., 2007. Evidence of arc-related Svecofennian magmatic activity in the southwestern margin of the East European Craton in Poland. Gondwana Research 12, 268-278.

Yedekar, D.B., Jain, S.C., Nair, K.K.K., Dutta, K.K., 1990. The Central Indian collision suture, in: Precambrian of Central India, Geological Survey of India, Special Publications 28, 1-37.

Yoshinobu, A.S., Barnes, C.G., Nordgulen, Ø., Prestvik, T., Fanning, M., Pedersen, R.B., 2002. Ordovician magmatism, deformation, and exhumation in the Caledonides of central Norway: An orphan of the Taconic orogeny? Geology 30, 883-886.

Zaman, M.N., Ahmed, S.S., Islam, M.B., Islam, M.S., Ishiga, H., Dozen, K., Daogong, C., Xiachen, Z., 2001. Trace and rare earth elements geochemistry of the basement complex in Madhyapara, Dinajpur, Bangladesh. Acta Mineralogica Pakistanica 12, 27-42.

Zaman, M.N., Ahmed, S.S., Islam, M.B., Islam, M.S., Ishiga, H., Dozen, K., Elahi, M.M.E., Daogong, C., Xiachen, Z., 2002. Geochemistry and Petrogenesis of the Basement Complex in Madhyapara Hard Rock Mine, Bangladesh. Bangladesh Journal of Geology 21, 23-40.

Zen, E., 1988. Phase relations of peraluminous granitic rocks and their petrogenetic implications. Annual Review of Earth and Planetary Sciences 16, 21-52.

Zen, E., 1989. Plumbing the depths of batholiths. American Journal of Science 289, 1137-1157.

Zhang, S.H., Liu, S.W., Zhao, Y., Yang, J.H., Song, B., Liu, X.M., 2007. The 1.75-1.68 Ga anorthosite-mangerite-alkali granitoid-rapakivi granite suite from the northern North China Craton: Magmatism related to a Paleoproterozoic orogen. Precambrian Research 155, 287-312.

Zhang, S.H., Zhao, Y., Song, B., 2006. Hornblende thermobarometry of the Carboniferous granitoids from the Inner Mongolia Paleo-uplift: implications for the tectonic evolution of the northern margin of North China block. Mineralogy and Petrology 87, 123-141.

Zhao, G.C., Wilde, S.A., Cawood, P.A., Sun, M., 2002. Review of global 2.1-1.8 Ga orogens: implications for a pre-Rodinia supercontinent. Earth Science Review 59, 125-162.

Zhao, G.C., Sun, M., Wilde, S.A., Li, S., 2003. Assembly, Accretion and Breakup of the Paleo-Mesoproterozoic Columbia Supercontinent: Records in the North China Craton. Gondwana Research 6, 417-434.

Zhao, G.C., Sun, M., Wilde, S.A., Li, S., Zhang, J., 2006. Some key issues in reconstructions of Proterozoic supercontinents. Journal of Asian Earth Science 28, 3-19.